Development of targeted exosomes for delivery of biotherapeutics



Eduard Frits Willms

Thesis submitted for the degree of Doctor of Philosophy

Department of Physiology, Anatomy, and Genetics

University of Oxford

New College

Trinity 2018

Declaration

The work presented in this thesis was undertaken in Professor Matthew Wood's laboratory at the Department of Physiology, Anatomy and Genetics (DPAG), University of Oxford, United Kingdom, between 2014 and 2018. All work presented is my own with the following exceptions: (1) Electron microscopy for the analysis of extracellular vesicle morphology, Chapter 3, Fiona Lee, Professor Matthew Wood laboratory, DPAG, University of Oxford. (2) Proteomics, Chapter 3, Henrik J. Johansson, Cancer Proteomics Mass Spectrometry, Science for Life Laboratory, Department of Oncology-Pathology, Karolinska Institutet, Stockholm, Sweden (3) Gene-array analysis, Chapter 2, Imre Mäger, Professor Matthew Wood laboratory, Department of Physiology, Anatomy and Genetics, University of Oxford, Oxford, OX1 3QX, United Kingdom (4) Design of CD19 and CD22 targeting constructs, Chapter 4, Natalie Tigue, Medimmune, Cambridge, United Kingdom (5) Quantification of exosome uptake images, Chapter 4, Carl Matthews, Medimmune, Cambridge, United Kingdom

The experimental findings have not been submitted for any other degree at the University of Oxford or any other institution. My thesis contains modified excerpts and figures of first-author manuscripts which have been published throughout the period of my DPhil in Open Access journals. Where required, permission from individual journals was obtained.

Acknowledgements

Firstly, I would like to thank Professor Matthew Wood for his guidance and advice, and most of all for offering me an environment which allowed me to follow my scientific curiosity and develop my own ideas. I've felt at home and welcomed in the Wood lab from the moment I arrived. Working in a big and vibrant lab like the Wood lab, means I have been able to interact with lots of interesting and great people, which has not only shaped me as a scientist, but also as a person. For that I would second of all like to say thank you to all the people that I have worked with in this lab over the last couple of years.

I would also like to thank Samir El Andaloussi for his guidance, advice, and support both scientifically and personally. His critical and challenging scientific views have always acted as a motivator - sometimes by trying to show his view was wrong, although it was usually not! I would also like to say thank you to all his lab members at the Karolinska Institutet in Stockholm.

Special thanks to Natalie Tigue. I've had a great time working at Medimmune, which wouldn't have been possible without Natalie's enthusiasm, friendliness, support, and patience. I would like to say thank you to all the people I worked with at Medimmune. In particular, Christina Schindler and Andrea Longatti for their help and having to endure me asking many questions. I would especially like to thank Carl Matthews for his help and advice with the microscopy work.

Before I move on to thank more people I would like to thank BBSRC, New College, DPAG, and University of Oxford for their support, which has made all of this possible.

Imre (Mäger), I just wrote "made all of this possible", but I think it's fair to say that most of it would not have been without you. There are numerous reasons I could list here that would show why, but you deserve a double thank you, thank you! The last couple of years have been tumultuous, but in you I've always found a person that would listen and offer valuable advice.

Pieter Vader, thank you for offering me the chance to come over to Oxford, for what was supposed to be a short internship. Little did I know I would end up enjoying research, science, and academia so much that it made me decide to stay in Oxford. Working together has been and still is great fun, your support and down-to-earth view and sense of calm have made both science and life easier. Thanks to for Professor Raymond Schiffelers (Ray), without you I would have never heard about an exosome and would have never met Pieter! Thanks to all his lab members and in particular, Maria Coimbra, Susan van Dommelen, and Sander Kooijmans.

Olivier de Jong, Olivier, Olly, too many good times come to mind writing this sentence. Thank you for all of them! I miss our discussions about science and life in general, sometimes accompanied by a pickled egg in a bag of plain crisps, but always by a pint or too many half pints.
Simon van de Wakker, thank you first of all for all your help in the lab and all the great Oxford memories. I couldn't have wished for a better, more motivated, and friendlier student to work with. I'm sure you will do well and we will cross paths again in the future.

Carlos Cabañas, working together in the lab with someone as knowledgeable, motivating, and energetic as you has been a great experience. I'm looking forward to continuing the interesting research journey you have sent me on.

I've extended my thanks to all the members of the Wood lab at the start, but I would like to take the opportunity to thank some people. First of all, all former and current members of the exosome team, Inna, Mariana, Hans, Anja, Ghulzar, Henok, Marie, Fiona, Jinhguan, Caz, Ashling, Chris, and Leslie. All former and current members of Wood lab, special thanks to: Anna, Graham, Corinne, Suzan, Miguel, Carlo, Melissa, Yoshi, and a special thanks to Amarjit for keeping up with all the things happening.

Special thanks to Gareth, Tom, and Justin! You made working in the lab sometimes feel a bit more like a party.

Kate, going to work and having a friend to chat to as soon as you step in the door is amazing. Your energy and our chats always makes me so happy, thanks!

Outside of work I would like to say thank you to Davide Carone and Frank Wolters, and all the other lovely people I was fortunate enough to meet during my time at the North Oxford Overseas Centre (NOOC).

Living life without cycling is probably like doing science without pipetting. Following on from that piece of wisdom I would like to say thank you to all the wonderful people I met through cycling with local Oxford teams Zappi's and VC Jericho. Special thanks to Hans van der Voorn, with whom I share my enthusiasm for both cycling and exosomes.

To my parents, grandparents, brother, sister, and all my family back home. I don't think a thank you is enough. Being abroad, although it's sort of only a stone's throw away, hasn't always made things easy. Thank you for being so understanding and supporting. Mam, Pap, Andy and Claire thanks for supporting me in all my decisions!

Miranda, a thank you is nowhere near enough to express how grateful I am for having you by my side. You are amazing and I admire and love you for many reasons. My time in Oxford has been good, but being here together with you has made it amazing! Thank you for making me laugh, smile, and happy – keep shining!

It felt appropriate to dedicate this entire page to my biggest fan. Thank you for always supporting me! Unfortunately you will never get to have a look at my thesis, but I think there's no better way to finish writing it, and my acknowledgments with your words: **'t is goud gewaes.**

Abstract

Development of targeted exosomes for delivery of biotherapeutics

Eduard Willms, New College, Doctor of Philosophy, Trinity 2018

Cells release nanosized membrane-enclosed vesicles termed extracellular vesicles. These naturally occurring vesicles have been established as important players in communication between cells, mainly through transfer of their content. This inherent ability makes extracellular vesicles outstanding candidates for development into drug delivery vehicles.

Cells are considered to release a number of extracellular vesicle types with unique size, biogenesis, and cargo: exosomes, microvesicles, and apoptotic bodies. Exosomes are the most well studied vesicle type and are considered to have homogenous characteristics. However, fractionation of isolated exosomes with sucrose density gradient flotation allowed for identification of two distinct exosome subpopulations with unique size and composition. Subpopulations derived from melanoma cells were found to have differential effects on gene expression of recipient cells. Secondly, development of a size exclusion chromatography based approach allowed for more in-depth study on exosome heterogeneity. Four exosome subpopulations with different size and composition were derived from ovarian cancer cells. Preliminary findings point to a potential pathophysiological role of ovarian-cancer derived exosomes, with unique roles of subpopulations in ovarian cancer metastasis.

In addition, differential properties of exosome subpopulations were explored in development of B cell targeted exosomes. Single chain variable fragments targeting B cell surface antigens CD19 and CD22 were successfully expressed on exosomes. Targeting of CD22 resulted in increased and rapid uptake as compared to targeting of CD19. Moreover, data suggested that specific exosome subpopulations are responsible for the latter observation. Findings demonstrate a promising approach for the delivery of biotherapeutics into malignant B cells.

In conclusion, this works shows the heterogeneous nature of exosomes and the release of subpopulations with potential unique biological roles. Addressing heterogeneity is one of the key topics of research on extracellular vesicles and will allow for in depth study on their underlying biogenesis and in turn benefit development of extracellular vesicle based therapeutics.

List of abbreviations

AF4	asymmetrical flow field flow fractionation
APO	apoptotic body
BSA	bovine serum albumin
CD	cluster of differentiation
DG	density gradient
DMEM	Dulbecco’s Modified Eagle’s Media
DMSO	dimethyl sulfoxide
DNA	deoxyribonucleic acid
DPhil	doctor of philosophy
dUC	differential ultracentrifugation
ESCRT	endosomal sorting complex required for transport
EV	extracellular vesicle
EXO	exosome
FBS	fetal bovine serum
FC	flow cytometry
Fig	figure
g	gravity
GO	gene ontology
h	hours
HD	high density
HR	high resolution
HRP	horseradish peroxidase
ILV	intraluminal vesicle
IM	Immunocapture
kDa	kilodalton
LD	low density
LO	large oncosomes
mAb	monoclonal antibody
MHC	major histocompatibility complex
mL	millilitre
MV	microvesicle
MVB	multivesicular body

MSC	mesenchymal stem cell
mRNA	messenger ribonucleic acid
miRNA	micro ribonucleic acid
nm	nanometre
nSMase	neutral sphingomyelinase
NTA	nanoparticle tracking analysis
qPCR	quantitative polymerase chain reaction
PAGE	polyacrylamide gel electrophoresis
PBS	phosphate buffered saline
PCR	polymerase chain reaction
PMT	pre metastatic niche
PS	phosphatidylserine
PVDF	polyvinyldene fluoride
RFP	red fluorescent protein
RNA	ribonucleic acid
SD	standard deviation
siRNA	small interfering ribonucleic acid
TBS	tris buffered saline
TEM	transmission electron microscopy
TFR	transferrin receptor
TRPS	tunable resistive pulse sensing
UF	ultrafiltration
SEC	size exclusion chromatography
µg	microgram

Table of Contents

1 Introduction 1

1.1 Intercellular communication 1

1.1.2 Experimental artefacts? 2

1.1.3 Extracellular vesicles 3

1.1.4 Biological functions of EVs 3

1.2 EV heterogeneity and classic EV populations 4

1.2.1 Exosomes 6

1.2.2 Microvesicles 8

1.2.3 Apoptotic bodies 9

1.2.4 Large Oncosomes 10

1.3 The role of EVs in cancer 11

1.3.1 EV Populations in cancer 17

1.3.2 Subpopulations based on size 17

1.3.3 Large oncosomes 20

1.3.4 Exosome subpopulations 21

1.3.5 Subpopulations based on EV surface composition 21

1.4 EV isolation and fractionation techniques 23

1.4.1 Differential ultracentrifugation (dUC) and density gradient (DG) 26

1.4.2 Size exclusion chromatography (SEC) 28

1.4.3 Ultrafiltration (UF) 30

1.4.4 Asymmetrical-Flow Field-Flow Fractionation (AF4) 31

1.4.5 Microfluidic isolation (MI) 32

1.4.6 Flow Cytometry (FC) 33

1.4.7 Immunocapture (IC) 34

1.5 EV-based therapeutics 36

1.6 Optimising EV-based therapeutics through elucidation of heterogeneity 37

1.7 Thesis aims 40

2 Materials and Methods 40

2.1 Cell culture 41
2.2 Recombinant cell line generation 41
2.3 EV isolation by dUC 42
2.4 EV isolation by SEC 43
2.5 Sucrose density gradient 43
2.6 EXO fractionation by HR-SEC 44
2.7 EXO fractionation by AF4 44
2.8 Nanoparticle tracking analysis 45
2.9 Tunable resistive pulse sensing 45
2.10 Immunoblotting 46
2.11 Dot blot 47
2.12 NanoLC-MS/MS Proteomic analysis 47
2.13 Transmission Electron Microscopy 49
2.14 RNA extraction and profiling 49
2.15 Gene array 50
2.16 Migration assay 52
2.17 Proliferation assay 52
2.18 Adhesion assay 53
2.19 Labelling of isolated EVs 53
2.20 Uptake microscopy 54

3 Results 1 55

3.1 Introduction 56

3.2 Results 58

3.2.1 Heterogeneity of isolated EXOs 58

3.2.2 EXO subpopulations have distinct protein compositions 65

3.2.3 Exosome subpopulations have distinct RNA profiles 71

3.2.4 Exosome subpopulations differentially affect gene expression in recipient cells 73

3.3 Discussion and conclusion 76

3.4 Supplementary figures 82

4 Results 2 90

4.1 Introduction 91

4.2 Results 94

4.2.1 HR-SEC allows for broad fractionation of EXOs 94

4.2.2 HR-SEC allows for isolation of LD-Exo and HD-Exo subpopulations 95

4.2.3 Identification of SKOV3-derived EXO Subpopulations 97

4.2.4 Functional roles of SKOV3-derived EXO subpopulations 101

4.2.5 The role of SKOV3-derived EVs in adhesion 103

4.2.6 SKOV3-derived EXO subpopulations show differential ability to support adhesion 105

4.3 Discussion and conclusion 108

4.4 Supplementary figures 115

5 Results 3 118

5.1 Introduction 119

5.1.1 Targeting of EVs 119

5.1.2 Single chain variable fragments for targeting of CD19 and CD22 121

5.1.3 Delivery of biotherapeutics 123

5.1.4 Intracellular targets for treatment of B cell malignancies 124

5.2 Results 126

5.2.1 Generation of targeted EXOs 126

5.2.2 Uptake by target-expressing recipient cells 127

5.3 Uptake of EV populations and EXO subpopulations 131

5.3.1 HR-SEC Subpopulations 133

5.3.2 AF4 Subpopulations 138

5.4 Discussion and conclusion 141

5.5 Supplementary figures 147

6 Discussion and conclusions 148

6.1 Summary of main findings 150

6.2 Future prospects for EV heterogeneity research 150

6.3 Future prospects for EV-based therapeutics 152

6.4 Concluding remarks 153

7 References 154

8 Appendices 174

8.1 Manuscripts accepted for publication 174

8.2 Attended conferences 175

Figures and Tables

Introduction

Figure 1.1 Cells secrete heterogeneous populations of EVs with overlapping sizes 15

Table 1 Advantages and disadvantages of commonly used EV isolation techniques 24

Results 1

Figure 3.1 B16F10 melanoma cells release EXO subpopulations with distinct biophysical characteristics and composition 59

Figure 3.2 Release of LD-Exo and HD-Exo subpopulations is not unique for B16F10 melanoma cells 64

Figure 3.3 Proteome characterisation of MV and EXO subpopulations by nano LC-MS/MS reveals differences in protein composition 66

Figure 3.4 MVs and EXO subpopulations have different RNA profiles 72

Figure 3.5 EXO subpopulations have different effects on gene expression in recipient endothelial cells 74

Figure S 3.1 EXO Subpopulations LD-Exo and HD-Exo are enriched in ALIX, but not Calnexin and GP96, compared to cell lysate 82

Figure S 3.2 HD-Exo subpopulation displays delayed flotation behaviour 83

Figure S 3.3 Detection of LD-Exo and HD-Exo subpopulations is not a result of isolation conditions, isolation method or fractionation method 84

Figure S 3.4 TRPS measurements confirm distinct size distribution of LD-Exo and HD-Exo 85

Figure S 3.5 Differential enrichment of late endosomal membrane proteins amongst MV, LD-Exo, and HD-Exo 86

Figure S 3.6 Good overlap in protein identification between proteomics replicates 87

Figure S 3.7 High correlation between proteomics replicates 88

Figure S 3.8 Size exclusion chromatography allows for fractionation and detection of LD-Exo and HD-Exo released by B16F10 melanoma cells 88

Figure S 3.9 ACTN4 and CCNY are enriched in LD-Exo derived from H5V endothelial cells 89

Results 2

Figure 4.1	Workflow for EXO isolation with SEC and fractionation with HR-SEC	93
Figure 4.2	HR-SEC fractionates purified EXOs according to size	94
Figure 4.3	HR-SEC allows for fractionation and detection of previously identified LD-Exo and HD-Exo released by B16F10 melanoma cells	96
Figure 4.3	Differential expression of a panel of EV proteins in individual HR-SEC fractions	98
Figure 4.4	SKOV3 HR-SEC pools contain EXOs with distinct size and protein composition	100
Figure 4.6	SKOV3-derived EXOs do not affect ovarian cancer proliferation	101
Figure 4.7	SKOV3 EXOs do not affect HMEC1 migration	102
Figure 4.8	SKOV3 –derived EXOs support adhesion of ovarian cancer cells in an integrin beta 1 dependent process	106
Figure 4.9	Large and small SKOV3-derived EXOs show differential ability in support of ovarian cancer adhesion	107
Figure S 4.1	Representative SKOV3 SEC elution profile	115
Figure S 4.2	Representative SKOV3 HR-SEC elution profile	115
Figure S 4.3	SKOV3 –derived EXOs support adhesion of ovarian cancer cells SKOV3 and mesothelial cells HMrSV5	116
Figure S 4.4	SKOV3 –derived EXOs support adhesion and spreading of ovarian cancer cells SKOV3 and mesothelial cells HMrSV5	117
Figure S 4.5	Asymmetrical flow field flow fractionation (AF4) allows for successful fractionation of SKOV3-derived EXOs	117

Results 3

Figure 5.1	Successful generation of CD19 and CD22 targeted EXOs through genetic manipulation of HEK293 cells	126
Figure 5.2	Dose-dependent uptake of targeted-EXOs by recipient hCD19 and hCD22 expressing cells	128
Figure 5.3	Time-dependent uptake of targeted-EXOs by recipient hCD19 and hCD22 expressing cells	130
Figure 5.4	EV Populations and HR-SEC EXO subpopulations isolated from RFB4 cells have distinct size distribution profiles	134
Figure 5.5	Labelled RFB4-EV Populations and RFB4-EXO subpopulations show different levels in uptake by hCD22 expressing recipient cells	136
Figure 5.6	HR-SEC EXO Pools show differences in uptake	137
Figure 5.7	Large and small EXOs show a difference in nuclear localisation	138
Figure 5.8	Uptake of labelled AF4-EXO subpopulations by hCD22 expressing recipient cells	139
Figure S 5.1	Fractionation of exosomes and exomeres with AF4	147

1 Introduction

Abstract

Chapter one of this DPhil thesis provides an overview of extracellular vesicles. I will briefly describe biological functions of EVs, different extracellular vesicle populations, their characteristics, and underlying biogenesis. The recently emerged challenges of extracellular vesicle heterogeneity, and the importance of addressing this topic will be discussed in the light of the well-explored role of extracellular vesicles in cancer. Current methods for isolation and novel developments for isolation and fractionation are described and compared. Furthermore the relevance of extracellular vesicle heterogeneity for successful development of extracellular vesicle-based therapeutics, which mainly relies on harnessing their unique characteristics for cell or tissue specific targeting, will be outlined as well.

1.1 Intercellular communication

Humans, reduced to their scientific essence, are complex multi-cellular organisms. Homeostasis is governed by the successful communication between the countless cells which compose the human body and its organs. This communication can occur through a number of mechanisms ranging from direct contact between cells (e.g. gap junctions) to distant signalling (e.g. hormones). Extracellular vesicles (EVs) have only recently been discovered as novel mediators in intercellular communication. They have been shown to play a role in intercellular communication through transfer of their content. A great deal of attention and effort has resulted in an understanding of their underlying biogenesis, characteristics, and biological functions, as described below.

1.1.2 Experimental artefacts?

Findings on what we now consider EVs go back to the late 1960s (1). Early observations were described as extracellular structures of lipid-rich particles “matrix vesicles” or “platelet-dust” (2,3). They were found to have coagulant properties and originated from platelets (2).

In the 1970s the term “microparticles” and “microvesicles” start to emerge, with exosomes (EXOs) and a description of their biogenesis being published in the 1980s by the groups of Johnstone and Stahl (4,5).

These initial findings were made in the study of the maturation of reticulocytes (immature red blood cells). Small membrane-enclosed structures of nearly uniform size were found to fuse with the reticulocyte plasma membrane and release their vesicular content into the extracellular space Harding et al 1983.

Interestingly, uptake of iron ceases during reticulocyte maturation which has been shown to coincide with loss of TFR. The authors were able to show that transferrin receptor (TFR) was not simply degraded or inactivated, but instead shed from the cell surface associated with vesicle-like structures during maturation (4,6,7). First regarded as ‘experimental artefacts’ due to induced anaemia in sheep reticulocytes, the authors resorted to studying the mechanism in animals with natural anaemia (piglets and embryonic chick reticulocytes), successfully establishing that EXO formation and release was indeed a natural occurring phenomenon. These findings laid the foundation for EV research, a field which has been growing rapidly ever since.

1.1.3 Extracellular vesicles

Extracellular vesicles (EVs) are naturally occurring membrane-enclosed vesicles ranging in size from 30 to 10,000 nm in diameter. Over the last couple of years interest of the scientific community in these extracellular signalling structures has significantly increased. Mainly because of their role as novel and important players in intercellular communication, through their ability to transfer their biological content, consisting of proteins, lipids, and nucleic acids, to recipient cells (8–10).

1.1.4 Biological functions of EVs

EVs are released by essentially all cell types under physiological as well as pathophysiological conditions. Findings have so far highlighted their physiological role in regulation of multiple processes (11). For example, mesenchymal stem cell (MSC)-derived EVs have been shown to aid tissue repair through transfer of their RNA cargo (12). Furthermore, embryonic stem cell (ES) – derived EVs play a role in stem cell maintenance (13), and coagulation (14).

In terms of pathophysiological processes EVs have established as important players as well. They have for example been found to play a role in neurodegenerative diseases (15), inflammatory diseases (16), and viral infection (17). Perhaps most well established and explored is the role of EVs in cancer (18), which will be described in more detail in section 1.3 of this DPhil thesis.

1.2 EV heterogeneity and classic EV populations

EVs are often conceptually portrayed as a uniform population of vesicles conveying a unified message. Over recent years multiple populations with distinct underlying biogenesis have been identified (19). Moreover, the vast dynamic range of EV cargos and cargo stoichiometry studies that have been described in literature suggests that even a single EV subpopulation may contain a spectrum of EVs with different cargo composition signatures (20–24).

Generally EVs are classified into three major vesicle populations: the non-apoptotic vesicle populations EXOs and MVs, and the apoptotic vesicle population APOs. A classification which is mainly based on a difference in underlying biogenesis, and biophysical characteristics. Additional populations which are unique to specific disease states and do not fall within the defined characteristics of the three populations have been identified as well (e.g. large oncosomes (LOs) in cancer) (25).

Lack of guidelines surrounding the nomenclature of EVs has resulted in numerous names being published for what are in essence overlapping populations (26).

Interestingly, very diverse biological effects reported for EVs indicate that either each individual EV may exert multiple functions, or cells release populations of EVs which carry out unique functions.

Analysis performed by Chevillet et al. on the number of EVs released by cells in comparison to the number of miRNA copies reveals that most EVs released by cells will not contain a biologically significant number of copies (27). Estimates on the number of copies of most abundant miRNA species ranged from one copy

per 9 EXOs to one copy per 47,162 EXOs. On the basis of their findings the authors propose stoichiometric models for EXO miRNA content, supporting release of miRNA rich EXO subpopulations. This possibility is supported by findings of Palma et al. on the packaging of miRNAs into unique EV subpopulations (23). Nevertheless, evidence supporting the role of EVs in functional transfer of miRNA is growing, and transfer appears to be a highly selective and infrequent occurrence (28–31).

Remarkably, the potential of heterogeneity within EVs released by cells was already postulated in the early work by Johnstone et al. The authors discuss that "It is also as yet unclear whether each EXO contains a mixture of all externalised components or if a mixed population is externalised." (6)

The functional role of EVs and differences in functionality of EV populations have mostly been studied in cancer (18,32–35), and will be outlined in section 1.3 - 1.3.6 of this DPhil thesis. However, both we and others have demonstrated heterogeneity in EVs obtained from non-cancerous sources, such as dendritic cells and mesenchymal stem cells (20,24,36).

Shedding light on EV heterogeneity and precisely defining secreted subpopulations and their unique functions will ultimately increase our understanding of EVs in physiology and pathophysiology, and aid development of EV-based biomarkers and therapies.

1.2.1 Exosomes

EXOs represent a population which is derived from intracellular endosomal compartments. Formation occurs through the endolysosomal pathway where EXOs start of as intraluminal vesicles (ILVs) sorted into multivesicular bodies (MVBs). Upon fusion of MVBs with the plasma membrane ILVs are released from the MVBs into the extracellular environment as EXOs. EXOs have a relatively homogenous and narrow size distribution ranging from 30 to 120 nm in diameter. As mentioned the underlying biogenesis of EXOs in particular and EVs in general has been widely studied, and reviewed in great detail by Van Niel et al. (19). Established pathways and important players will be briefly discussed below.

Formation of ILVs and sorting of proteins has been shown to rely on the endosomal sorting complex required for transport (ESCRT) machinery (37,38). This machinery consists of over twenty proteins assembled into 4 unique complexes (ESCRT-0, -I, -II, and -III) and associated proteins (e.g. vacuolar protein sorting-associated protein 4, ALG-2 interacting protein X (ALIX)) (39).

Findings from a comprehensive RNA interference screen, inhibiting individual ESCRT components in HeLa-CIITA-OVA and dendritic cells (DCs), highlight that alterations in this machinery can cause heterogeneity in EXO size and composition (40). ESCRT-0 silencing (hepatocyte growth factor-regulated tyrosine kinase substrate (HRS) and signal transducing adapter molecule 1 (STAM1)) and ESCRT-1 silencing (tumour susceptibility gene 101 protein TSG101) decreased secretion of exosomal proteins CD63 and MHC II. A decrease of EXOs ranging in size from 50 – 200 nm was observed after ESCRT-0 silencing, indicating HRS is not involved in the secretion of EXOs smaller than 50 nm. On the other hand, STAM1 and ALIX seemed to play a role in the

secretion of EXOs smaller than 50 nm. Changes in composition, reduction of exosomal CD63 and MHC II, after depletion of TSG101 and STAM1 were observed as well. Most interestingly, quantification of the expression of CD63 and MHC II indicated that only 20% of the total EXOs released by cells express both markers. This striking finding clearly demonstrates the heterogeneous nature of secreted EXOs.

MVB formation can also occur in the absence of ESCRT machinery (41). Tetraspanins, a family of membrane proteins with four transmembrane domains, seem to be pivotal in ESCRT-independent mechanisms. CD63, a frequently reported tetraspanin in the EV field, has been shown to directly participate in protein sorting and ILV formation in melanocytes, although EXO secretion was not assessed (42,43). The role of another frequently reported exosomal tetraspanin CD9 in EXO secretion has been evaluated in DCs derived from CD9 knockout mice, resulting in a reduction of EXO secretion after knockout (44).

The sphingolipid ceramide seems to represent another important player in ESCRT-independent EXO biogenesis (45). Inhibition of neutral sphingomyelinases (nSMase), an enzyme which is responsible for breaking sphingomyelin (SM) down into phosphocholine and ceramide, has been reported to result in a reduction of EXO release (45). As such, nSMase inhibition is widely employed in the EV field as a simple tool to evaluate EXO biogenesis (24,41,46). Edgar et al. have shown that a competitive relationship between aforementioned ESCRT-dependent and -independent mechanism seems to exist. Interestingly this competition appears to influence formation of differently sized ILV subpopulations within MVBs (47). Based on these findings, it is tempting to

speculate that this competitive relationship may contribute to heterogeneity of released EVs.

The Rab proteins represent another group of essential players in EXO biogenesis and intracellular vesicle trafficking in general. They comprise the largest part of the Ras-like small GTPase superfamily (reviewed in 48). A number of Rab proteins has been shown to be involved in EXO release. Knockdown of Rab 11 has been shown to inhibit the release of transferrin receptor- and heat-shock protein 70 kDa-expressing EXOs in a chronic myeloid leukemia cell line (50). Silencing of Rab35 has been shown to inhibit release of proteolipid protein- and ALIX-expressing EXOs from primary oligodendrocytes (51).

Perhaps most well established is the role of Rab27s (i.e. Rab27a and Rab27b), inhibition of which has been shown to result in decreased release of CD63-, CD81- and MHC II-expressing EXOs by HeLa cells (52). Importantly, Rab27a knockdown in melanoma cells has been shown to decrease EXO production and subsequently inhibit tumour growth and metastasis in mice (53,54). The exact roles of Rab proteins and their involvement in EV biogenesis, secretion, and intercellular interactions has been reviewed in great detail by Colombo et al. (11).

1.2.2 Microvesicles

MVs are derived directly from the plasma membrane of cells. They are a non-apoptotic EV population with a broad size, ranging from 50 to 1,000 nm in diameter. Numerous different names have been used to refer to MVs, such as shedding vesicles, ectosomes, and microparticles. Although the underlying biogenesis of MVs does, in contrast to EXOs, not proceed through a complex

network of intracellular steps, a number of processes and players have been shown to play essential roles in their biogenesis (55). In short, activating signals resulting in an increase of cytosolic Ca^{2+} levels, result in changes in transbilayer lipid distribution and membrane blebbing. Mainly resulting from changes in activity of the transmembrane lipid transporter proteins: flippase, translocase, and scramblase (55,56).

A number of key players in MV release have been identified, such as ADP-ribosylation factor 6 (ARF6), a member belonging to the Ras superfamily of small GTPases (57,58). As well as ATP-mediated activation of P2X receptors, which have been shown to lead to rearrangements of the cell membrane and subsequent MV release (59).

Changes in cytoskeletal actin dynamics and reorganisation of actin through the small GTPase Ras homolog gene family member A (RhoA) and subsequent activation of associated kinase Rho-associated coiled coil-containing kinases are involved in MV formation as well (60).

1.2.3 Apoptotic bodies

APOs are released as a product of apoptotic cell disassembly, through outward blebbing and fragmentation of the cell membrane (61,62). APOs have a very broad size range between 50 and 2,000 nm in diameter. Although their content is generally thought of as randomly packaged, sorting of RNA and DNA into separate distinct APO subpopulations seems to occur (63). Interest in this apoptotic EV population is growing since evidence suggests that APOs have important immune regulatory roles, a concept relevant across different disease

settings including autoimmunity, cancer, and infection (61).

1.2.4 Large Oncosomes

The release of LOs seems to be restricted to cancer cells (25). As their name suggests, LOs represent a population of unusually large non-apoptotic EVs (1–10 μm) that bears the ability of transferring oncogenic material.

Although unusual in size, their biogenesis resembles that of other EV populations. Membrane shedding occurs from cancer cells with an amoeboid phenotype, a process which can be induced through overexpression of oncoproteins (e.g. myristoylated Akt1, heparin-binding epidermal growth factor, and caveolin-1 (Cav-1), silencing of the cytoskeletal regulator Diaphanous-related formin-3, or activation of Akt1 and EGFR pathways. Importantly, their formation does not coincide with increased apoptosis, indicating that LOs are a unique class of EV. Furthermore, tetraspanins CD9, CD63, and CD81 are in contrast to EXOs expressed at very low levels. Membrane localised cytokeratin-18 is a protein which is abundantly expressed by LOs as well as Cav-1. The latter has been reported as a marker for LOs, with findings suggesting that Cav-1 positive LOs can be used to detect metastatic disease in patients with prostate cancer (64,65). Furthermore, sorting of specific miRNA species into LOs has been observed (25). The authors also report the presence of programmed cell death 6 interacting protein, also known as ALIX, in LOs. This finding contradicts increasing evidence from in depth proteomics, which has highlighted ALIX as a reliable marker for EXOs. Since LOs originate from the plasma membrane it is not surprising that ARF6 has been found in LOs as well. The observed overlaps

in composition and biogenesis highlight the complexity of obtaining and characterising, pure EV populations.

1.3 The role of EVs in cancer

The diverse roles of EVs in cancer and tumour metastasis have been extensively reviewed (32,66). I will here briefly describe supporting findings of the main functions of tumour-derived EVs in cancer. EVs have established as major players in the tumour microenvironment, by influencing both the environment directly surrounding the primary tumour as well as distant sites (67). The influence of EVs on key processes such as transfer of oncogenic traits, angiogenesis, immune modulation, thrombosis, and pre-metastatic niche formation promote successful metastasis of disseminated cancer cells (68–73).

The development of cancer initially involves accumulation of genetic alterations. Tumour-derived EVs have been shown to exhibit the capability of transferring oncogenic cargo and traits (e.g. anchorage- independent growth and enhanced survival capability) and in this way promote tumourigenesis (68). Furthermore, tumour-derived EVs have been shown to transfer mutant KRAS proto-oncogene to wild-type KRAS- expressing recipient colon cancer cells, and melanoma-derived EVs are capable of activating mitogen-activated protein kinase pathways in non-metastatic recipient cancer cells (74). Luhtala et al. have recently published their findings on functional transfer of active K-Ras protein through glioblastoma-derived EVs into recipient cells in culture. The authors hypothesise that if transfer of functional K-Ras from EVs into the cytoplasm of recipient cells occurs, it must do so at an extremely low efficiency and therefore is unlikely to

initiate Ras-ERK MAP kinase pathway signalling. Although the authors were making use of a different type of cancer, reported findings claiming functional transfer of proteins through EVs should be interpreted with caution (75).

Angiogenesis is required for supplying tumours with adequate nutrients and oxygen, ultimately allowing tumour growth beyond microscopic size. Tumour-derived EVs are capable of influencing the vasculature surrounding the primary tumour by induction of pro-angiogenic processes (70,76), EV mediated transfer of oncogenic epidermal growth factor receptor (EGFR) to endothelial cells plays a key role in this process (77).

Tumour-derived EVs can influence coagulation and development of thrombosis, contributing to thrombotic events more frequently observed in cancer patients (71). Tissue factor (TF) and P-selectin glycoprotein ligand-1 (PSGL-1) expressed on tumour-derived EVs have been implicated as the most important players in cancer-associated thrombosis (78).

Modulation of multiple immune related processes is another way in which tumour-derived EVs have been shown to increase peripheral tolerance of tumours and support immune evasion of cancer (79–81). Inducing apoptosis of anti-cancer effector cytotoxic T cells through FasL (Fas ligand) positive EVs and influencing T regulatory cells (Tregs) are amongst the main processes involved (82,83). Furthermore, it has been shown that tumour-derived EVs are able to promote T cell-dependent immunosuppressive functions of myeloid-derived suppressor cells (MDSCs), through transfer of heat-shock protein 72 (Hsp72), prostaglandin 2, and transforming growth factor beta (72,84).

Recent findings emphasise the important role of the immunosuppressive molecule programmed cell death ligand 1 (PD-L1) present on EVs. Glioblastoma-derived EVs were found to directly bind programmed cell death protein-1 (PD-1), ultimately leading to immune evasion through inhibition of T cell activation and proliferation (85).

Influencing the metastatic behaviour of tumour cells is the most well described role of tumour-derived EVs. Metastasis or simply spread of cancer from the primary site is a crucial moment in cancer. Interestingly the spread of cancer seems to occur in a predictable pattern, and relies on the interaction between the receiving cells or organ (i.e. “the soil”) and the circulating tumour cell (i.e. “the seed”) as postulated over a century ago by Stephen Paget (86). Tumour-derived EVs seem to affect both “the soil” through stimulating the formation of so-called pre-metastatic niches which favour outgrowth of disseminated tumour cells, as well as “the seed” through affecting the behaviour of cancer cells (66).
Melanoma-derived EVs are able to travel sentinel lymph nodes, leading to recruitment of disseminated melanoma cells. Subsequent stimulation of metastatic factors involved in angiogenesis and extracellular matrix remodelling prepare the lymph node for successful metastasis (87). Transfer of MET through melanoma-derived EVs has been shown to affect bone marrow-derived cells (BMDCs), which are essential for the generation of a tumour microenvironment favouring establishment of secondary outgrowths (53).

Aforementioned findings highlight the diverse role of tumour-derived EVs in cancer. Importantly, taking into account the heterogeneous nature of tumour

cells, the fact that tumour cells release large numbers of EVs, and secreted tumour-derived EVs are very heterogeneous adds another layer of complexity to the role of EVS in cancer which remains to be addressed. Current evidence on unique roles of tumour-derived EV (sub)populations will be summarised and described in the sections below.

Figure 1.1 schematically illustrates the heterogeneous nature of secreted EVs. An overview of EV populations and their reported size range, including the cancer-specific population large oncosomes (LOs) is given. Most commonly reported functions of cancer-derived EVs are listed as well.

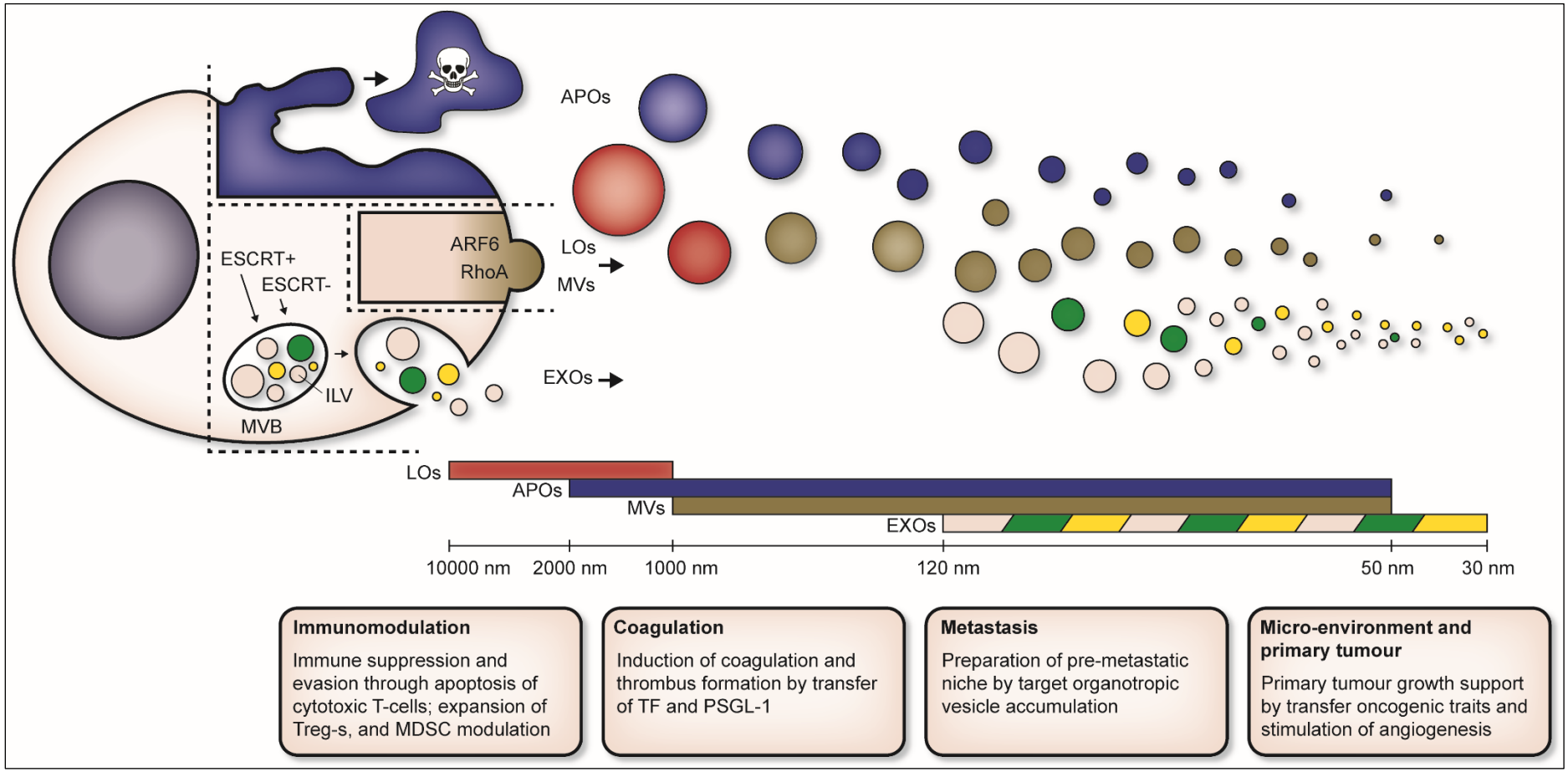

APOs
LOs
MVs
EXOs
ARF6
RhoA
ESCRT+
ESCRT-
ILV
MVB
LOs
APOs
MVs
EXOs
10000 nm
2000 nm
1000 nm
120 nm
50 nm
30 nm
Immunomodulation
Immune suppression and evasion through apoptosis of cytotoxic T-cells; expansion of Treg-s, and MDSC modulation
Coagulation
Induction of coagulation and thrombus formation by transfer of TF and PSGL-1
Metastasis
Preparation of pre-metastatic niche by target organotropic vesicle accumulation
Micro-environment and primary tumour
Primary tumour growth support by transfer oncogenic traits and stimulation of angiogenesis

Figure 1.1 Cells secrete heterogeneous populations of EVs with overlapping sizes. EXOs (pink) are derived from intracellular endosomal compartments. ILVs form within MVBs and are subsequently released as EXOs upon MVB fusion with the plasma membrane. Both ESCRT-dependent (ESCRT+) and -independent (ESCRT−) pathways (e.g. ceramide-dependent pathways) are involved in biogenesis of EXOs. Recently identified unique subpopulations of EXOs are indicated by green and yellow EVs. APOs (blue) are exclusively released by cells undergoing apoptosis. LOs (red) and MVs (brown) are derived directly from the plasma membrane, ARF6 and RhoA are key players in biogenesis of MVs. **Abbreviations: MVB**, multivesicular body; **ILV**, intraluminal vesicle; **ESCRT+**, endosomal sorting complex required for transport-dependent; **ESCRT**-, endosomal sorting complex required for transport-independent; **ARF6**, ADP-ribosylation factor 6; **RhoA**, Ras homolog gene family, member A; **EVs**, extracellular vesicles; **APOs**, apoptotic bodies; **LOs**, large oncosomes; **MVs**, microvesicles; **EXOs**, exosomes; **Treg-s**, T regulatory T cells; **MDSCs**, myeloid-derived suppressor cells; **TF**, tissue factor; **PSGL-1**, P-selectin glycoprotein ligand-1.

1.3.1 EV Populations in cancer

Findings described below provide an overview of currently available evidence on functional differences between tumour-derived EV populations in cancer. It has to be taken into consideration that commonly used methods of isolation and fractionation often result in mixtures of EV populations (88). We will here focus on reported functional differences between tumour EV populations based on size (i.e. LOs, APOs, MVs, and EXOs, including emerging evidence on EXO heterogeneity and the role of specific EXO subpopulations). Furthermore recent important findings on differences in tumour-derived EV populations based on surface composition (i.e. integrin and tetraspanin expression) will be discussed.

1.3.2 Subpopulations based on size

Differences between the functions of the classic EV populations (i.e. APOs, MVs, and EXOs) in cancer have been evaluated in only a handful of studies. Proteomic analysis of EXOs and MVs isolated from SH-SY5Y neuroblastoma cells highlight the differences in composition between these major EV populations (89).

EVs were isolated by dUC (100,000 × g) and subsequently purified by iodixanol DG. A homogenous EXO population (30–100 nm in diameter) highly enriched in exosomal markers TSG101 and ALIX was retrieved from low-density fractions of the gradient, whereas MVs (>200 nm in diameter) were retrieved from higher density fractions (with low TSG101 and ALIX expression). EXOs were enriched with ESCRT components (e.g. VPS24, VPS32, and VPS36), tetraspanins (e.g. CD81, TSPAN9, and TSPAN14), annexins (ANXA7), flotillins, and integrins (ITGA3).

MVs, on the other hand, were found to be enriched in Rac GTPase-activating protein 1, protein disulfide-isomerase A3, spectrin beta chain, non-erythrocytic 2, Mucin-19, 3 ubiquitin-protein ligase, keratin, type I cytoskeletal 18 (KRT18), kinesin-like protein 14, kinesin-like protein 4A, vimentin, 40S ribosomal protein S9, 40S ribosomal protein S18, and matrix metalloproteinase-2 (MMP2). On top of that, CD81 and MMP2 were exclusively found in, respectively, EXOs and MVs, suggesting their potential use as bona fide markers for these EV populations. Functional enrichment analysis hinted to the fact that EXOs and MVs might function through different biological pathways. EXOs were found to be enriched in signalling proteins (e.g. proteins implicated in ESCRT, syndecan signalling, and membrane trafficking), whereas MVs were found to be enriched in enzymes and proteins implicated in gene expression and translation. Comparison of the identified MV and EXO content against COSMIC (Catalogue of Somatic Mutations in Cancer) and EST (Expressed Sequence Tag) databases revealed that proteins exclusively identified in EXO were highly abundant in most cancer types, whereas exclusive MV content was found to be less common in other types of cancer. Upon evaluation of functional effects, SH-SY5Y EXOs were indeed found to stimulate SK-N-BE2 neuroblastoma cells *in vitro* proliferation and cell migration to a higher extent compared with MVs.

On the contrary, it has been reported that colon cancer derived MVs (LIM1863 cells) induce higher invasive activity in recipient fibroblasts cells (NIH3T3 cells) than EXOs (90). Based on proteomic enrichment of invasion, migration, and motility- related components in the LIM1863 EXOs and MVs, the authors argued that these EV populations might stimulate invasion through different

mechanisms. However, the difference in tumour cell source (SH-SY5Y neuroblastoma vs. LIM1863 colon cancer) and isolation technique (UF versus dUC) may have strongly accounted for the observed difference in functionality of the populations.

Investigations into the procoagulant and immunogenic properties of B16-F1 melanoma populations provide an interesting body of evidence on functional differences between APOs, MVs, and EXOs in cancer (91). Fibrin and thrombin generation assays revealed a higher coagulative potential of APOs compared with MVs and EXOs. EXOs were found to be the least coagulative vesicle population. Evaluation of the immunogenic potential of the populations revealed that APOs offer protection against *in vivo* B16 tumour formation and could therefore play a major role in anti-cancer immunity. Thrombotic events are a major cause of death in cancer patients and EVs have been shown to be involved in thrombotic events (92). This finding is interesting in the light of therapeutic approaches taken in anti-cancer therapy and the diverse roles of EVs in cancer. Cytoablative therapy might promote release of APOs, in that way increasing the risk of thrombotic events, while at the same time stimulating an anti-cancer immune response.

1.3.3 Large oncosomes

LOs represent an unusual EV population, mainly because their release seems to be restricted to cancer cells (25). Findings describe their functional role in cancer. Prostate cancer (LNCaP)-derived LOs have been found to affect stroma cells surrounding the tumour, establishing a positive feedback loop affecting tumourigenesis and tumour progression (93). The authors established that active EV-associated Akt1, found to be enriched in prostate cancer-derived LOs compared with EXOs, is a key player both *in vitro* and *in vivo*. *In vitro*, conditioned medium of normal prostate associated fibroblasts (NAFs) treated with LOs induced a significant increase in tube formation of endothelial cells (HUVECs), compared with EXO-treated NAFs. Alterations in expression of factors (e.g. interleukin-6, MMP1, MMP9, α-smooth muscle actin, TGFb1, and thrombospondin 1) in fibroblasts treated with LOs reflected a pro-vascularisation phenotype. Moreover, *ex vivo* treatment of NAFs with LOs before combined *in vivo* injection with DU145 (human prostate cancer cells) resulted in significantly enhanced tumour growth compared with DU145 injection alone. Stimulation of MYC-dependent processes was found to mediate the observed fibroblast reprogramming. Importantly, inhibition of LO uptake through interference with active endocytic pathways prevented the observed effects. Proteomic analysis of LO revealed enrichment of proteins involved in metabolic processes relevant to cancer, including the metabolic enzyme aspartate transaminase (GOT1). LOs were able to transfer GOT1 and increase glutamate production in recipient cells, suggesting an effect of LOs on metabolic functions in cancer cells. Furthermore, it has been shown that LOs mediate transfer of miR-1227, influencing migration of cancer-associated fibroblasts (CAFs) (64).

1.3.4 Exosome subpopulations

As discussed, there is increasing appreciation and evidence for the fact that cells secrete a heterogeneous mix of EVs both in size and composition. The EXO population is generally portrayed throughout literature as a homogenous EV population in both size and composition. Contrary to this view, the reported effects and reported observed functions mediated by EXOs are diverse. This could indicate that each individual EXO has the capability to carry out multiple effects, perhaps depending on secondary effects or the model in which their function is studied, or EXO subpopulations with unique functions are present in the seemingly homogenous EXO vesicle population. Work presented in this thesis will address EXO heterogeneity and the potential different functional roles of EXO subpopulations released by B16F10 melanoma cells.

1.3.5 Subpopulations based on EV surface composition

Study of EV heterogeneity and concretely defining (sub)populations has been hampered due to overlaps in EV size (schematically illustrated in Fig. 1.1) and lack of bona fide EV population markers. An updated categorisation of populations mainly based on enrichment of tetraspanins has recently been put forward (20). Tetraspanins are consistently and abundantly found in EVs, regardless of the EV source (e.g. cell culture supernatant or other biological fluids). Interestingly, integrins and other adhesion receptors are proteins associated with tetraspanins in so-called tetraspanin-enriched microdomains (TEMs) (94–96). Tetraspanins exert important regulatory control on the adhesive and signalling capacities of associated adhesion molecules. Differences and

alterations in tetraspanin and integrin composition could thus result in unique functional roles of EV subpopulations.

EVs secreted by the highly metastatic rat pancreatic adenocarcinoma cell line BSp73ASML preferentially target lung fibroblasts and lymph node stroma cells, triggering upregulation or *de novo* expression of several adhesion molecules, chemokines, growth factors, and proteases. This ultimately results in a phenotype promoting pre-metastatic niche formation. Changes in the EV expression of Tspan8 (released from the Tspan8-transfected non-metastatic variant BSp73AS-Tspan8 cell line) results in targeting of endothelial cells (97). Transfecting the aforementioned cell line with integrin increases their metastatic capacity, and EVs derived from these cells are no longer targeted to endothelial cells but show a preferential binding and incorporation into stromal cells, accumulating in the liver and lung after their intravenous injection (98). These findings clearly highlight that minor changes in EV expression, of tetraspanins and associated integrins, can have significant effects on the function of tumour-derived EVs.

Metastasis occurs in an organ-specific pattern, and it has become evident that EVs and their associated integrins play a key role in directing organotropism (99). Findings indicate that organ specific metastasis is directed by EV integrins, with tumour-derived EVs being capable of redirecting metastasis of tumour cells which normally lack metastatic capacity. EV integrins α6β4 and α6β1 were found to favour binding to lung-resident fibroblasts and epithelial cells, governing the lung metastasis tropism, while EV integrin αvβ5 dictates binding of EVs to Kupffer cells and associates with liver metastasis. The authors also proposed that EV integrins not only mediate the adhesion, but also influence signalling and

inflammatory responses in target cells. Interestingly, packaging of integrins into EVs seems to be a selective process, since EV integrin expression did not reflect cellular expression.

Aforementioned findings on significant changes in EV functionality after only minor changes in composition highlight the importance of addressing EV heterogeneity.

1.4 EV isolation and fractionation techniques

Great advances have been made in development of techniques for isolation of EVs, which have allowed dissection of EV heterogeneity. To date, dUC remains the most commonly used technique for isolation of EVs (88). However, multiple techniques used in other fields (e.g. SEC and FC) have now been successfully adapted for EV isolation. Application of these optimised techniques will allow more in-depth study on EV heterogeneity. Each technique has its own specific advantages (e.g. high resolution and/or purity) and drawbacks (e.g. time-consuming and/or expensive), as summarised in **Table 1**. Selection of the most suitable technology therefore highly depends on the research question and definition of EV subtype (size versus marker expression).

	dUC	UF	DG	SEC	FC	IC	AF4	MI
Sample purity	med.	low	high	high	high	high	high	high
Ability to resolve subpops	low	med.	med.	med.	high	high	med.	med.
Ease of use	mod.	easy	dif.	easy	mod.	mod.	dif.	mod.
Time	long	short	long	inter.	inter.	inter.	inter.	inter.
Scalable	no	yes	no	yes	yes	yes	yes	yes
Possibility to automate	dif.	dif.	dif.	mod.	mod.	mod.	dif.	mod.
Downstream application	char. func.	char. func.	char. func.	char. func.	char.	char.	char. func.	char. func.
Cost	med.	low	med.	med.	high	high	high	med.

Table 1 Advantages and disadvantages of commonly used EV isolation techniques. dUC, differential ultracentrifugation; **UF**, ultrafiltration; **DG**, density gradient; **SEC,** size exclusion chromatography; **FC**, flow cytometry; **IC**, immunocapture; **AF4**, asymmetrical flow field flow fractionation; **MI**, microfluidic isolation; **med.**, medium; **mod.**, moderate; **dif.**, difficult; **char.**, characterisation; **func.**, functionality. **Sample purity**—Are obtained samples free of contaminating proteins, lipids, and fragments? **Ability to resolve subpopulations**—Is the method able to isolate homogenous populations, and as such suitable for population studies? **Ease of use**—Is the method easy to use, are special training or equipment needed? **Time**—Is the method time-consuming? **Scalable**—Is the isolation process scalable? **Possibility to automate**—Is it possible to automate the isolation process? **Downstream application**—Is it possible to use the obtained samples for functional assays (i.e., in vitro and in vivo)? **Cost**—What are the costs associated with method of isolation (e.g., specialised equipment, time, and consumables)?

1.4.1 Differential ultracentrifugation (dUC) and density gradient (DG)

Ultracentrifugation remains the most well-known and commonly employed technique for EV-isolation. Successive centrifugation at high centrifugal forces allows for elimination of dead cells and cellular debris, and subsequent enrichment of EV populations. A detailed protocol for isolation of EV populations was published by Théry et al. in 2006 (100). In short, large EVs (e.g. LOs and APOs) are pelleted by centrifugation at 2,000 × *g*, MVs are pelleted by centrifugation at 10,000 × *g*, whereas EXOs are pelleted at centrifugal forces of 100,000 × *g* and above. Pelleted EVs are washed by resuspension and a subsequent second round of pelleting. dUC has been successfully applied to isolate distinct populations of EVs (101,102). Throughout literature slight alterations to this protocol are reported by many groups over the years, such as centrifugation force and time. Interestingly, such alterations have been described to result in large differences between sedimentation patterns and efficiency of EVs derived from different cell lines (103). More importantly, it has since then been shown that yield and purity of dUC-isolated EVs is greatly influenced by rotor type and centrifugation time (104). Differences in applied isolation techniques and lack of standardisation may affect reported findings of EV composition and functionality. Furthermore, dUC does not allow for absolute separation of EV populations, since smaller EVs will also pellet at lower centrifugal forces and *vice versa*. Subsequently resulting in heterogeneity within isolated populations, in turn making the study of EV subtypes using dUC only very difficult. As a result density gradient flotation (DG) has been employed in the EV field to increase purity of isolated EVs, eliminating potential copurified non-EV material or EV fragments which arise during dUC. In DG, EVs are allowed to

float into a gradient of increasing dilutions of viscous solutions,such as sucrose or iodixanol. Upon centrifugation, EVs migrate to their (equilibrium) density. Migration speed or rate of flotation depends on the size, shape, and density of the EV.

Chapter 3 of this DPhil thesis will provide a large body of evidence on successful application of DG for addressing EV heterogeneity. Aalberts et al. utilised a similar approach and highlighted the existence of populations of prostasomes in seminal plasma from vasectomised men (105). Prostasomes are small membrane vesicles which have been proposed to be secreted after fusion of MVBs with the plasma membrane of prostate epithelial cells (106). Similar to reports on functionality of EVs, a wide variety of effects have been reported for prostasomes, suggesting the likelihood of distinct subpopulations. Sucrose DG allowed for identification of two subpopulations with distinct size (56±13 versus 105±25 nm), but similar equilibrium buoyant density (105). Findings on protein composition further highlighted prostasome heterogeneity, with CD9 present in both subpopulations, whereas GLI pathogenesis-related 2 (GLIPR2) was enriched in smaller prostasomes and Annexin A1 in larger prostasomes.

DG has also been employed to show copurification of different types of EXOs from 4T1 mouse breast cancer cells, when relying on dUC for EXO isolation only. Isolated EXOs (100,000 × *g*) were fractionated using a sucrose DG. Using this methodology, Bobrie et al. detected CD9 in all sucrose fractions, with a strong enrichment in CD9 expressing EXOs present in specific low-density fractions (1.11 and 1.14 g/ml) and high-density fractions (1.26 and 1.29 g/ml) (107). A similar pattern was observed for CD63. In contrast, Mfge8 was enriched in EXOs present in the low-density fraction (1.14 g/ml). Interestingly, inhibition of the small

GTPase Rab27a decreased CD63 levels in all fractions, whereas levels of CD9 and Mfge8 were only moderately reduced. Immuno electron microscopy allowed for detailed study of the CD9 distribution within the seemingly heterogeneous EXO populations. A reduction of CD9 was observed in larger EXOs, indicating that secretion might require Rab27a.

dUC and DG remain most commonly applied techniques for EV isolation and subsequent purification. However, their time-consuming nature, low resolution, operator-dependent yield, and lack of automatisation remain major drawbacks. Recent reports on reduced functionality of dUC isolated EVs further undermine its widespread application (108).

1.4.2 Size exclusion chromatography (SEC)

Over the last couple of years SEC has emerged as a user-friendly alternative to dUC and DG. SEC is performed using a column containing small porous polymer beads (referred to as the stationary phase). As the particle-containing solution travels through the stationary phase, small particles are able to enter the porous beads. As a result, larger particles travel through the column more quickly than small particles and leave the column (i.e. elute) at an earlier time point than small particles. SEC is now widely utilised by researchers in the EV field, mainly as a straightforward method that overcomes problems associated with dUC (e.g. vesicle disruption, aggregation, and co-purification of non-EV material) (109,110). Importantly, clear differences between functionality of dUC-isolated EVs (dUC-EVs) and SEC isolated EVs (SEC-EVs) were observed (108). Comparison of dUC-EVs and SEC-EVs showed no major morphological

differences or differences in protein composition. However, a clear increase in EV-induced ERK1/2 phosphorylation in recipient endothelial cells was observed after treatment with SEC-EVs compared to dUC-EVs, highlighting increased functionality of EVs isolated with SEC. As outlined in Chapter 3 of this thesis, through the appropriate choice of column resin SEC may also be suitable for fractionation of EVs and separation of EV subpopulations. Willms et al. utilised a custom SEC method (based on Sephacryl S-1000 resin) for the fractionation of B16F10 dUC-isolated EXOs according to size. On the basis of enrichment profiles of ACTN4, CCNY, and EPHA2, the presence of two distinct subpopulations of EXOs previously identified by sucrose DG was confirmed (24). Along similar lines, Willis et al. were able to separate EXO sub-types derived from human mesenchymal stem/stromal cells from bone marrow and Wharton's jelly (111). EXOs were isolated by dUC, followed by tangential flow filtration and iodixanol density flotation, and subsequently fractionated by SEC. Large EXOs (>80 nm in size) were found to be enriched in CD63 and flotillin-1, whereas small EXOs (<80 nm in size) were found to be enriched in ALIX and TSG101. These findings further highlight the heterogeneity within EXO preparations, and the potential of SEC for isolation of specific EV and EXO subpopulations, whilst preserving functionality.

1.4.3 Ultrafiltration (UF)

Modern techniques allow for production of filters with extremely low pore size. Making use of semipermeable membranes with defined molecular weight cut-off or pore size it's possible to concentrate EVs according to size. EVs which are smaller than the applied pore size pass through the pores in the membrane, whereas larger EVs are retained. Similar to SEC, UF-based techniques may offer a less harsh and straightforward alternative to dUC, minimising the exposure of EVs to high-centrifugal forces for prolonged periods of time (112,113). Simpson et al. were able to obtain EXOs and MVs released from LIM1863 colon cancer cells using a method based on a series of four filtration steps through hydrophilic PVDF membrane filters with different pore sizes (0.65, 0.45, 0.22, and 0.1 µm) (113).

Obtained populations, correlating to retained particles after filtration, were termed Fn1 (i.e. retentate after 0.65 µm filtration, pelleted by centrifugation 10,000 × *g*) to Fn5 (i.e. retentate after 0.1 µm filtration, pelleted by centrifugation 100,000 × *g*). Strong enrichment of ALIX, TSG101, and tetraspanins CD63 and CD81 was observed in Fn5 compared to Fn1. Based on these findings the authors concluded that fraction Fn5 contained EXOs and fraction Fn1 MVs. Fractions 2–4 were excluded for any further characterisation due to low EV yield. Cryo-EM revealed a homogenous distribution of particles in fraction Fn5 (i.e. EXOs), whereas Fn1 (i.e. MVs) was heterogeneous in size containing a small percentage of very large EVs consistent with LOs. Analysis of the protein content revealed 256 proteins common to both fractions, 98 unique proteins in EXOs, and 350 in MVs. EXOs were found to be enriched in common EXO marker proteins (TSG101, ALIX, and Syntenin) and a number of tetraspanins (e.g. CD9, CD63,

CD82, CD151, TSPAN6, and TSPAN8) and integrins (ITGA2, ITGA6, ITG1, and ITGB4). MVs were found to be enriched in cytoskeletal elements (e.g. microtubules) and septins (along with their associated binding partners), and cytoskeleton associated proteins (e.g. Actin, Actinin, Dynamin, Myosins, Tubulin, and VDAC1/2). These findings provide further evidence for the unique composition of MVs and EXOs. UF allows for straight-forward isolation of EV populations, although limitations in choice of membrane pore size present drawbacks. Furthermore, clogging of membrane pores may affect EV isolation as well (114). Optimised filtration methods such as tangential flow filtration and hollow fiber filtration could overcome such drawbacks (115).

1.4.4 Asymmetrical-Flow Field-Flow Fractionation (AF4)

Interest in this novel technique has grown rapidly, mainly due to a recent publication by Zhang et al. describing the fractionation of EXO subpopulations and discovery of a novel population of very small non-membranous nanoparticles (approximately 35 nm) termed exomeres (116). Application of flow field flow fractionation (FFFF) was first published by Giddings et al. in 1966 (117). Asymmetrical-flow field-flow fractionation (AF4), a type of FFFF, is a relatively new technique to the EV field and only a small number of groups have reported using AF4 (118–123). Similar to SEC, AF4 represents an isolation technique with a mild character and ability to separate materials over a wide colloidal size range. A4F allows for fractionation of distinct EV populations (e.g., EXO, MV, and APO) and even EXO subpopulations, while preserving intact biophysical characteristics (124). Reduced risk of potential EV-loss resulting from adherence to membranes

(UF) or a stationary phase (SEC) are other advantages. Zhang et al. have recently shown that A4F allows for fractionation of EXOs, and isolation of EXO subpopulations based on size. Two distinct subpopulations, Exo-L (large EXO vesicles, 90–120 nm) and Exo-S (small EXO vesicles, 60–80 nm) were isolated. Detailed characterisation on both biophysical characteristics, composition, and bio-distribution were performed. Aforementioned findings highlight the strong fractionation capability of AF4, allowing in-depth study of EV and EXO heterogeneity.

1.4.5 Microfluidic isolation (MI)

The application of micro-fluidic systems for isolation of EVs is relatively new to the EV field. Application of MI devices for EV isolation, which is based on precise control and manipulation of geometrically constrained fluids on a very small (submillimetre) scale, has been extensively reviewed by Gholizadeh et al. (125). Although the prospects are very promising, MI is not widely applied yet. Shin et al. highlight its potential for isolation of classic EV populations (EXOs and APOs) based on size (126). Separation of these two populations was confirmed based on TEM analysis and expression of the EXO marker syntenin and the exclusion marker calreticulin. Mild external forces, possibility to apply low sample volumes, and minimal sample dilution make MI a very attractive technique for EV isolation. Further advances could result in potential application of MI for fractionation of EVs.

1.4.6 Flow Cytometry (FC)

In contrast to aforementioned techniques, which all rely on differences in EV size for separation, FC allows for separation based on EV surface composition. FC has been widely used for counting, characterising, and sorting of individual cells in heterogeneous cell populations.

In FC, particles are suspended in a hydrodynamically focused stream (i.e. flow) and passed through a series of lasers. Scattering of particles, or fluorescence in case fluorescently labelled antibodies or fluorescent dyes are utilised, is recorded.

Application of this technique for detection and potential sorting of EV populations has been held back mainly by the submicron size, complex composition, and low refractive index of EVs. Different FC techniques, optimisation of experimental parameters, and the application of FC in the EV field have been extensively reviewed by Welsh et al. (127). FC has been successfully applied for detection of EVs and distinct EV subpopulations (128,129). Nolte-'t Hoen et al. combined general PKH67 labelling of EVs isolated by dUC (100,000 × *g* pellets), with selective labelling using fluorescently labelled antibodies. This approach allowed for discrimination between T-cell- and DC-derived EXOs. Importantly, a double labelling approach with MHC II and MFG-E8 antibodies allowed for detection of subtle changes in the composition of EVs derived from LPS stimulated DCs. This finding highlights the potential strength of FC for detection of EV subpopulations.

Physical changes in the mechanics and technical parameters of FC equipment (e.g. varying nozzle size and sheath pressure), can allow for increases in sensitivity and subsequent particle analysis (129). The authors describe the successful development of a method for high-resolution FC-based particle

quantification, characterisation, and sorting. EVs were isolated from bone marrow-derived mast cells using dUC (100,000 × *g*). The entire population of isolated EVs was subsequently labelled with CFSE, followed by population specific labelling with R-PE-labelled CD63 and APC-labelled CD9 antibodies. Following this approach the authors were able to accurately separate and sort CD63 positive EVs from CD9-positive EVs. Along similar lines, Higginbotham et al. were able to detect distinct human colorectal cancer (DiFi) EV subpopulations expressing conformationally active EGFR (130). Aforementioned findings outline the strength of applying FC for EV characterisation and potential sorting, based on surface composition. Further optimisation is however needed to allow accurate detection of very small EVs. Application of sorted EVs in functionality assays is hampered by antibody binding to the EV surface.

1.4.7 Immunocapture (IC)

Koliha et al. recently published findings on the combination of FC and IC, a novel multiplex bead-based platform, allowing analysis of the EV-surface protein composition (131). Findings on heterogeneity in expression of tetraspanins on EVs, and between EVs derived from different sources highlight the strength of this approach. NK-cell derived EVs were found to be devoid of tetraspanin CD9 whilst expressing CD63 and CD81. In contrast, platelet-derived EVs express abundant CD9 and CD63, but lack CD81. In addition, different subpopulations of EVs derived from activated B lymphocytes were identified, based on the relative expression of B cell markers CD19 and CD20, and activation markers CD80 and CD86.

Aforementioned findings show that IC can allow for identification and potential physical separation of different EV subpopulations from a heterogeneous mixture. Physical binding of EVs to beads does however interfere with EV characteristics, hampering study of biological functionality. Development of methods which will allow dissociation of bound EVs would allow a broader application of this technique. In the present circumstances the technique could be employed to deplete EV samples of all EVs expressing a specific surface marker (i.e. deplete of all CD9-bearing EVs), which would subsequently allow for study of differences in functional effects of EV subpopulations. IC and the approach described by Koliha et al. are very powerful techniques, relatively easy to use, and quick. Most importantly they can even be performed without extensive prior sample purification steps.

1.5 EV-based therapeutics

The inherent ability of EVs to deliver cargo into the intracellular environment of recipient cells makes them excellent candidates for development into drug-delivery vehicles. EVs might have multiple advantages over currently available drug delivery vehicles, such as their ability to cross natural barriers, their intrinsic cell targeting properties, and stability in the circulation (132,133). These advantages could be exploited for delivery of therapeutics, by encapsulating therapeutics into EVs. The lipid bilayer could offer protection of therapeutic cargo from degradation, but also presents a barrier for therapeutics to be encapsulated (i.e. loaded) into EVs. Several methods of EV loading have been described, they can generally be divided into two types: exogenous loading and endogenous loading. The former approach involves loading after the EVs have been isolated. For example, electroporation of therapeutic cargo or membrane incorporation of lipid-conjugated therapeutics, have been successfully employed to exogenously load EVs with siRNAs (134,135). EVs electroporated with BACE1 siRNA caused strong *in vivo* knockdown of BACE1 mRNA (60%) and protein (62%) in wild-type mice (135).

Endogenous loading can be achieved through manipulation of the EV producing cells. Relatively straightforward approaches such as transfecting EV producing cells with miRNA (136), or incubating EV producing cells with the desired therapeutic to be encapsulated have been successful (137). Using the latter approach Pasccucci et al. were able get MSC cells to incorporate paclitaxel into EVs. EVs isolated from the exposed cells were found to have incorporated paclitaxel, and more importantly they were found to inhibit tumour growth (137).

Endogenous loading can also be achieved through fusion of therapeutic cargo to proteins enriched in EVs. Kanuma et al. recently employed this approach to increase delivery of an antigen to $CD8^+$ T cells, and improve vaccine immunogenicity (138). The antigen was fused to tetraspanin CD63, which is abundantly expressed in EVs. In a mouse tumour model the EV-delivered antigen significantly inhibited tumour growth.

The aforementioned findings are examples of the successful application of EV-based therapeutics. In addition to their therapeutic application, EVs have been established as promising biomarkers. This area of EV research, although highly interesting, is beyond the scope of this DPhil thesis. However, some excellent reviews on the application of EVs as biomarkers have been published (139–141).

1.6 Optimising EV-based therapeutics through elucidation of heterogeneity

Heterogeneity of secreted EVs and the existence of unique subpopulations within currently established populations creates a number of challenges as well as opportunities for the development of EV-based therapeutics. As previously hypothesised and outlined, cells secrete a large number of EVs, as such the assumption that there are populations with differences in characteristics favourable to drug deliver (ability to cross natural barriers, intrinsic cell targeting properties, and stability in the circulation), seems therefor highly likely.

EXOs are currently the most widely studied EV population, which perhaps falsely depicts them as more important and interesting than other populations in terms

of development into therapeutics. This assumption is however not supported by current scientific evidence (142). On the contrary, Kanada et al. were able to show differential loading of HEK293FT-derived MVs and EXOs with pDNA, mRNA, siRNA, and protein (143). Loading of MVs was found to be more efficient than loading of EXOs. More importantly, the authors only observed functional transfer of pDNA to recipient cells when using MVs both *in vitro* as well as *in vivo*.

These findings clearly highlight the relevance of elucidating heterogeneity for the development of EV-based therapeutics. This could in turn allow for identification of the optimal population to be employed therapeutically. Observed differences may arise from differences in uptake by recipient cells and/or differences in subsequent intracellular localisation. Interestingly, uptake studies performed by Kanada et al. with RFP-labelled MVs and EXOs revealed no difference in level of uptake by recipient cells (143), possibly indicating that observed functional differences result from a difference in intracellular localisation or intracellular release between the populations.

Caponnetto et al. observed that cells preferentially take up smaller glioma-associated stem cell EXOs, which subsequently led to a stronger effect on glioma cell motility (144). Although the observed difference in size of the populations were isolation method-dependent (dUC vs. precipitation), the findings suggest that size could have major consequences on EV therapeutic potential. However, it has to be taken into consideration that although a higher activity was observed for smaller precipitation-isolated EVs, precipitation methods have been reported to result in co-precipitation of NON-EV material (145). In addition, the EV field has a number of other aspects that remain to be addressed in order to accelerate the therapeutic application of EVs.

These aspects, although relevant, are beyond the scope of this thesis. Briefly, applications have so far been limited by lack of methods for scalable EV isolation and efficient drug loading (132). Key aspects such as effects of storage conditions on EVs remain to be studied in greater detail. However, a growing body of evidence on these aspects is emerging (146–148).

1.7 Thesis aims

In summary, findings described in this introduction clearly outline the important role of EVs in intercellular communication, in both physiological as well as pathophysiological processes. An increasing amount of evidence points towards vast heterogeneity existing within secreted EVs and hitherto defined populations.

The following hypotheses will be addressed in this thesis:

1 Despite a wide range of putative biological functions being attributed to EXOs, they are assumed to represent a homogenous population of EVs. I propose the existence of subpopulations of EXOs with defined molecular compositions and biological properties.

2 Development of novel methods for EXO isolation and fractionation will allow for more in-depth studies of EXO heterogeneity. To this end, a chromatography approach for EXO fractionation can facilitate identification of subpopulations and additionally more detailed studies on unique functions of secreted subpopulations.

3 The natural characteristics of EXOs can be harnessed for intracellular delivery of biotherapeutics, and target cell specificity of EXOs can be influenced by expression or targeting moieties on their surface. Engineered EXO producing cells might release subpopulations with different delivery and targeting characteristics. As a result development of EXO based therapies can benefit from elucidation of heterogeneity.

2 Materials and Methods

2.1 Cell culture

B16F10 cells (ATCC, Manassas, VA, USA), A431 cells (ATCC), Neuro2a (ATCC), H5V cells (ATCC), HEK293 (ATCC), and SKOV3 cells (kindly provided by Professor Ahmed lab (Ovarian Cancer Cell Laboratory in The Weatherall Institute of Molecular Medicine, Oxford, United Kingdom) were cultivated in DMEM (Life Technologies, Carlsbad, CA, USA). Human microvascular endothelial cells HMEC-1 (CDC; Atlanta, GA, USA) were maintained (up to passage number 27) in MCDB131 medium (Life Technologies) containing 10% fetal bovine serum (FBS), 50 nm Hydrocortisone, 10 mM L-glutamine and 10 ng/ml rhEGF. hTERT immortalised mesenchymal stem cells were kindly provided by St. Jude Children's Research Hospital, and were cultivated in RPMI (Life Technologies). Media were supplemented with 10% heat-inactivated FBS (Life Technologies), 100 U/mL penicillin (Sigma-Aldrich, St. Louis, MO, USA) and 250 ng/mL amphotericin B (Sigma), cells were cultivated at 37 ℃ in 5% CO2. Cells were routinely checked for mycoplasma contamination by PCR Mycoplasma Test Kit I/C (Promokine, Heidelberg, Germany).

2.2 Recombinant cell line generation

Sequences to generate HEK293 cells expressing hCD19, hCD22, αCD19 - 6C11 - scFv, or αCD22 - RFB4 - scFv were provided by Medimmune. HEK293FT cells were co-transfected with lentiviral vector constructs and pPACKH1 packaging plasmid mix (System Biosciences) using Lipofectamine 2000 (Thermo Fisher Scientific) according to manufacturer's instructions. 48 h post-transfection,

culture supernatants containing lentiviral particles were harvested and used to infect HEK293 at 70–80% confluency in media containing 8 μg ml−1 polybrene (Sigma-Aldrich). Transduced cells were selected by addition of 1 μg ml−1 puromycin (Thermo Fisher Scientific) 48 h after transduction. Cells were maintained in selective media throughout.

2.3 EV isolation by dUC

Cells were seeded in 150 cm^2 polystyrene dishes (Corning, NY, USA). After 24h, cells were washed with PBS and medium was replaced for OptiMEM (Life Technologies) or DMEM (Life Technologies) supplemented with 10% HI FBS (Life Technologies) depleted of EVs. EVs were removed by overnight centrifugation at 110,000 x g. Condition medium (CM) was collected 48h after media exchange when cells had reached 90 -100 % confluency. First, CM was spun at 2,000 x g for 10 minutes to remove cells and cell debris. Microvesicles (MV) were isolated by centrifugation at 10,000 x g for 30 minutes, and subsequently washed by resuspending the pellet in 25 mL of PBS (Life Technologies) and centrifugation at 10,000 x g for 30 minutes. EXOs were isolated by centrifugation of the 10,000 x g supernatant for 70 minutes at 110,000 x g, and subsequently washed by resuspending the pellet in 25 mL of PBS (Life Technologies) and centrifugation at 110,000 x g for 70 minutes. For EV isolation from plasma, whole blood from healthy volunteers was collected in vacuum tubes containing trisodium citrate (final concentration 0.32% (w/v)) and centrifuged twice for 10 min at 2000 x g at room temperature to generate platelet-free plasma. Procedures were approved by the University Medical Center Utrecht Ethical Committee. Plasma was diluted six times in PBS, and MVs and EXOs were

isolated as above. All ultracentrifugation steps were performed using the Beckman Coulter (Brea, CA, USA) Type 55.2 Ti rotor (k factor 64) at 4℃.

2.4 EV isolation by SEC

Cells were handled as described under 'EV isolation with dUC'. EXOs were isolated as previously described (Nordin et al. 2015 (109)). Briefly, the 10,000 x g supernatant was concentrated with 100 kDa molecular weight cut-off Amicon centrifugal filter units (Merck Millipore, Billerica, Massachusetts, USA) to 1.0 mL and subsequently loaded on a HiPrep Sephacryl S-400 HR 16/60 size exclusion chromatography column (GE Healthcare, Buckinghamshire, UK) connected to the ÄKTA prime system (GE Healthcare), and eluted at 0.5 ml/min flow rate using PBS as the eluent. Chromatogram was recorded using absorbance at 280 nm. 2.0 mL fractions were collected, and EV-containing fractions were pooled and concentrated with 10 kDa molecular weight cut-off Amicon centrifugal filter units (Merck Millipore).

2.5 Sucrose density gradient

EXOs were either covered with (=bottom loading/upward displacement) or loaded on top of a discontinuous sucrose step-gradient ranging from 2.5 – 0.4M sucrose (Sigma) in HEPES buffer pH 7.4 (Sigma), and centrifuged at 200,000 x g for 16 hours (unless otherwise indicated) in a SW41 swinging bucket (Beckman) at 4 ℃. After centrifugation, 1.0 mL fractions were collected and each fraction was weighed to determine its density. The low density exosome subpopulation (LD-Exo) was obtained by pooling sucrose fractions 3-5, the high

density subpopulation (HD-Exo) was obtained by pooling sucrose fractions 8-9. Pooled fractions were diluted in PBS and placed on a SSL4 See-saw rocker (Stuart, Staffordshire, UK) at 4℃ for 24 h. EXOs were collected by centrifugation at 110,000 x g for 70 minutes.

2.6 EXO fractionation by HR-SEC

Eluted SEC fractions containing EXOs (i.e. unfractionated exosomes (EXO)) were pooled, mixed, and subjected to fractionation through high resolution size exclusion chromatography (HR-SEC). For this purpose a XK 16/70 SEC column (GE Healthcare) packed with Sephacryl® S-1000 Superfine SEC medium (GE Healthcare) was used. Elution was performed in PBS, at a flow rate of 0.5 mL/min, and monitored through absorbance at 280 nm. A representative elution profile is shown in Supp). Thirty individual HR-SEC fractions of 4.0 mL were collected using a fraction collector (F9-R Ge Healthcare), and stored at 4℃. Representative elution profile is shown in Supplementary. Fig. S 3.2. Required concentration of fractions was performed using 10 kDa centrifugal filters (Amicon Ultra-2).

2.7 EXO fractionation by AF4

EXOs were isolated from HEK293 - αCD19- 6C11 and HEK293 - αCD22 - RFB4 cells as described under ‘EXO isolation’ and subsequently labelled with NHS-Alexa647 as described under ‘Labelling of isolated exosomes’. Isolated and Alexa647 – labelled - EXOs were fractionated according to the protocol published by Zhang et al. Protocol Exchange (A protocol for Asymmetric-Flow Field-Flow Fractionation (AF4) of small extracellular vesicles - Haiying Zhang & David

Lyden (149)). Fractions containing large EXOs (Exo – L), small EXOs (Exo – S), and exomeres were pooled identical to Zhang et al. and concentrated using 10 kDa centrifugal units. Fractionation and collection was performed at room temperature.

2.8 Nanoparticle tracking analysis

Nanoparticle tracking analysis (NTA) was performed with a NS500 nanoparticle analyser (NanoSight, Malvern, Worchestershire, UK). Camera level was set at 14 for all recordings. Camera focus was adjusted to make the particles appear as sharp individual dots. Three 30-second videos were recorded for each sample with a delay of 7 seconds between each recording. All post-acquisition functions were set at automatic, except detection threshold, which was set at 4.

2.9 Tunable resistive pulse sensing

TRPS measurement was performed on a qNano gold (Izon science, Christchurch, New Zealand), making use of a NP150 nanopore (Izon science). Calibration using carboxylated polystyrene particles CPC100 calibration particles (Izon science) was performed prior to measurement of samples. All reagents and diluents were 0.22 µm filtered before application. The Data was analysed and processed making use of Izon Control Suite version 3.3.

2.10 Immunoblotting

Samples were resuspended in Laemmli sample buffer (Bio-Rad, Hercules, CA, USA) with freshly added β-mercaptoethanol (5 % (v/v)) (Sigma). Samples were subsequently heated for 10 minutes at 95 ℃ and separated on a 1.5 mm, 10% SDS (Sigma) polyacrylamide gel alongside a molecular weight marker (Rainbow Protein Marker, Coloured, GE Healthcare). Blotting was performed on an Immobilin®-FL membrane (Merck Millipore). Membranes were blocked in 5% skimmed milk in TBST 1% for 1 hour, primary antibodies (mouse anti-Alix (Abcam, ab117600, Cambridge, UK) at 1:1000, rabbit anti-TSG101 (Abcam, ab30871) at 1:1000, rabbit anti-alpha actinin 4 (Abcam, ab137564) at 1:500, rabbit anti-cyclin Y (Abcam, ab114186) at 1:500 and rabbit anti-Eph receptor A2 (Abcam, ab5387) at 1:1000), mouse anti-syntenin (Origene, TA50479) at 1:1000, rabbit anti-CD81 (Santa Cruz Biotechnology, sc-9158) at 1:500, rabbit anti-CD63 (Santa Cruz Biotechnology, sc15363) at 1:500, mouse anti-CD9 (Santa Cruz Biotechnology, sc-13118) at 1:500, rabbit anti-calveolin-1 (Cell Signalling Technology, 3238S) at 1:500, rabbit anti-calnexin (Abcam, ab22595), anti-c-Myc (Abcam, ab56), and anti-beta tubulin (Abcam, ab6046) were incubated overnight in 5% skimmed milk in TBS-Tween 1% at 4 ℃. After incubation, membranes were washed three times in TBS-Tween 1% for 10 minutes at RT. Membranes were subsequently probed with IRDye® 680RD Goat anti-Rabbit (Li-Cor, Nebraska, USA) or IRDye® 800CW Goat anti-Mouse (Li-Cor) at 1:10,000 in TBS-Tween 1% with 0.01% SDS for 2 hours at RT. After incubation, membranes were washed three times in TBS-Tween 1% for 10 minutes at RT and imaged on an Odyssey FC Imager (Li-Cor). Alternatively, membranes were incubated with secondary HRP-labelled antibodies anti-rabbit (Promega, W401B) or anti-mouse (Promega,

W402) at 1:5.000 in TBS-T with 0.01% SDS for 1 hour at RT. After incubation, membranes were washed two times with TBS-T for 15 minutes and once with TBS for 15 minutes. Proteins were detected with Clarity™ Western ECL Substrate (Bio-Rad), detection was performed with Odyssey FC Imager (Li-COR).

2.11 Dot blot

For dot blot analysis a Minifold Dot Blot Apparatus (GE Healthcare) was used at room temperature according to manufactures' instructions. Samples were blotted onto a nitrocellulose membrane (0.2 µm pore size) (Bio-Rad, Hercules, CA, USA) which was pre-wetted for 5 minutes in TBS. Prior to blotting samples were lysed using RIPA buffer (Merck Millipore, Billerica, Massachusetts, USA) including protease inhibitors (cOmplete™, Mini, EDTA-free Protease Inhibitor Cocktail, Roche, Penzberg, Germany) and were heated for 5 minutes at 95 °C. Samples were allowed to cooled down to room temperature and subsequently allowed to blot under gentle vacuum. After the entire volume had ran through the membrane was taken out off of the dot blot Apparatus and blocked overnight with Odyssey blocking buffer (Li-COR, Nebraska, USA) at 4 °C. Incubation with primary and secondary antibodies, and detection of signal was performed as described under '2.10 Immunoblotting'.

2.12 NanoLC-MS/MS Proteomic analysis

Purified EVs were lysed with 1% SDS, 25 mM HEPES, 1 mM DTT. Lysates were heated to 95°C for 5 min followed by sonication for 1 min and centrifugation at 14,000g for 15 min. The supernatant was mixed with 1 mM DTT, 8 M urea, 25

mM HEPES, pH 7.6 and transferred to a 10-kDa cut-off centrifugation filtering unit (Pall, Nanosep®, NY, USA), and centrifuged at 14,000g for 15 min. Proteins were alkylated by 50 mM iodoacetamide (IAA) in 8 M urea, 25 and centrifugations with 8 M urea, 25 mM HEPES. Trypsin (Promega) in 250 mM urea, 50 mM HEPES was added to the cell lysate at a ratio of 1:50 trypsin:protein and incubated overnight at 37°C. The filter units were centrifuged at 14,000g for 15 min followed by another centrifugation with MQ and the flow-through was collected. Peptides were cleaned by a strata-X-C-cartridge (Phenomenex).

Before analysis on the Q Exactive (Thermo Fischer Scientific, San Jose, CA, USA), peptides were separated using an Ultimate 3000 RSLCnano system. Samples were trapped on an Acclaim PepMap nanotrap column (C18, 3 µm, 100Å, 75 µm x 20 mm), and separated on an Acclaim PepMap RSLC column (C18, 2 µm, 100Å, 75 µm x 50 cm), (Thermo scientific). Peptides were separated using a gradient of A (5% DMSO, 0.1% FA) and B (90% ACN, 5% DMSO, 0.1% FA), ranging from 6 % to 37 % B in 240 min with a flow of 0.25 µl/min. The Q Exactive was operated in a data dependent manner, selecting top 10 precursors for fragmentation by HCD. The survey scan was performed at 70.000 resolution from 400-1600 m/z, with a max injection time of 100 ms and target of 1 x 106 ions. For generation of HCD fragmentation spectra, a max ion injection time of 140 ms and AGC of 1 x 105 were used before fragmentation at 30% normalised collision energy, 35.000 resolution. Precursors were isolated with a width of 2 m/z and put on the exclusion list for 70 s. Single and unassigned charge states were rejected from precursor selection.

Peptide, protein identification and data analysis. Proteome discoverer 1.4 with SequestHT was used for protein identification. Precursor mass tolerance was set

to 10 ppm and for fragments to 0.02 Da. Oxidised methionine was set as dynamic modification, and carbamidomethylation as static modification. Spectra were matched to a mus musculus, Ensembl 75 database, supplemented with the 250 most abundant bos taurus proteins from FBS, and results were filtered to 1% FDR. Identifications in bos taurus were considered to originate from FBS and removed. Protein areas were normalised to the median between each replicate to account for uneven peptide loading. Proteins were considered identified if they had quantifiable protein area in 2 or more of the 3 biological replicates. GO term enrichment analysis was done using Panther (Huaiyu Mi, Anushya Muruganujan and Paul D. Thomas, Nucl. Acids Res. (2012)).

2.13 Transmission Electron Microscopy

10 µL of MV or EXO suspension was added onto formvar-carbon coated electron microscopy grids (Agar Scientific, Elektron Technology UK Ltd, Essex, UK) for 20 min. The grid was blotted dry with filter paper and 15 µL of 2% uranyl acetate Sigma) was added on the grid for 1 minute. Next, uranyl acetate was removed and 15 µL of distilled water was added for 1 minute. The water droplet was then removed and the grid was left to air dry for 15 minutes. The grids were then visualised using a transmission electron microscope (JEM-1010, JEOL Ltd, Tokyo, Japan).

2.14 RNA extraction and profiling

RNA was extracted using TRIzol®-LS Reagent (Life Technologies) according to manufacturer's instructions. Isolated RNA was resuspended in RNase free water

and RNA yield was determined with Quant-iT™ RiboGreen® RNA assay (Life Technologies) according to the manufacturer's protocol. Quality and size of RNA in EXOs were determined using capillary electrophoresis with the Agilent RNA 6000 Pico kit and Agilent RNA small RNA kit on an Agilent 2100 Bioanalyzer® (Agilent Technologies, Santa Clara, CA, USA) according to the manufacturer's protocol.

2.15 Gene array

H5V cells were seeded in 24 well plates at a density of 60,000 cells per well in DMEM (Life Technologies) supplemented with 10% FBS depleted of serum EVs. After 24 h, cells were incubated with LD-Exo or HD-Exo isolated from ~500 mL conditioned medium, at a concentration of 15 µg/mL (or 30 µg/mL for RT-qPCR validation) or PBS for 24 h. Cells were washed three times with PBS, and RNA was isolated using RNeasy Mini Kit (Qiagen, Hilden, Germany) according to the manufacturer's protocol, Isolated RNA was resuspended in Nuclease free water (Life Technologies) and RNA yield was determined using the NanoDrop 2000 UV-Vis Spectrophotometer (Thermo Scientific). The RNA quality was assessed using Agilent 2100 Bioanalyzer® (Agilent Technologies, Santa Clara, CA, USA). 100 ng of total RNA was run for each sample on Mouse Gene ST 2.1 Array plates (Affymetrix, Santa Clara, CA, USA). Labelling and hybridisation were performed according to standard Affymetrix protocols at the Bioinformatics and Expression Analysis (BEA) core facility, at Novum, Huddinge, Sweden. The processing and data analyses were performed in Affymetrix Expression Console Software. The arrays were analysed using Median Polish, RMA background correction and

Sketch-Quantile normalisation (RMA-Sketch in Expression Console Software). Only the signals from the probe sets in the main category were used. If a probe set signal was below 20 in all the groups, it was removed. False Discovery Rate (FDR) estimations were done calculating q values (qvalue R package) from the p-value lists. The criterion for differentially expressed transcripts was set to $q < 0.15$. The microarray data are accessible through GEO (GSE72351). To analyse whether certain gene ontology (GO) terms were enriched among the genes that were differentially regulated by LD-Exo and HD-Exo treatment, we used the PANTHER Gene Ontology Classification System tool. We calculated fold changes in gene expression between samples treated with LD-Exo and HD-Exo, and subjected these data to statistical enrichment analysis using the Mann-Whitney test39. The Mann-Whitney test is a rank-sum test that compares whether the distribution of LD-Exo/HD-Exo fold-change values of a given GO term is statistically different to the distribution of all fold-change values in the data set. If the genes of a given GO term are sampled in a statistically significant manner from among the higher ranking genes of the distribution of all fold-change values, the given GO term is said to be “statistically enriched/upregulated” (+) in the dataset. Accordingly, vice versa, when genes of the GO term are sampled from among the lower ranking genes, the GO term is said to be “statistically de-enriched/downregulated” (-) in the dataset. The results include also the number of genes (#) belonging to those GO terms. Note that the Mann-Whitney test compares the distributions of gene expression fold-changes, and not the expression level of individual genes separately. For selected genes, changes were validated with RT-qPCR. cDNA was synthesised from 200 ng RNA using a High Capacity cDNA Reverse Transcriptation Kit (Life Technologies) according

to the manufacturer's protocol. 1/50th of the obtained cDNA was used for each qPCR reaction. Reactions were performed in triplicate using TaqMan® Fast Universal PCR Master Mix (Life Technologies) and the StepOnePlus™ Real-Time PCR System (Life Technologies). Gene expression analysis was performed using the Pfaffl method in order to account for qPCR efficiency (150), whereas the qPCR efficiency was determined by LinRegPCR software. Gene expression levels were normalised to GAPDH.

2.16 Migration assay

HMEC-1 cells (60,000 cells/well) were seeded in 96-well IncuCyte® ImageLock Plates (Essen BioScience) and cell were starved by replacing the medium with MCDB 131 medium not containing supplements. Scratches in the confluent cell monolayer were made with a Woundmaker 96 (Essen BioScience) and detached cells were washed away. Subsequently, the cells were treated in triplicate and migration of the cell monolayer was followed over time using IncuCyte ZOOM (Essen BioScience), which was set to take images every hour. Migration was quantified by making use of an ImageJ plugin kindly written by Oliver Gerrit De Jong.

2.17 Proliferation assay

SKOV-3 cells were seeded in a 96-well plate at a concentration of 2,000 cells/well in DMEM supplemented with 10% FBS and antibiotics. 24 h after seeding the medium was replaced for DMEM medium supplemented with 0.5 % FBS and antibiotics. Cells were incubated with 1.0 µg/mL SKOV3 EXOs treatments, 1.0 µg/mL BSA (negative control), or 1.0% FBS (positive control). Cells were

incubated for 48 h, and proliferation was followed over time using the IncuCyte (Essen BioScience) set to take photos every 4 h, rate of proliferation was calculated with built-in software.

2.18 Adhesion assay

Samples were coated onto 96 - well plates (Greiner) overnight at 4 °C, protein from the non-EXO fraction was coated as a negative control (all 1.0 µg per well). Wells were washed with PBS to remove any unbound sample, and subsequently blocked with PBS + 1.0% BSA for 2 hours. SKOV3 cells were washed with PBS, trypsinised, and resuspended in DMEM (without supplements) to create a cell suspension with a final concentration of 200,000 cells/mL. 100 uL of this cell suspension was added to each well and left to incubate and adhere for 30 minutes. Where indicated incubation was performed in presence of mAb Lia1/2, which was kindly provided by Dr. Carlos Cabanas. Each well was subsequently washed three times with PBS to remove any unadhered cells. Images were taken on an EVOS FL Cell Imaging System (ThermoFisher) to evaluate level of adhesion, number of adhered cells were quantified using ImageJ – Analyze Particles.

2.19 Labelling of isolated EVs

Alexa Fluor™ 647 NHS Ester (Thermo Fisher Scientific) was dissolved in DMSO at a final concentration of 10 mg/mL (=stock), 5 µL aliquots were stored at – 20 °C in presence of desiccants in a well closed container to prevent hydrolysis. Isolated EXO were diluted in PBS to a concentration of 200 µg/mL in 100 µL, and subsequently 1 µL Alexa647 NHS stock was added. This mixture was incubated

for 2 h at 37 °C under gentle shaking. Labelling was followed by purification through three successive Zeba Spin Desalting Columns (0.5mL, 4K MWCO, Thermo Fisher Scientific) to remove free dye. Zeba spin columns were used according to the manufacturer's instructions. A "Free dye" control sample that contained the same amount of Alexa647 NHS stock in PBS was used as a control.

2.20 Uptake microscopy

For microscopy, cells were seeded at 20,000 cells per well into black 96 well Greiner µClear plates (Greiner Bio-One #655946) and treated as described previously. Following treatment, cells were fixed for 10 minutes at room temperature using 4% paraformaldehyde (Thermo Fisher Scientific) diluted into PBS containing Hoechst 33342 (Thermo Fisher Scientific) at 1µg/ml for labelling of nuclei. Plasma membrane was labelled using CellMask Green (Thermo Fisher Scientific) diluted into PBS/0.1% TritonX-100 added to fixed cells for 20 minutes at room temperature before being washed three times with PBS. If images were not acquired immediately, plates were stored at 4°C until acquisition. Four images per well were acquired using a 20x objective (NA 0.75) on a Molecular Devices ImageXpress Micro XLS widefield High Content microscope. Images were analysed using the MultiWaveLength Cell Scoring application module built into the MetaXpress analysis software (Molecular Devices).

3 Results 1

Cells release distinct exosome subpopulations

Abstract

According to current conventional understanding cells seem to release three major extracellular vesicle populations: apoptotic bodies, microvesicles and exosomes. Despite their proposed homogenous characteristics, exosomes have been reported to mediate a plethora of biological functions. Leading on from this, we hypothesised the existence of subpopulations of exosomes with unique molecular compositions and inherent biological properties. Fractionation of melanoma exosomes using sucrose density gradient centrifugation allowed for detection of two distinct subpopulations, differing in biophysical properties, protein composition, and RNA cargo. The subpopulations were found to mediate differential effects on gene expression in recipient endothelial cells.

Presented findings highlight the heterogeneous nature of exosomes, and confirm the release of distinct exosome subpopulations with unique effects on recipient cells. Gaining a better insight into exosome heterogeneity will advance our understanding of exosomal biology in health and disease and benefit development of exosome-based diagnostics and therapeutics.

3.1 Introduction

As outlined in detail in chapter one of this thesis, EVs are heterogeneous populations of endogenous nano-sized cell-derived membrane vesicles released by eukaryotic and prokaryotic cells (133). Although there is ongoing discussion in the field, the field has categorised EVs into three main populations, mainly based on their biogenesis pathways: exosomes, microvesicles and apoptotic bodies (26,151).

In short, Microvesicles (MVs) range in size from 50 nm to 1,000 nm in diameter and originate directly from the cell surface, where they are released by outward budding of the plasma membrane. Apoptotic bodies, only formed by cells undergoing apoptosis, are released through outward blebbing and fragmentation of the cell membrane of apoptotic cells. APOs have a broad size range of 50–2,000 nm in diameter.

EXOs have an endolysosomal origin and are formed as intra luminal vesicles (ILVs) within multivesicular bodies (MVBs). They are released as EXOs by cells upon fusion of MVBs with the plasma membrane (40). In contrast to MVs, EXOs are presumed to represent a more homogenous population of EVs, ranging in size from 30 nm to 120 nm in diameter. Interestingly, a wide spectrum of effects from EXOs on recipient cells have been described, despite their seemingly homogenous characteristics. This finding could indicate that either each individual exosome has multiple functional effects, or cells release unique subpopulations of EXOs which display distinct compositions and related functions. Studies on EXO cargo (23), and MVB sorting mechanisms highlight the potential heterogeneous nature of EXOs (47,107,152,153).

Alterations in exosome release, resulting in increased release of specific subpopulations have been reported as well (154,155).

Aforementioned observations support the idea that EXOs represent a heterogeneous population of EVs. Throughout this chapter we describe findings providing more evidence for the heterogeneous nature of EXOs. On top of that we show that cells release distinct subpopulations of EXOs. As described EXO subpopulations were isolated from different cell lines, with detailed characterisation being performed on B16F10 mouse melanoma cell-derived EVs. Biophysical characteristics, composition, and cargo of the B16F10 subpopulations were studied in detail. Leading on from observed differences we further evaluated whether EXO subpopulations have different biological effects on recipient cells. The results from this work may have important implications for future studies on EXO biology and (patho)physiology. Furthermore it can potentially benefit development of exosome-based biomarkers and therapeutics, as shown in Chapter 4 of this thesis.

3.2 Results

3.2.1 Heterogeneity of isolated EXOs

EV populations, MVs and EXOs, were isolated from conditioned medium (Opti-MEM 48 h) of B16F10 melanoma cells by differential ultracentrifugation (dUC). A schematic overview of the isolation protocol including wash steps is shown in Figure 3.1A EXOs (P110) were subsequently subjected to sucrose density gradient centrifugation (DG). It has previously been shown that DG allows for fractionation of EXOs and separation of EXO subpopulations (23,105,107). When the common approach of downward displacement or top loading of P110 was taken, we detected the vast majority of particles, as well as the EXO marker proteins ALIX and TSG101 in sucrose fractions 3 -5 (Fig. 3.1B). This finding corresponds to the originally proposed density of EXOs, ranging from 1.12–1.19 g/mL (11). Interestingly and in contrast with this finding, upward displacement or bottom loading of P110, allowed for detection of two distinct particle populations, in both of which ALIX and TSG101 were detected (Fig. 3.1C). One population was recovered from the lower density sucrose fractions 3–5 (LD-Exo), while the second population associated with the higher density sucrose ranging from 1.26–1.29 g/mL (i.e. fractions 8–9 or HD-Exo).

Immunoblot and proteomic analysis showed the presence of common EXO marker proteins (e.g. ALIX, CD63, CD81, and CD9) and absence of the endoplasmic reticulum proteins calnexin and GP96 (Supplementary Fig. S 3.1A) in both LD-Exo and HD-Exo compared to MVs.

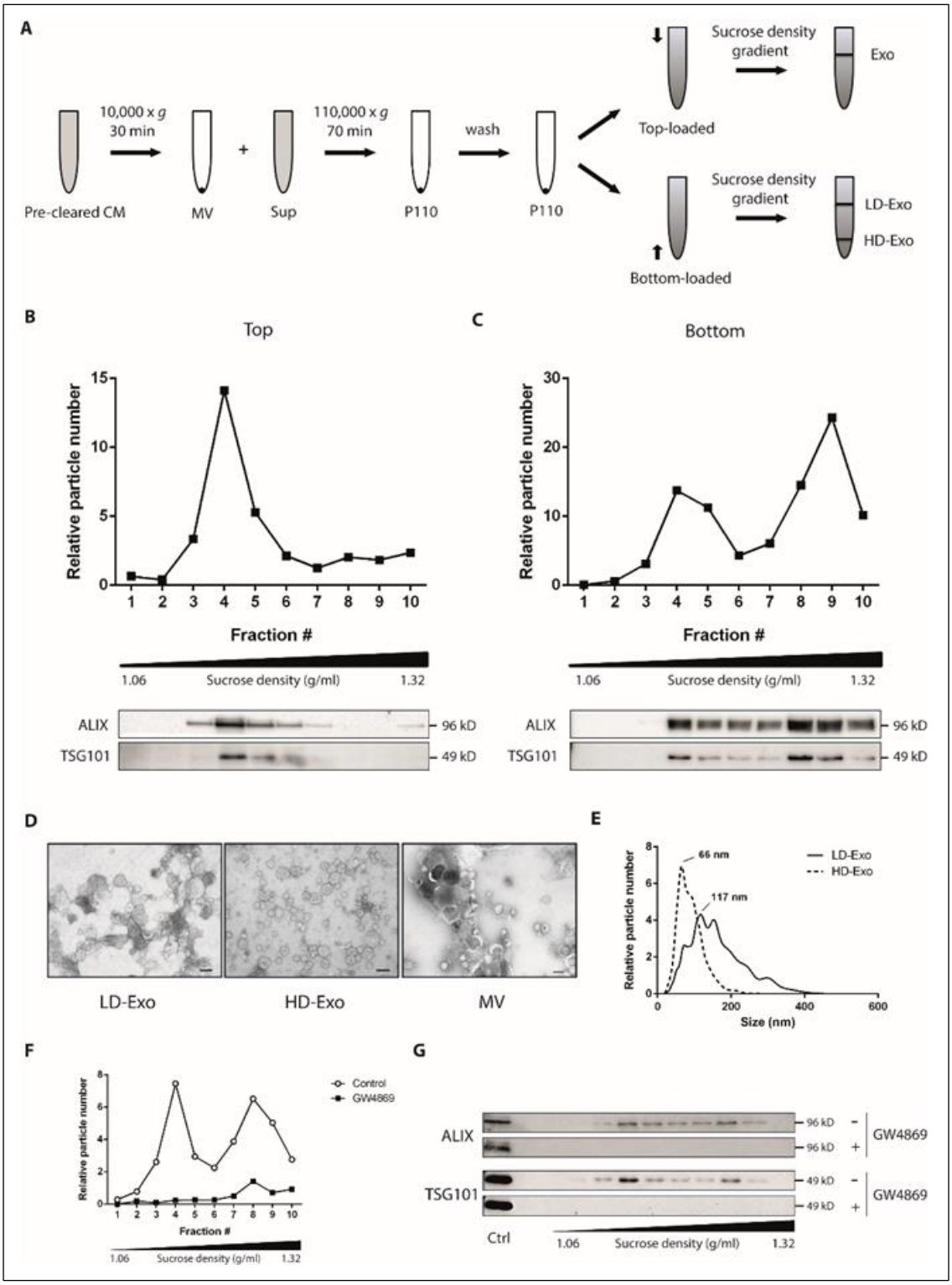

A
10,000 x g
30 min
110,000 x g
70 min
wash
Pre-cleared CM
MV
Sup
P110
P110
Top-loaded
Bottom-loaded
Sucrose density gradient
Exo
LD-Exo
HD-Exo
B
Top
C
Bottom
Relative particle number
Fraction #
1.06
Sucrose density (g/ml)
1.32
ALIX
TSG101
96 kD
49 kD
D
LD-Exo
HD-Exo
MV
E
66 nm
117 nm
LD-Exo
HD-Exo
Size (nm)
F
Control
GW4869
G
GW4869
Ctrl

Figure 3.1 B16F10 melanoma cells release EXO subpopulations with distinct biophysical characteristics and composition (A) Overview of isolation protocol used to obtain MV and EXO subpopulations (B,C) P110 was loaded on top (B) or at the bottom (C) of a sucrose density gradient and subjected to ultracentrifugation for 16 h. The resulting fractions (1–10) with increasing density were analysed for particle number by NTA (upper panels) and the presence of EXO marker proteins ALIX and TSG101 by Western blotting (lower panels). For Western blots, an equal volume of each sample was analysed. Fractions 3–5 (LD-Exo) and 8–9 (HD-Exo) were pooled for further analysis. (D) EXOs or MVs were negatively stained with uranyl acetate and visualised by transmission electron microscopy. Scale bars represent 100 nm. (E) Size distribution profiles as determined by NTA. Data shown are representative of three independent experiments. (F, G) EXOs from B16F10 melanoma cells cultured for 48h in the absence or presence of 7.5 μM GW4869 were isolated as in Fig. 3.1A. P110 was loaded at the bottom of a sucrose gradient and subjected to ultracentrifugation for 16 h. The resulting fractions (1–10) with increasing density were analysed for particle number by NTA (F) and the presence of exosome marker proteins ALIX and TSG101 by western blotting (G). A control sample (Ctrl) was included to show consistent analysis across the membranes. For western blots, an equal volume of each sample was analysed.

Similar findings were made when P110 was isolated from B16F10 melanoma cells cultured under regular conditions (i.e. presence of EV-depleted 10% FBS instead of serum starvation using Opti-MEM), ruling out the that observed difference in EXO flotation behaviour resulted from differences in culture conditions (Supplementary Fig. S 3.2A).

Both upward and downward displacement of P110 for 72 h resulted in both particles as well as EXO markers ALIX and TSG101 ending up in fractions 3–5, which suggests that both populations equilibrate at the same density of 1.12–1.19 g/ml, but HD-Exo display delayed flotation behaviour (Supplementary Fig. S 3.3A).

dUC has been found to affect EV integrity and subsequent activity (108,109). To rule out the possibility that LD-Exo and HD-Exo were an artefact of the ultracentrifugation method, we also employed ultrafiltration followed by size-exclusion chromatography (UF-SEC) for the initial EXO isolation prior to the DG experiment. Following upward displacement of UF-SEC-purified EXOs two distinct subpopulations could again be recovered (Supplementary Fig. S 3.2B).

Given the fact that sucrose exerts high osmotic pressure on isolated EXOs we wanted to exclude the possibility of this causing damage or changes in biophysical characteristics of EXOs, ultimately leading to differences in flotation behaviour. For this purpose the nonionic gradient-forming material Nycodenz was employed. Similar to sucrose this material allowed for formation of a density gradient with high density, however the osmolarity of Nycodenz solutions is considerably lower than that of sucrose. Importantly, also using a Nycodenz gradient, two distinct exosome subpopulations were clearly observed (Supplementary Fig. S 3.2C).

Study of the particle morphology using TEM analysis indicated that both LD-Exo and HD-Exo are spherical, membrane-encapsulated particles with a cup-shaped

appearance, characteristic of EXOs (Fig. 3.1D). In contrast, MVs represent a heterogeneous population of EVs, differing greatly in size, shape and electron-density. LD-Exo was found to contain particles in a size range of 75–200 nm, while particles in HD-Exo were found to be smaller and more homogeneous in size, with most vesicles smaller than 100 nm.

The aforementioned finding was confirmed by two additional techniques commonly used to characterize EVs, NTA and tunable resistive pulse sensing (TRPS). NTA showed distinct size distribution profiles for the LD-Exo and HD-Exo populations, with LD-Exo displaying a mode size of 117 nm and HD-Exo 66 nm (Fig. 3.1E). TRPS characterisation confirmed the difference in size distribution of LD-Exo and HD-Exo (Supplementary Fig. S 3.4), although the mode size of particles in both LD-Exo and HD-Exo was found to be slightly larger, 153 nm and 109 nm respectively.

To evaluate the role of the enzyme neutral sphingomyelinase (nSMase) and ceramide in the formation of both subpopulations of EXOs, B16F10 cells were treated cells with the nSMase inhibitor GW4869 (152). Based on the number of particles (Fig. 3.1F) and the expression levels of ALIX and TSG101 (Fig. 3.1G), release of LD-Exo was found to be almost completely inhibited after treatment with GW4869, whereas release of HD-EXO was partially reduced (approx. 80 %). This finding indicates that both EXO subpopulations are derived through a ceramide-dependent pathway, although some EXOs seem to be present in HD-EXO which are potentially derived from different pathways.

To confirm that the observed findings were not exclusive to B16F10 mouse melanoma cells, EXOs were isolated from multiple other cellular sources and subjected to the same upward displacement approach and characterisation by NTA and Western blotting. Although subtle differences were observed, two distinct subpopulations were detected in EXOs from all studies sources (i.e. N2a mouse neuroblastoma cells, A431 human squamous carcinoma cells, H5V mouse heart endothelial cells, MSC hTERT human immortalised mesenchymal stem cells, and human plasma), as shown in Fig. 3.2.

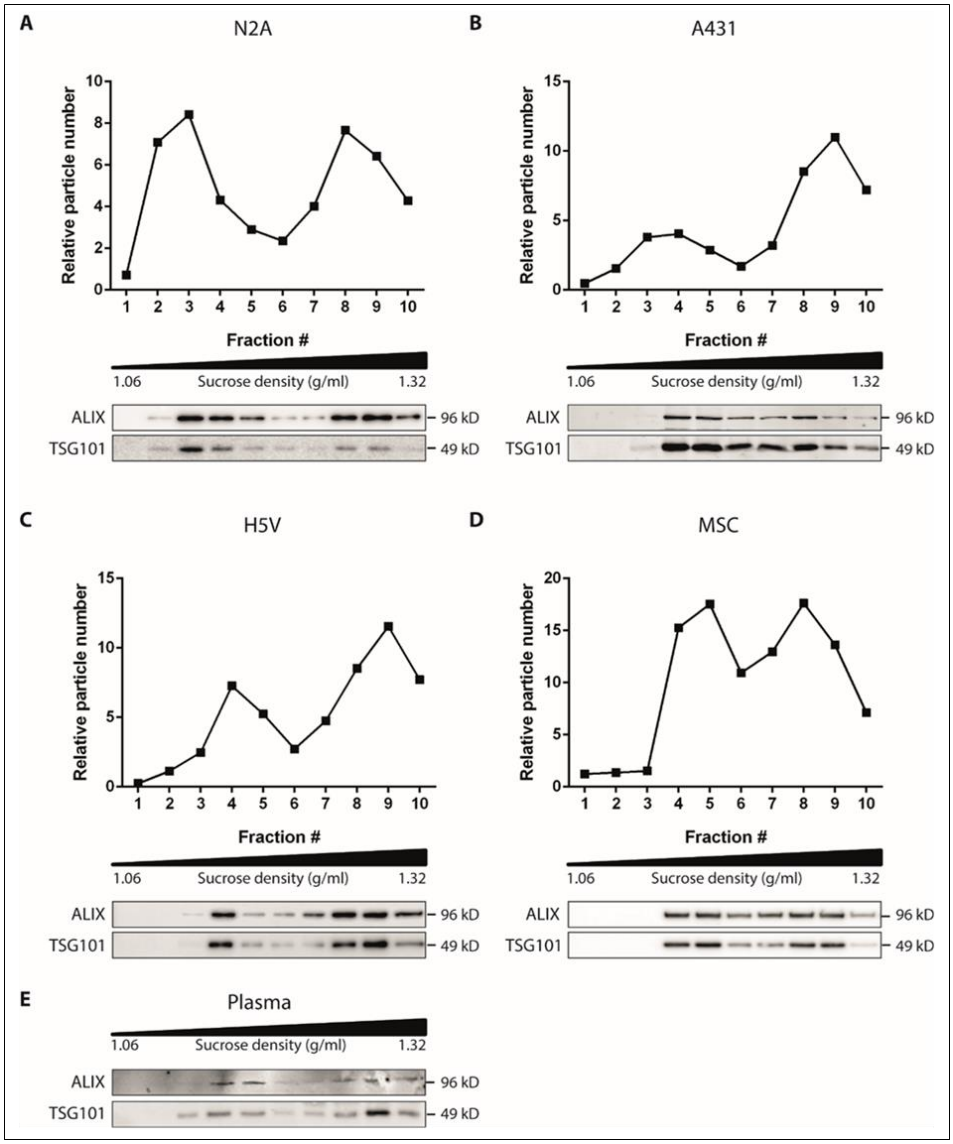


Figure 3.2 Release of LD-Exo and HD-Exo subpopulations is not unique for B16F10 melanoma cells. EXOs were isolated using dUC from other cell sources (N2a, mouse neuroblastoma cells; A431, human squamous carcinoma cells; H5V, mouse heart endothelial cells, MSC hTERT, human immortalised mesenchymal stem cells; and human plasma. Presence of LD-Exo and HD-Exo subpopulations after sucrose density gradient centrifugation was evaluated using NTA (upper panels) and presence of ALIX and TSG101 by western blotting (lower panels).

In summary, the aforementioned findings clearly demonstrate that cells release subpopulations of EXOs with distinct biophysical characteristics which can be separated through upward displacement in density gradient centrifugation.

3.2.2 EXO subpopulations have distinct protein compositions

We next set out to study the protein composition of MVs and EXO subpopulations released by B16F10 melanoma cells. Label-free mass spectrometry-based proteomics was performed in triplicate for LD-Exo and HD-Exo, and MVs. Good overlap in protein identification between replicates, and a median number of peptide spectrum matches (psms)/protein between 4 and 7 (Supplementary Fig. S 3.5) allowed for identification of 4421 proteins in total from all EV samples. Subsequently, a more conservative filtering was applied for quantification where proteins were considered detected if they were identified (1% FDR) and in at least 2 of the 3 replicates. Using this criterion, 1540 proteins were identified in all EV populations, and 533, 354 and 110 proteins were identified exclusively in MV, LD-Exo and HD-Exo, respectively. 769 proteins were identified in both MV and LD-Exo, while 183 proteins were identified in both LD-Exo and HD-Exo, and only 51 proteins in both MV and HD-Exo (Fig. 3.3A, B).

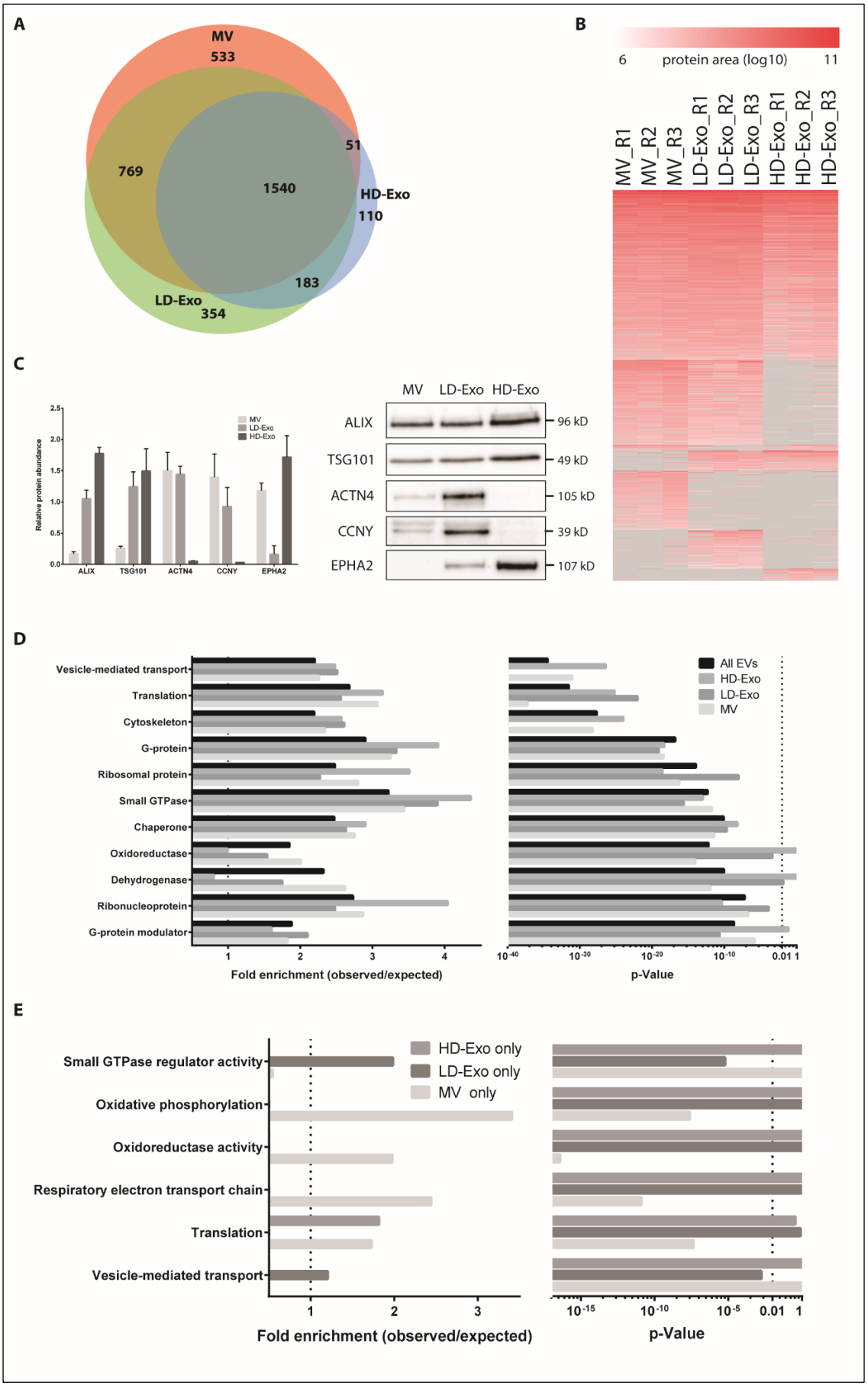

A
MV
533
769
1540
51
HD-Exo
110
183
LD-Exo
354
B
6
protein area (log10)
11
MV_R1
MV_R2
MV_R3
LD-Exo_R1
LD-Exo_R2
LD-Exo_R3
HD-Exo_R1
HD-Exo_R2
HD-Exo_R3
C
Relative protein abundance
MV
LD-Exo
HD-Exo
ALIX
TSG101
ACTN4
CCNY
EPHA2
MV LD-Exo HD-Exo
ALIX 96 kD
TSG101 49 kD
ACTN4 105 kD
CCNY 39 kD
EPHA2 107 kD
D
Vesicle-mediated transport
Translation
Cytoskeleton
G-protein
Ribosomal protein
Small GTPase
Chaperone
Oxidoreductase
Dehydrogenase
Ribonucleoprotein
G-protein modulator
Fold enrichment (observed/expected)
All EVs
HD-Exo
LD-Exo
MV
p-Value
E
Small GTPase regulator activity
Oxidative phosphorylation
Oxidoreductase activity
Respiratory electron transport chain
Translation
Vesicle-mediated transport
HD-Exo only
LD-Exo only
MV only
Fold enrichment (observed/expected)
p-Value

Figure 3.3 Proteome characterisation of MV and EXO subpopulations by nanoLC-MS/MS reveals differences in protein composition. (A) Overlap of identifications between MV, LD-Exo and HD-Exo. Proteins were considered identified if they had quantitative protein area in at least 2 of the 3 replicates. (B) Heatmap showing protein intensity (area) for each replicate. Subpopulations were grouped based on overlap in identifications as in (A), and subsequently ranked from highest to lowest average protein area. (C) Validation of proteomics data for selected proteins ALIX, TSG101, ACTN4, CCNY, and EPHA2 (left panel) by western blotting (right panel). Equal amounts of protein were analysed. (D) GO enrichments of all identified proteins and proteins identified in MV, LD-Exo and HD-Exo. (E) GO enrichments of proteins uniquely identified in MV, LD-Exo and HD-Exo.

Protein quantitation was found to correlate well between replicates (Supplementary Fig. S 3.6). Proteins common to all populations included suggested EV and exosome marker proteins ALIX, TSG101, CD9, CD81 and CD63, although their relative abundance was higher in the EXO subpopulations as compared to MV.

As shown in Fig. 3.3C a number of proteins were found to be enriched in EXOs and subpopulations LD-Exo and / or HD-Exo in particular. In accordance with the proteomic results, Western blotting confirmed that actinin alpha 4 (ACTN4) and cyclin Y (CCNY), were enriched in LD-Exo versus HD-Exo, and ephrin type-A receptor 2 (EPHA2) in HD-Exo versus LD-Exo (Fig. 3.3). A more stringent GO-enrichment analysis revealed differential enrichment patterns of proteins annotated to the PANTHER GO-Slim Cellular Component 'Late endosomal membrane' (Supplementary Fig. S 3.5).

Interestingly, after sucrose density gradient centrifugation for 72 h, EPHA2 was mainly detected in fractions 3–5 (LD fractions). The latter finding confirmed that particles present in the higher density sucrose fractions display delayed flotation behaviour (HD-Exo), but eventually equilibrate at a density of 1.12–1.19 g/ml (Supplementary Fig. S 3.2B).

Ultracentrifugation has been reported to compromise the integrity of isolated EVs (108). To rule out that observed subpopulations were the result of potential disruption of EV integrity, EVs were isolated following an optimised size exclusion chromatography (SEC) isolation approach. B16F10 P110 was fractionated using SEC, making use of a column packed with Sephacryl S-1000 resin which allowed for separation of EXOs into two fractions (Supplementary Fig. S 3.7A). Fraction

1, which contained larger EXOs, was found to be enriched for ACTN4 and CCNY, while fraction 2, which contained smaller EXOs, was enriched for EPHA2 (Supplementary Fig. S 3.7B,C). This further indicates that these proteins are indeed selectively enriched in large or small EXOs, respectively. Additionally, this finding confirms that the existence of LD-Exo and HD-Exo are not the result of influences exerted by density gradient medium (i.e. sucrose or Nycodenz) and overnight centrifugation. Selective enrichment of ACTN4 and CCNY in LD-Exo was also observed for EXOs isolated from H5V endothelial cells (EPHA2 could not be detected in H5V EXOs) (Supplementary Fig. S 3.8).

Differences in protein composition of the obtained vesicle populations suggested that LD-Exo and HD-Exo could have differences in functionality. We performed GO enrichment analysis in order to get insight into these potential differences. Four different protein lists were used for this analysis: (1) the full list of all identified proteins across EV populations, (2) MV, (3) LD-Exo and (4) HD-Exo protein identifications, compared to the whole proteome database (Fig. 3.3D). Commonly enriched terms in all 3 subpopulations included ‘vesicle mediated transport’, ‘translation’, ‘cytoskeleton’, ‘G-protein’, ‘ribosomal protein’, ‘small GTPase’ and ‘chaperones’, aligning with previous observations on exosome content analysis performed by members of the Wood lab. ‘Oxidoreductases’ and their subgroup ‘dehydrogenases’ were enriched in MV, and slightly enriched in LD-Exo but not in HD-Exo, potentially reflecting the presence of mitochondrial components in MV and LD-Exo. The terms ‘translation’, ‘ribonucleoproteins’ and ‘ribosomal proteins’ displayed higher enrichment in HD-Exo than in LD-Exo. ‘G-

proteins' were enriched in both HD-Exo and LD-Exo, while only LD-Exo reached significant enrichment for 'G-protein modulators'.

When looking at proteins considered unique in one of the EV subpopulations (Fig. 3.3A), LD-Exo showed enrichment in 'small GTPase regulatory activity' and 'vesicle mediated transport'. HD-Exo unique proteins did not show any enrichment in a GO-specific category. In contrast, MV unique proteins displayed enrichment in 'oxidoreductase', 'oxidative phosphorylation' and 'respiratory electron transport chain' (Fig. 3.3E). Analysis of uniquely identified proteins, using the functional enrichment analysis tool FunRich, highlighted potential differences in cellular origins. The cellular component 'mitochondrial' was found enriched in the MV-population. Cellular components 'cytoplasm and cytosol' were enriched in LD-Exo, whereas HD-Exo was enriched in the 'lysosome' component.

On the basis of these findings, LD-Exo and HD-Exo represent two distinct EXO subpopulations with unique protein compositions, both differing from larger MVs.

3.2.3 Exosome subpopulations have distinct RNA profiles

There is strong evidence for the role of EVs in the functional transfer of RNA species between cells. EVs can carry different RNA species, including mRNA (and fragments thereof), long and small non-coding RNA and ribosomal RNA (rRNA). However, the relative amounts vary depending on the EV source and methodology used to isolate EVs and analysis of data (22). To get a better insight into the distribution of different RNA species between B16F10 MVs and EXO subpopulations RNA was isolated and analysed by Bioanalyzer ®.

As shown in Fig. 3.4 the profiles for MVs and LD-Exo show high similarity. When analysed on an Agilent RNA 6000 Pico chip (left panel), three dominant peaks were observed for MV and LD-Exo, two of which corresponded to rRNA subunits 18S and 28S. The third peak was found at ~60 nt. In contrast, HD-Exo did not contain rRNA, and a broader RNA size distribution profile was observed in the range of 50–200 nt. On an Agilent RNA small RNA chip (right panel), again one dominant peak was observed at ~60 nt for MV and LD-Exo, while for HD-Exo, RNA sizes ranged from 30–150 nt. Although the RNA content profiles of the EV populations are very similar (in particular MVs and LD-Exo), the profiles of EXO subpopulations, indicate that LD-Exo and HD-Exo have a distinct RNA content.

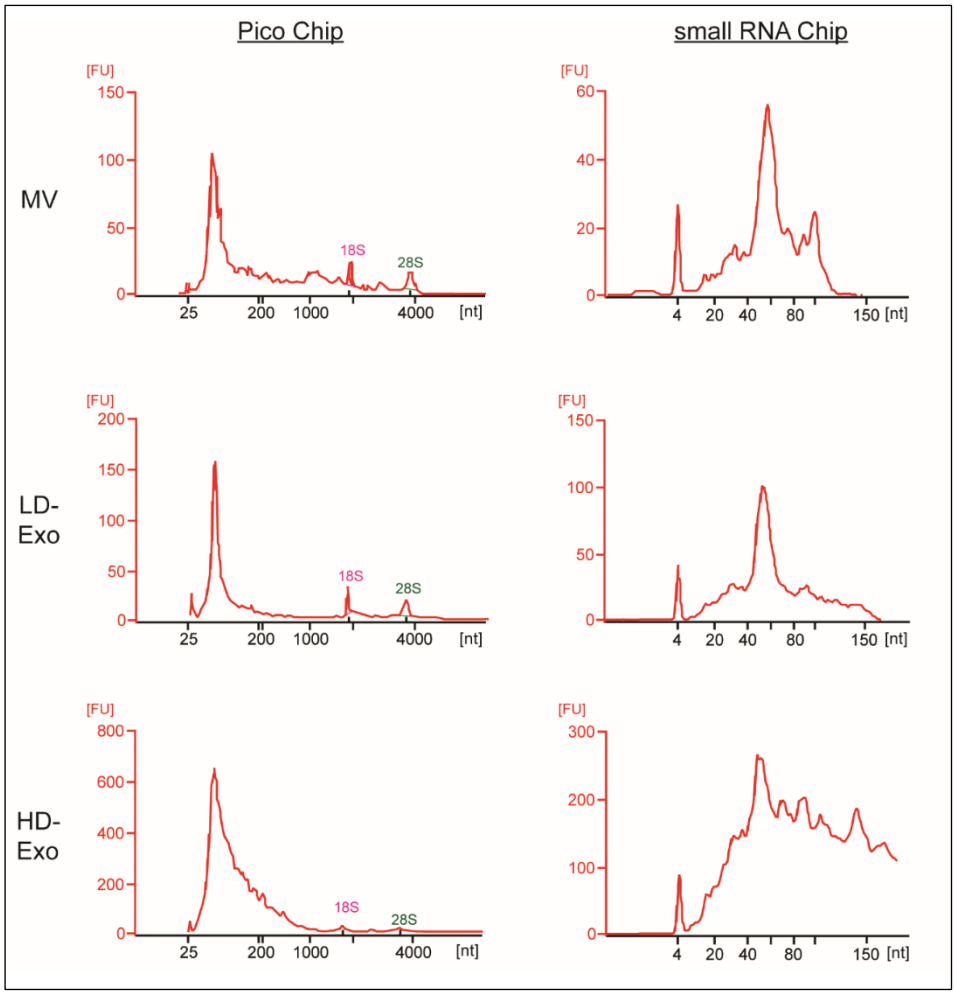
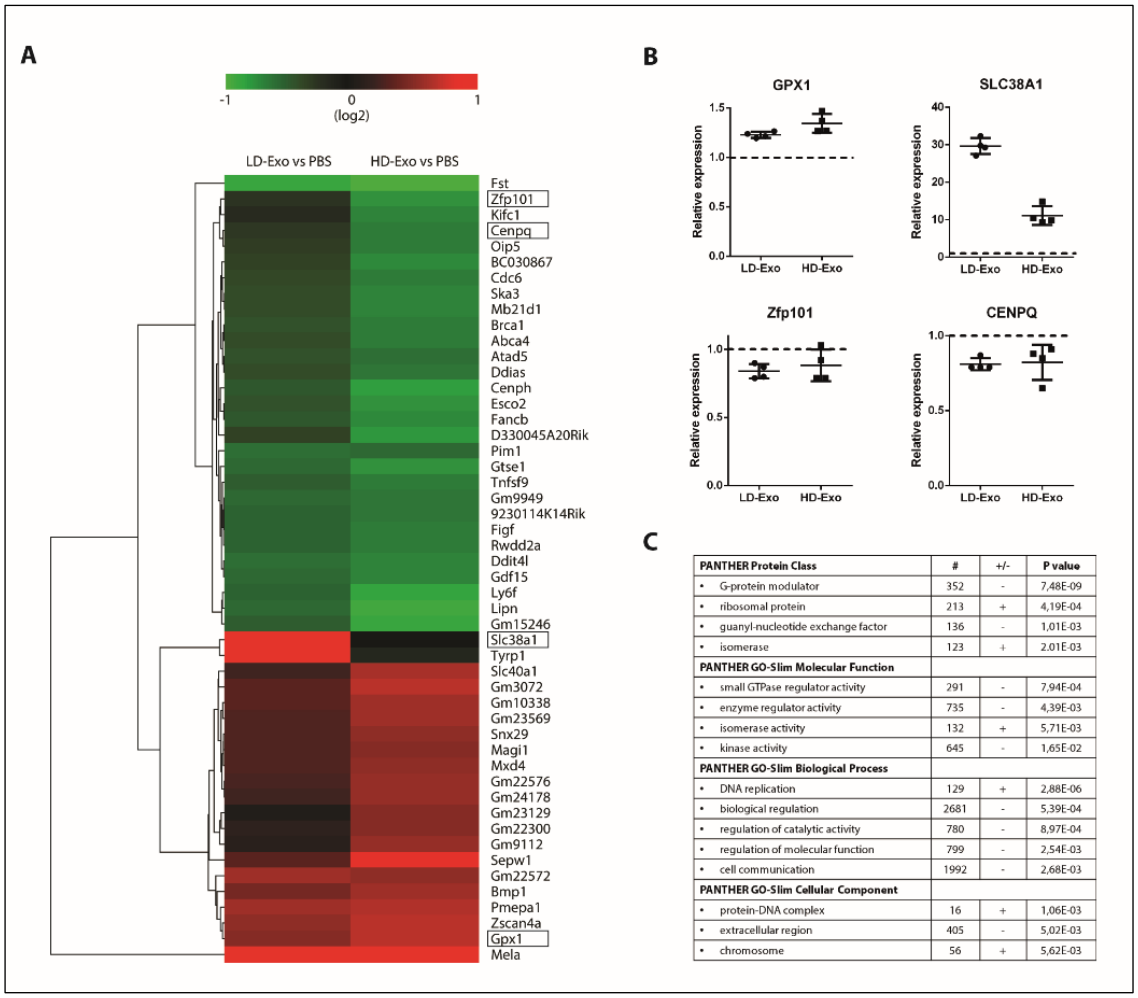


Figure 3.4 MVs and EXO subpopulations have different RNA profiles. RNA from MV, LD-Exo and HD-Exo was extracted using Trizol-LS and analysed using capillary electrophoresis with the Agilent RNA 6000 Pico chip (left panel) and Agilent small RNA chip (right panel) on an Agilent 2100 Bioanalyzer®. The y-axis of the electrophoretograms represents fluorescence units (FU) and the x-axis represents the nucleotide length of the RNA (nt). Peaks at 25 nt (left panels) or at 4 nt (right panels) represent internal standards. Data shown are representative of two independent experiments.

3.2.4 Exosome subpopulations differentially affect gene expression in recipient cells

Taken together the aforementioned findings indicate that LD-Exo and HD-Exo are biophysically distinct and have different protein and RNA compositions. We next examined whether these observed differences might result in differences in gene expression of recipient cells. Given the described role of tumour-derived EXOs on endothelial cells we decided to evaluate potential differences in effects of LD-Exo and HD-Exo on recipient H5V endothelial cells. H5V endothelial cells were exposed to EXO subpopulations for 24 h, and changes in the gene expression in the recipient cells were evaluated using a Genechip gene array. Overall, 257 and 1116 genes were found to be differentially expressed in endothelial cells after exposure to LD-Exo and HD-Exo, respectively, compared to control cells exposed to PBS.

As shown in Fig. 3.5A. 42 genes had a greater than 1.5-fold expression change upon exposure to either LD-Exo or HD-Exo (11 genes upregulated (red), 31 genes downregulated (green)).



PANTHER Protein Class	#	+/-	P value
• G-protein modulator	352	-	7,48E-09
• ribosomal protein	213	+	4,19E-04
• guanyl-nucleotide exchange factor	136	-	1,01E-03
• isomerase	123	+	2,01E-03
PANTHER GO-Slim Molecular Function			
• small GTPase regulator activity	291	-	7,94E-04
• enzyme regulator activity	735	-	4,39E-03
• isomerase activity	132	+	5,71E-03
• kinase activity	645	-	1,65E-02
PANTHER GO-Slim Biological Process			
• DNA replication	129	+	2,88E-06
• biological regulation	2681	-	5,39E-04
• regulation of catalytic activity	780	-	8,97E-04
• regulation of molecular function	799	-	2,54E-03
• cell communication	1992	-	2,68E-03
PANTHER GO-Slim Cellular Component			
• protein-DNA complex	16	+	1,06E-03
• extracellular region	405	-	5,02E-03
• chromosome	56	+	5,62E-03

Figure 3.5 EXO subpopulations have different effects on gene expression in recipient endothelial cells. LD-Exo and HD-Exo were isolated as depicted in Fig. 3.1A and incubated with H5V endothelial cells for 24 h. (A) Heat map displaying genes that were upregulated (in red) or downregulated (in green) in response to LD-Exo or HD-Exo exposure (> 1.5 fold change, q-value < 0.15). (B) RT-qPCR validation of array results making use of a new biological replicate. Transcript levels were measured relative to GAPDH and plotted relative to levels in PBS-treated cells. Dot plots represent mean ±SD. (n = 4). (C) Representative GO enrichments differentially regulated (upregulated (+), or downregulated (-)) by LD-Exo versus HD-Exo. #, number of genes.

The findings of the gene array were subsequently validated using RT-qPCR analysis on a number of genes. As shown in Fig. 3.4B. validation experiments confirmed upregulation of glutathione peroxidase 1 (GPX1) and downregulation of zinc finger protein 101 (Zfp101) and centromere protein Q (CENPQ) by both exosome types, and a much more pronounced upregulation of solute carrier family 38 member 1 (SLC38A1) by LD-Exo compared to HD-Exo.

GO statistical enrichment analysis on affected genes was performed in order to get an idea of the more global effects elicited by these two distinct EXO subpopulations. Several classes of genes were found to be differentially affected by the EXO subpopulations, most significantly PANTHER protein classes ‘G-protein modulator’ and ‘ribosomal protein’, GO molecular function ‘small GTPase regulator activity’ and ‘enzyme regulator activity’, GO biological process ‘DNA replication’ and ‘biological regulation’ and GO cellular component ‘protein-DNA complex’ and ‘extracellular region’ (Fig. 3.5C).

The observed differences in effects on endothelial gene expression and subsequent GO analysis indicate that B16F10 EXO subpopulations LD-Exo and HD-Exo display different effects on recipient endothelial cells.

3.3 Discussion and conclusion

EXOs are assumed to represent a homogenous population of EVs, and research has mainly focussed on comparing differences between the classic EV populations (i.e. EXOs, MVs, and APOs) (90,156,157). Here we describe findings indicating heterogeneity within the EXO population released by multiple cell lines and human plasma, and the existence of two distinct EXO subpopulations therein, which were found to have distinct protein and RNA compositions. Furthermore we observed differences in biological properties of B16F10 melanoma derived EXO subpopulations.

EXOs were isolated according to an elaborate dUC isolation protocol with multiple wash steps to ensure high purity. Isolated EXOs were subsequently fractionated by sucrose density gradient centrifugation, a method previously used by others to study the heterogeneity of EXOs (23,105,107).

Two distinct particle populations were observed within the ten sucrose fractions obtained after upward displacement of the isolated EXOs (Fig. 3.1C). Particles pooled from fractions 3–5 (LD-Exo) and 8–9 (HD-Exo) both expressed the EXO marker proteins ALIX and TSG101, displayed the typical cup-shaped morphology when observed with electron microscopy, and were formed through a ceramide-dependent pathway. Furthermore, both populations displayed the originally proposed equilibrium density for EXOs, respectably 1.12–1.19 g/ml. Taken together these findings strongly suggest that both particle populations are EXOs. With observed difference in migration speed resulting from different particle sizes for each subpopulation (LD-Exo: mode size 117 nm, HD-Exo: mode size 66 nm, Fig. 3.1E), as besides density, the rate at which particles migrate also depends on their size. As described, multiple experiments were performed to successfully

rule out the potential of the experimental procedures (i.e. culture conditions, EXO source, isolation method, and density gradient medium) causing disruption of the isolated EXO population, and as a result the occurrence of smaller EXO-like particle population.

In depth proteomic analysis revealed common as well as unique proteins among the MVs and EXO subpopulations. Commonly reported EV marker proteins (ALIX, TSG101, CD9, CD81 and CD63) were detected in MVs as well as EXO subpopulations. Their relative abundance was higher in the EXO subpopulations compared to MVs, indicating successful enrichment of EXOs using the dUC isolation approach. Detection of EXO marker proteins in MVs could either mean that a small number of EXOs co-sediment at 10,000 x g, or the reported EXO marker proteins are not suitable for accurate distinction between these two major EV populations.

When comparing the two EXO subpopulations LD-Exo and HD-Exo, interesting differences in composition were found. We observed enrichment of ACTN4 and CCNY in larger LD-Exo versus HD-Exo (Fig. 3.3C) derived from both B16F10 and H5V endothelial cells (Supplementary Fig. S 3.8), suggesting that these proteins could be used as marker proteins specifically for larger EXOs. ACTN4 is a cytoskeleton-associated protein, shown to be involved in metastasis of cancer (158), and has also been identified as a potential biomarker for cervical cancer (159). Interestingly, Kowal et al. report abundant expression of ACTN1 and ACTN4 in larger EVs obtained by centrifugation at only 10,000 x g (20). CCNY is a highly conserved membrane associated cyclin, and part of the cyclin

superfamily of proteins which play a crucial role in cell cycle regulation and transcription (160).

On the contrary, EPHA2 was found to be enriched in HD-Exo versus LD-Exo. Eph-Ephrin interactions are involved in numerous cellular processes, such as regulation of vascular endothelial growth factor (VEGF) signalling and angiogenesis (161). Interactions of Eph receptor-ephrins were typically thought to be subject to strict spatial constraints. In other words, Eph receptor–ephrin binding and subsequent signalling requires close juxtaposition of two cells with appropriate localisation of the Eph receptor and the ephrin on their respective plasma membranes. Recent findings indicate a novel mechanism of ephrin-Eph signalling independent of direct cell contact through EVs (162–164).

GO enrichment analysis provided us with a better understanding of potential functional differences between the studied populations. In line with previous findings by our group on EXO content, vesicle mediated transport', 'translation', 'cytoskeleton', 'G-protein', 'ribosomal protein', 'small GTPase' and 'chaperones', were commonly enriched terms. GO terms 'translation', 'ribonucleoproteins' and 'ribosomal proteins' were found to be more enriched in HD-Exo than in LD-Exo, further highlighting the unique protein composition of LD-Exo and HD-Exo.

Study of the RNA content revealed that HD-Exo contained a broad range of RNA species ranging in size from 30 – 150 nt, whereas LD-Exo and MVs seem to contain a smaller range of RNA species. Interestingly we only found 18S and 28S ribosomal RNA (rRNA) in MVs and LD-Exo. rRNA has previously been detected

in MVs, and also in EXOs (22,165), although others have reported that EXOs are negative for intact 18S and 28S rRNA (15,102). These differences could arise from differences in experimental parameters (i.e. isolation protocols, cell type) or, as our data seems to indicate, the presence of distinct EXO subpopulations.

Observed differences in biophysical characteristics, protein composition, and RNA content could suggest that different biogenesis pathways or cargo sorting mechanisms are underlying the release of the observed subpopulations. However, GO enrichment analysis did not provide direct evidence regarding differences in biogenesis. Treatment with GW4869 reduces cellular ceramide formation through inhibition of neutral sphingomyelinase (nSMase) activity, which resulted in a substantially decreased release of both subpopulations (Fig. 3.1F,G), indicating that both subpopulations are formed through a ceramide-dependent pathway. This may suggest both are of endosomal origin. The role of ceramides in the formation of other types of EVs remains to be determined.

It has previously been shown that MVBs present in cells can contain both large as well as small intraluminal vesicles (ILVs) (47). The size of ILVs is influenced by both cargo and formation mechanisms, which comprise of ESCRT-dependent and –independent processes operating within the same cell and/or MVB. It is therefore tempting to speculate that LD-Exo and HD-Exo are derived from different types of ILVs. Whether the observed difference in size results from different cargo being packaged, potentially through different mechanisms, remains to be investigated.

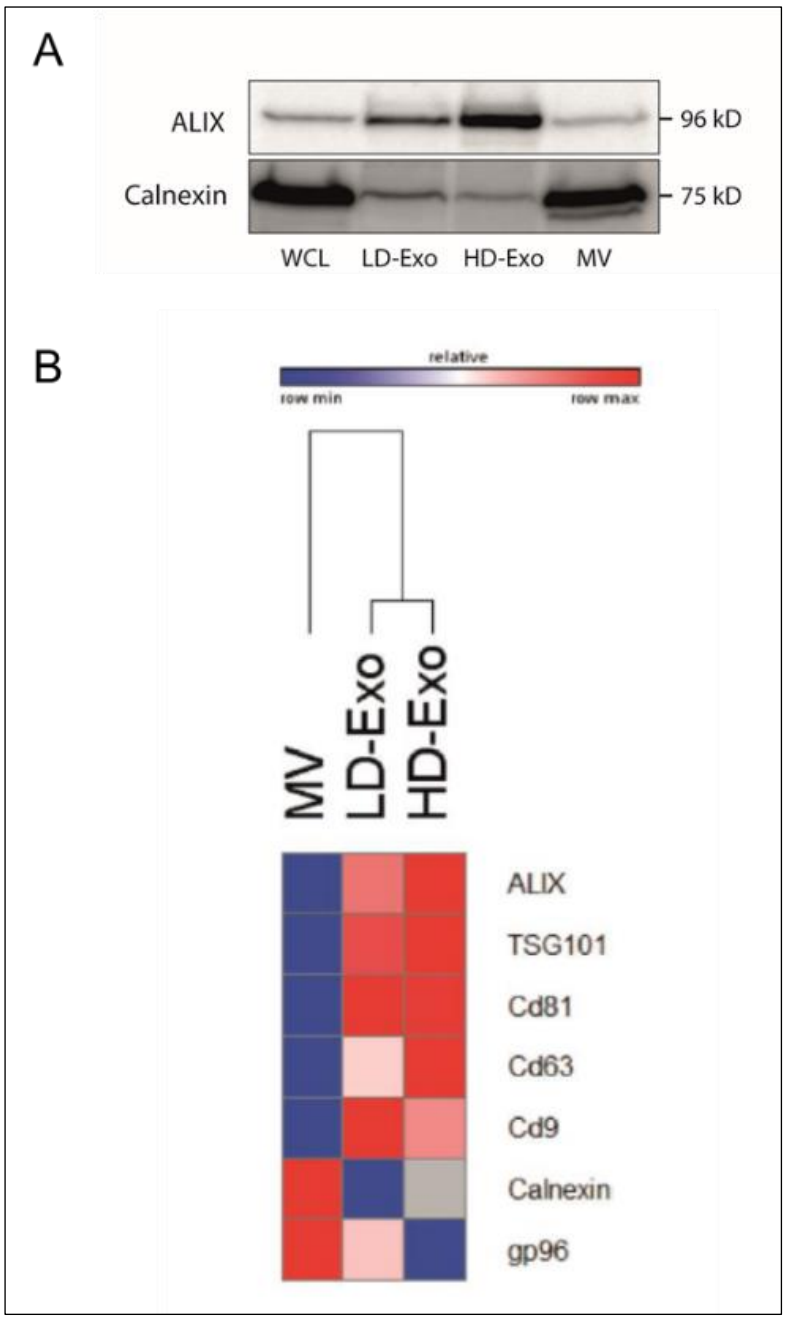
EXOs can affect recipient cells by transfer of their cargo, hence the observed differences in cargo of LD-Exo and HD-Exo could result in different functional effects.

We evaluated potential functional differences by exposing recipient endothelial cells to the EXO subpopulations, and subsequently looking at changes in gene expression of the recipient cells (Fig. 3.5). For LD-Exo, 257 genes were significantly changed versus control cells, while for HD-Exo, 1116 genes were significantly altered. A closer look at 42 genes with a fold change greater than 1.5-fold revealed upregulation of 11 genes and a downregulation of 31 genes. These findings highlight the heterogeneous effects that EXOs can mediate. GO statistical enrichment analysis revealed that a number of protein classes, molecular functions, biological processes and cellular components were differentially regulated by LD-Exo versus HD-Exo.

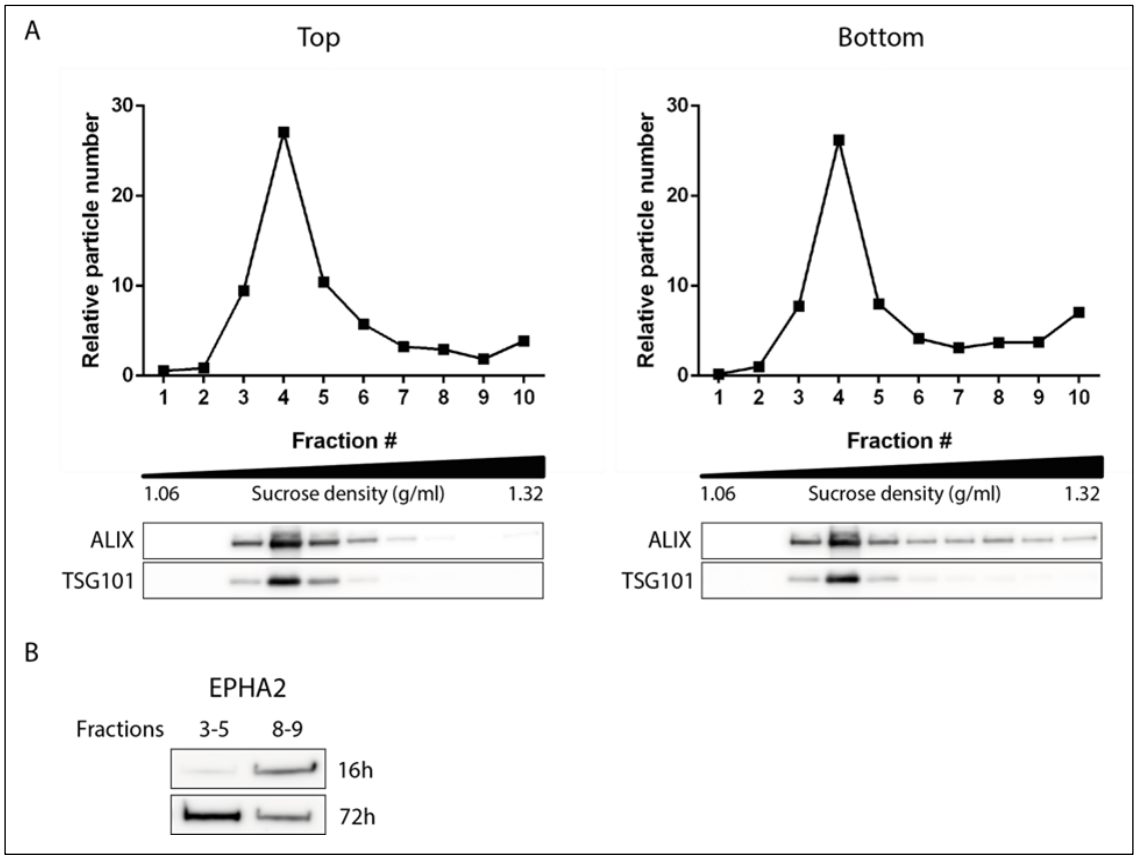
However, it is as yet unclear how the observed differences between LD-Exo and HD-Exo in changes of gene expression profile in target cells translate to phenotypic functional effects. For example, it must be determined in detail whether changes in gene expression lead to effects of protein expression level, and subsequent alterations in cell activation, signalling or differentiation. Furthermore, it should also established whether the differential effects of EXO subpopulations are connected only to differences in their biofunctional cargoes or whether they also differ in intracellular localisation after cell uptake. Potential differences in the latter characteristic are of great interest for development of EXOs into therapeutic drug-delivery vehicles.

Taken together, our results clearly show the heterogeneous nature of EV populations and the existence of distinct EXO subpopulations. Subpopulations with unique size, protein and RNA composition, which result in different effects on recipient cells. A better understanding of differences between subpopulations of EXOs will be of great importance for studies on exosome physiology, and subsequently accelerate development of exosome-based diagnostics and therapeutics.

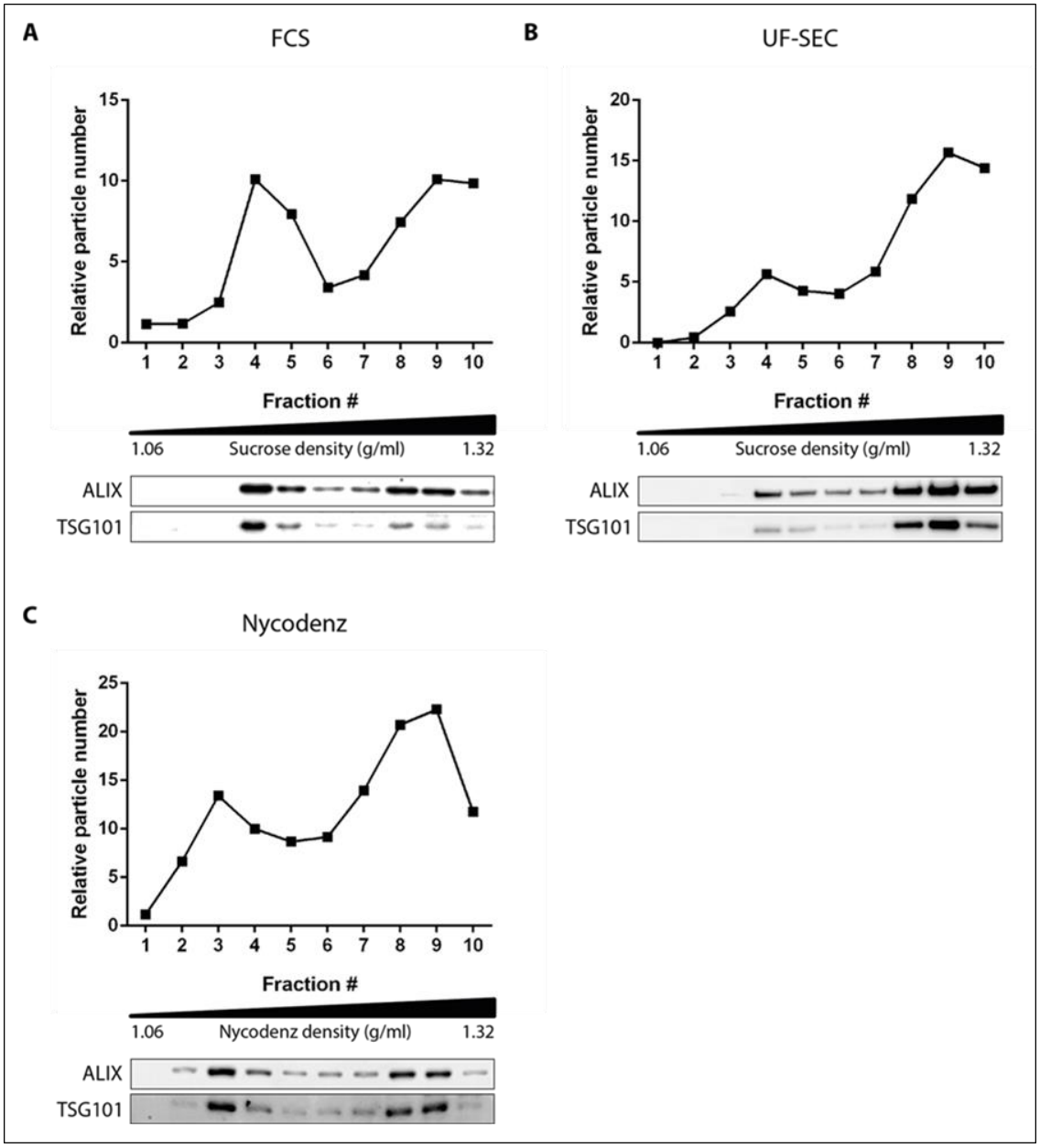
3.4 Supplementary figures



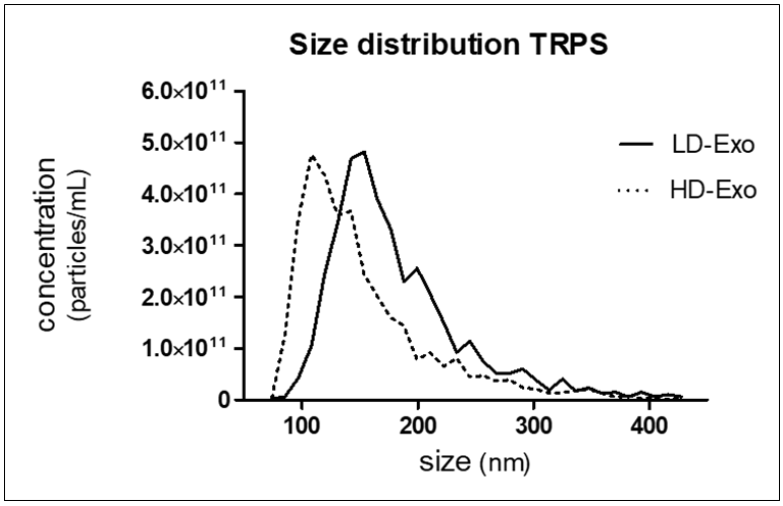
Supplementary Figure S 3.1 EXO Subpopulations LD-Exo and HD-Exo are enriched in ALIX, but not Calnexin and GP96, compared to cell lysate. EXOs were isolated as in Fig 3.1A. P110 was loaded at the bottom of a sucrose density gradient and subjected to ultracentrifugation for 16 h. Fractions 3-5 (LD fractions) and 8-9 (HD fractions) were analysed for the presence of Alix and Calnexin by Western blotting (A) and proteome analysis (B). Equal amounts of proteins were analysed. WCL, whole cell lysate.



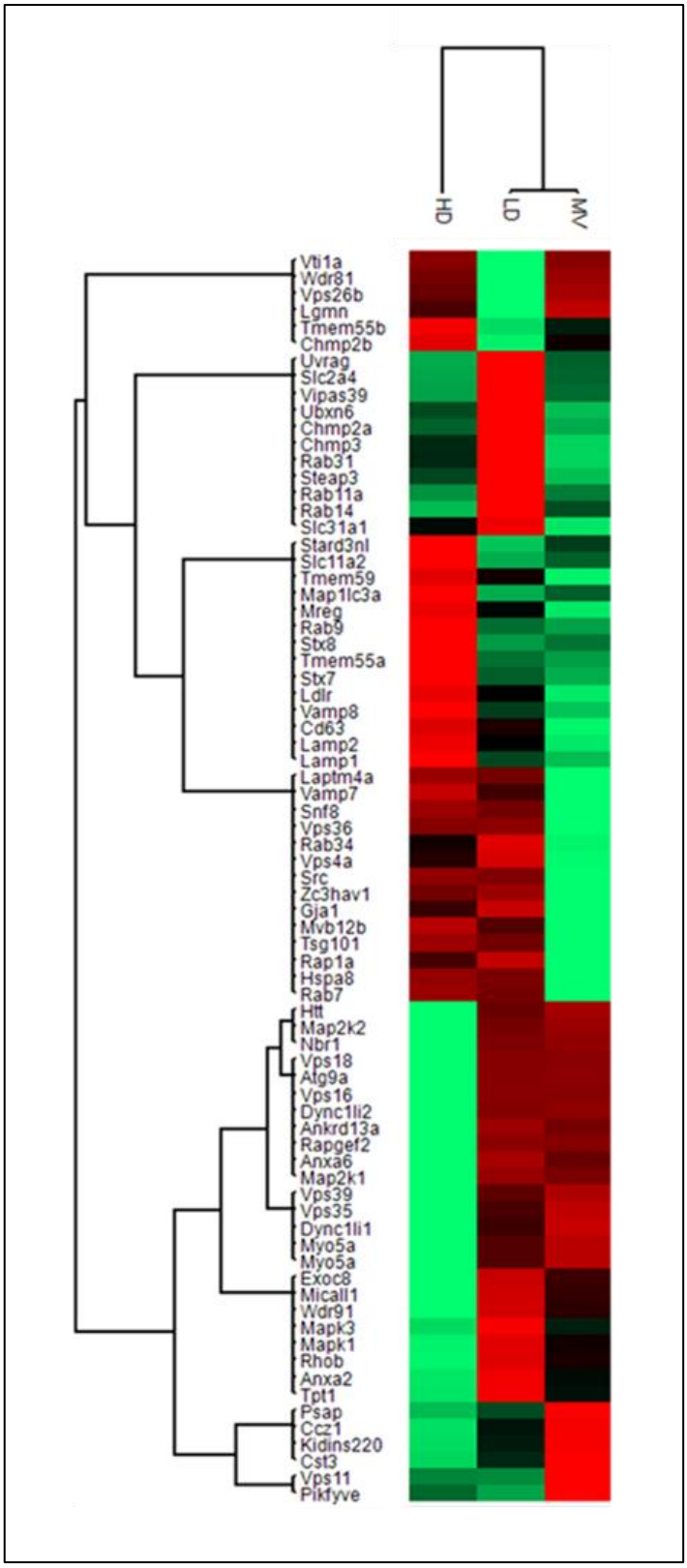
Supplementary Figure S 3.2 HD-Exo subpopulation displays delayed flotation behaviour. (A) dUC isolated B16F10 EXOs (P110) was loaded on top or at the bottom of a sucrose density gradient and subjected to ultracentrifugation for 72 h. EPHA2 is mainly detected in sucrose fractions 3-5 after 72 h centrifugation confirming association with smaller EXOs.



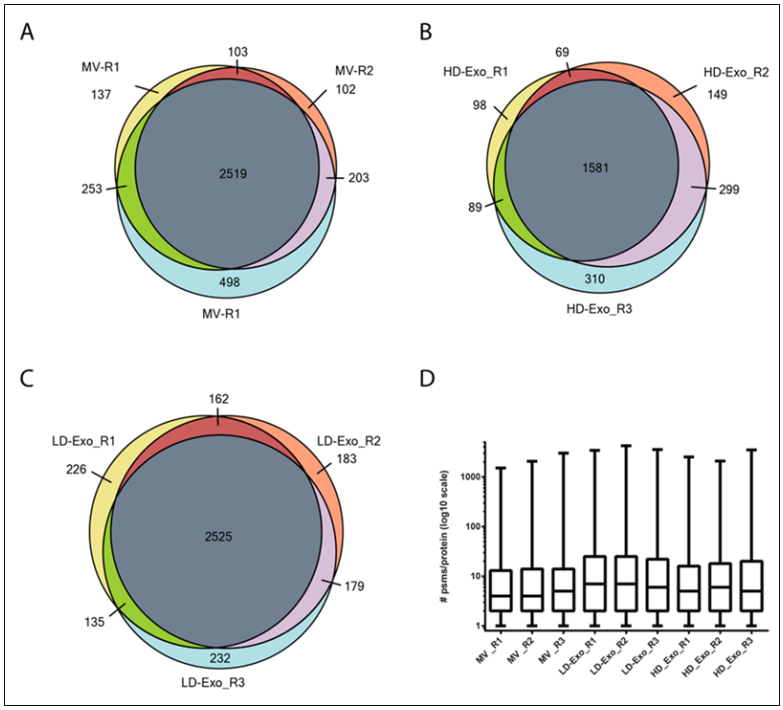
Supplementary Figure S 3.3 Detection of LD-Exo and HD-Exo subpopulations is not a result of isolation conditions, isolation method, or fractionation method. (A) EXOs were isolated from B16F10 melanoma cells cultured in presence of EXO depleted FBS instead of Opti-MEM (B) EXOs were isolated from B16F10 melanoma cells using an ultrafiltration (UF) and size exclusion chromatography (SEC) based method instead of dUC (C) EXOs were isolated from B16F10 melanoma cells using dUC and subjected to Nycodenz density gradient centrifugation instead of sucrose density gradient centrifugation.



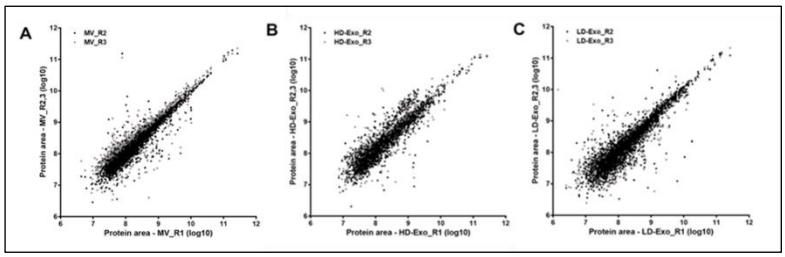
Supplementary Figure S 3.4 TRPS measurements confirm distinct size distribution of LD-Exo (153±58.3 nm) and HD-Exo (109±29.9 nm). B16F10 EXOs (P110) were isolated and EXO subpopulations (LD-Exo and HD-Exo) were obtained as shown in Fig. 3.1A. Number and size of particles were determined on a qNano gold making use of an NP150 nanopore.



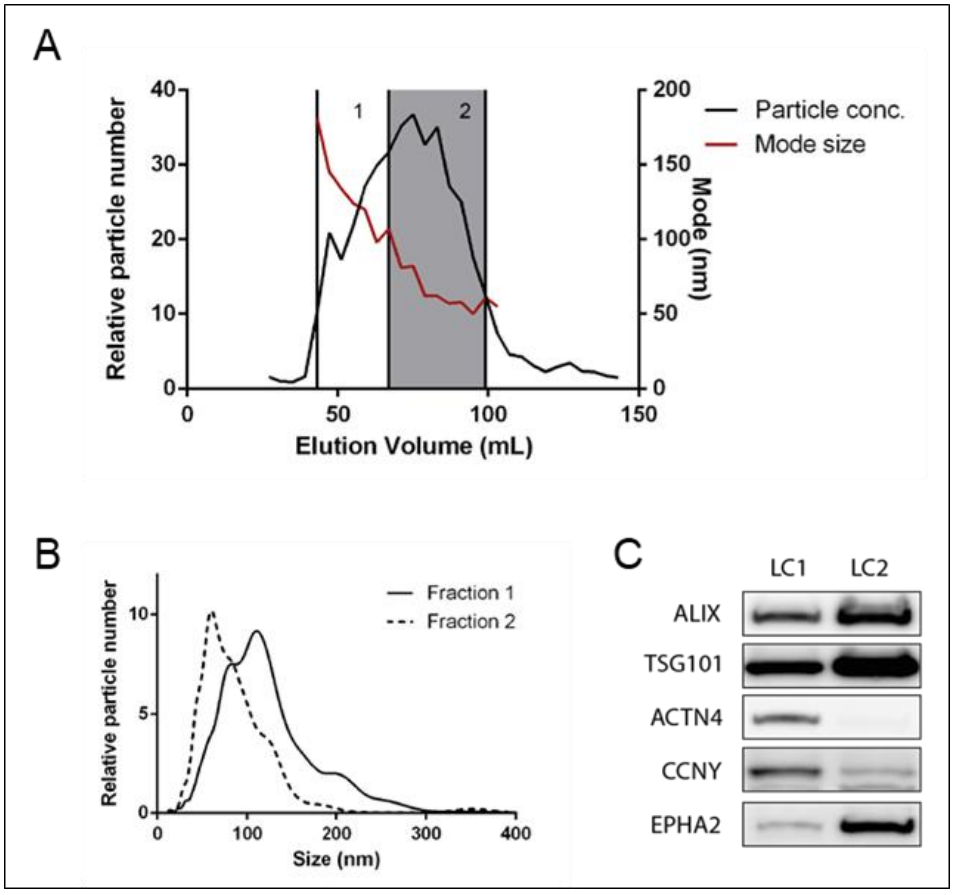
Supplementary Figure S 3.5 Proteins of the PANTHER GO-Slim Cellular Component 'Late endosomal membrane' display differential enrichment amongst MV, LD-Exo, and HD-Exo.



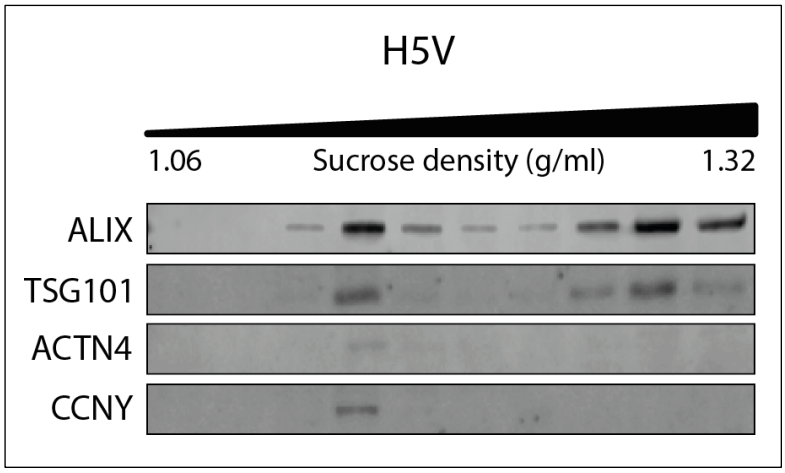
Supplementary Figure S 3.6 Good overlap in protein identification between proteomics replicates (A) MV replicates (B) HD-Exo replicates (C) LD-Exo replicates (D) Median number of peptide spectrum matches (psms)/ protein between 4 and 7.



Supplementary Figure S 3.7 High correlation between replicates (A) MV replicates (B) HD-Exo replicates (C) LD-Exo replicates.



Supplementary Figure S 3.8 Size exclusion chromatography allows for fractionation and detection of LD-Exo and HD-Exo released by B16F10 melanoma cells. EXOs were isolated using dUC (P110) and fractionated by SEC. The resulting fractions 1 and 2 (A) were analysed for particle size by NTA (B) and the presence of ALIX, TSG101, ACTN4, CCNY and EPHA2 by Western blotting (C). For Western blots, equal amounts of protein were loaded.



Supplementary Figure S 3.9 ACTN4 and CCNY are enriched in LD-Exo derived from H5V endothelial cells. EXOs were isolated using dUC, P110 was loaded at the bottom of a sucrose density gradient and subjected to ultracentrifugation for 16 h. The resulting fractions (1-10) with increasing density were analysed for the presence of ALIX, TSG101, ACTN4 and CCNY by Western blotting. For Western blots, an equal volume of each sample was analysed.

4 Results 2

In-depth investigation of exosome heterogeneity

Abstract

As described in the previous section cells release subpopulations of exosomes with defined biophysical characteristic, composition, and content. These differences can subsequently result in unique biological functions of exosome subpopulations. Through density gradient centrifugation we were able to identify two subpopulations. However, given the fact that exosomes have been reported to mediate a multitude of effects it seems highly likely that multiple subpopulations are released by cells. In order to explore exosome heterogeneity in more detail, a high resolution size exclusion chromatography based approach was optimised for fractionation of exosomes isolated from the cell culture supernatant of SKOV3 ovarian cancer cells. This approach confirmed that exosomes represent a heterogeneous extracellular vesicle population, vesicles ranging from 168 nm down to 68 nm in diameter were detected. Dot blot analysis performed on individual fractions revealed differential distribution patterns for a number of common exosomal markers. ACTN4 was more abundantly expressed in fractions containing larger exosomes, whereas CD9, ALIX, and SDCBP, were found to be more abundant in HR-SEC fractions containing smaller exosomes. Based on observed expression patterns, individual fractions were pooled to obtain four subpopulations with distinct size and protein composition. Functional effects on recipient cells were studied using proliferation, migration, and adhesion assays. Preliminary findings highlight the potential unique biological role of ovarian cancer-derived exosome subpopulations in cellular adhesion.

4.1 Introduction

Fractionation of purified EXOs using density gradient flotation (DG) allowed for identification of two distinct exosome subpopulations (LD-Exo and HD-Exo). This method of fractionation has however got a number of drawbacks: 1) gradient layering is a delicate process (i.e. time-consuming and potential loss of sample); 2) DGs have to be centrifuged at high speed overnight (i.e. time-consuming and energy intensive); and 3) necessity of DG medium removal afterwards (i.e. time-consuming and sample loss). Furthermore, DG is limited by the fact that only a small volume of a sample can be fractionated and the resolution is relatively low.

Over the last couple of years size exclusion chromatography (SEC) has emerged as a user-friendly alternative EV purification technique next to methods such as DG and dUC (109,166). SEC is performed using a column containing small porous polymer beads (referred to as the stationary phase). As the particle-containing solution travels through the stationary phase, small particles are able to enter the porous beads. As a result, larger particles travel through the column more quickly than small particles and elute at an earlier time point than small particles. SEC has been used widely by researchers in the EV field, to overcome problems associated with dUC (e.g. vesicles disruption, aggregation, and co-purification of non-EV material). More importantly, SEC does not seem to impact EV integrity and as such it preserves functionality (108,109). Clear differences between functionality of dUC-isolated EVs (dUC-EVs) and SEC isolated EVs (SEC-EVs) have been reported (108). Analysis of dUC-EVs and SEC-EVs morphology (TEM) and composition (western blot for ALIX and CD63) showed no major size differences between both preparations. However, a clear increase

in EV-induced ERK1/2 phosphorylation in recipient endothelial cells was observed after treatment with SEC-EVs compared with dUC-EVs, highlighting increased functionality of EVs isolated with SEC. In the EV field SEC is now commonly used for the isolation of EVs from many different types of biological fluids.

We hypothesised that through the appropriate choice of column dimension and resin, SEC may also be used to fractionate EXOs according to size and ultimately separate EV subpopulations. For this purpose we made use of a SEC column with larger dimensions, and a stationary phase containing Sephacryl® S-1000 Superfine beads. The larger pore size accommodates particles up to 400 nm, which in combination with larger column dimensions should allow for fractionation. From here on onwards this method will be referred to as high resolution SEC (HR-SEC). Fig. 4.1 describes the general workflow followed for isolation and fractionation of EXOs from cell culture supernatant.

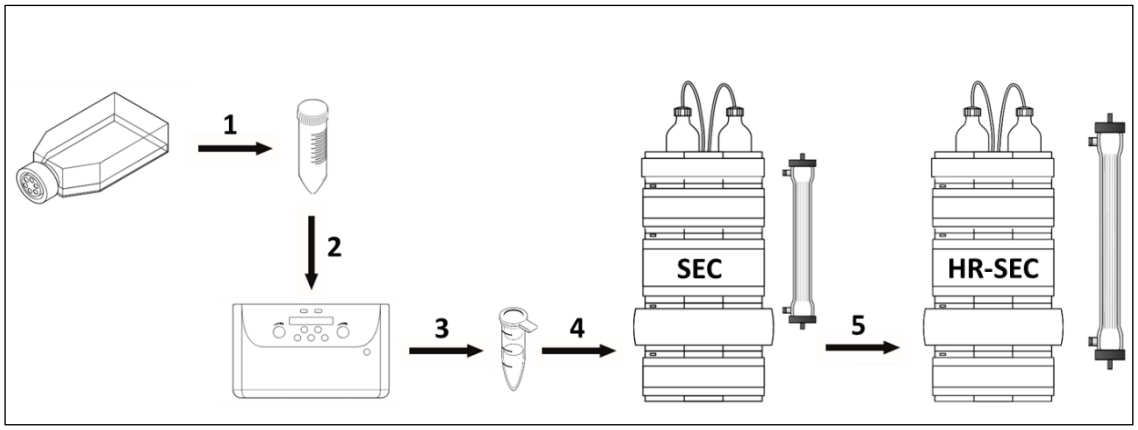


Figure 4.5 Workflow for EXO isolation with SEC and fractionation with HR-SEC. Cell culture supernatant collected after 48 hours in OptiMEM (1) and centrifuged at 300 x g for 5 minutes, followed by 2,000 x g for 10 minutes (2). Pre-cleared supernatant 10 kDa concentrated using filters and subsequently centrifuged at 10,000 x g for 10 minutes to pellet MVs (3). EXOs are isolated from the MV-cleared supernatant through SEC (4), and subsequently fractionated through HR-SEC (5).

4.2 Results

4.2.1 HR-SEC allows for broad fractionation of EXOs

HR-SEC resulted in fractionation of EXOs into 30 individual (4.0 mL) fractions. Nanoparticle tracking analysis was performed to determine the size and concentration of EXOs present in each individual fraction. As shown in Fig. 4.2, larger EXOs (max 186 nm) were detected in the fractions eluted earliest and as elution continued exosome size decreased (min 68 nm). The majority of isolated particles seem to be within the commonly reported EXO size of approx. 100 nm. These findings confirmed first of all that HR-SEC, through the appropriate choice of column dimension and resin, can be used to fractionate EXOs according to size.

More importantly the observed particle distribution indicates that the isolated population of vesicles (i.e. EXOs) contain a wide and distinct range of large as well as small particles, which is not revealed during conventional EXO bulk analysis.

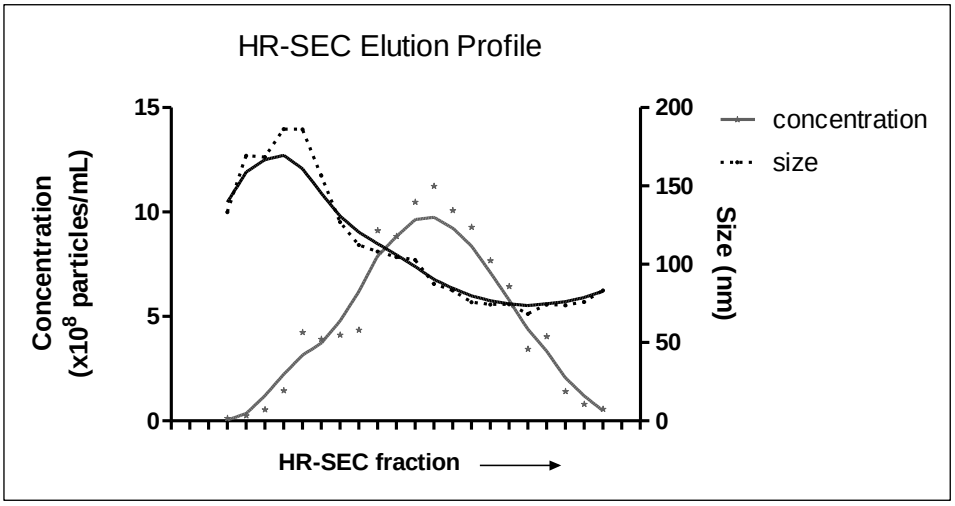


Figure 4.6 HR-SEC fractionates purified EXOs according to size. SKOV3 EXOs were fractionated and individual HR-SEC fractions were analysed for particle concentration (grey solid) and diameter (black solid) by NTA. Representative elution profile of HR-SEC.

4.2.2 HR-SEC allows for isolation of LD-Exo and HD-Exo subpopulations

We firstly set out to determine whether LD-Exo and HD-Exo subpopulations could be derived using HR-SEC instead of previously used DG approaches. For this purpose EXOs isolated from B16F10 cells using dUC (P110 Fig. 3.1 Chapter 3) were fractionated using HR-SEC. Fractions containing EXOs in the size ranges of LD-Exo (i.e. Pool 1 (white background)) and HD-Exo (i.e. Pool 2 (grey background)) were pooled and concentrated (Fig. 4.3A). As shown in Fig. 4.3B, Fraction 1 contained larger EXOs with a broader size distribution and Fraction 2 contained smaller EXOs with a narrower size distribution. Western blot analysis revealed a similar enrichment profile for a number of proteins present in Fraction 1 and Fraction 2, compared to LD-Exo and HD-Exo (Fig. 4.3C). On the basis of overlapping size distribution profiles and enrichment profiles of ACTN4, CCNY, and EPHA2, the presence of two distinct subpopulations of EXOs previously identified by sucrose DG was confirmed.

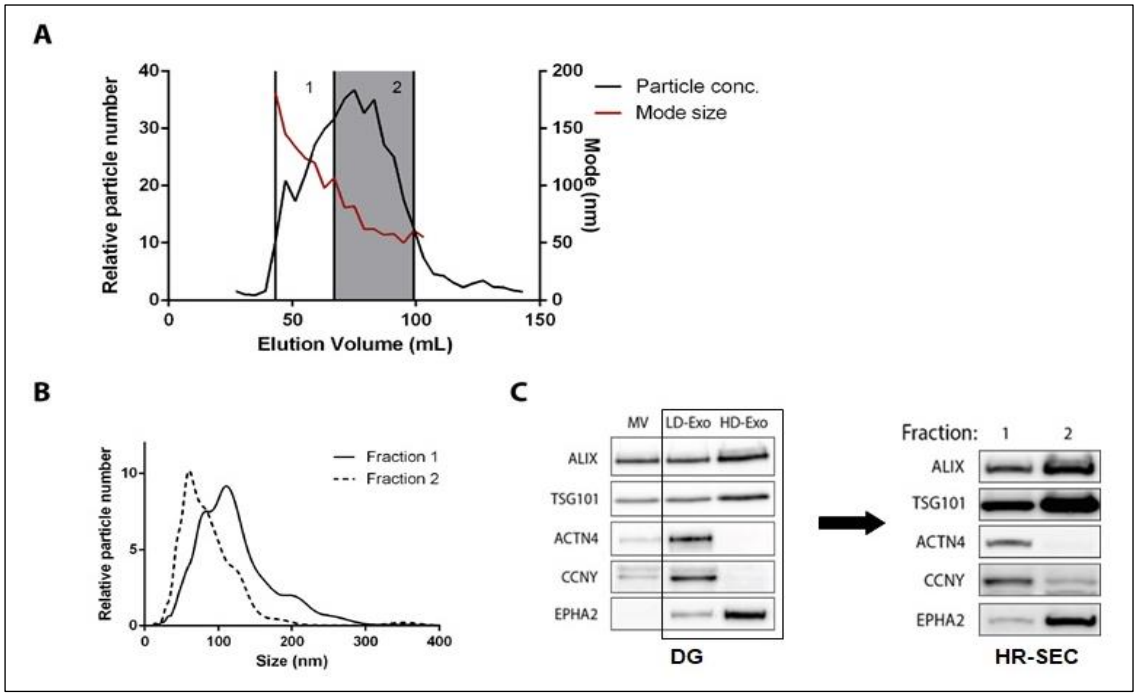


Figure 4.3 HR-SEC allows for fractionation and detection of previously identified LD-Exo and HD-Exo released by B16F10 melanoma cells. EXOs were isolated as described in Chapter 2. EXOs were fractionated by HR-SEC. The resulting fractions 1 and 2 (A) were analysed for particle size by NTA (B) and the presence of ALIX, TSG101, ACTN4, CCNY and EPHA2 by western blotting (C). For western blots, equal amounts of protein were analysed.

The aforementioned findings clearly highlight that EXO released by cells represent a heterogeneous population of EVs. Taking into consideration that EXOs have been reported to mediate a vast number of functional effects it is highly likely that more than two subpopulations are released. HR-SEC allows for a higher degree of fractionation than DG, enabling potential identification of more subpopulations.

4.2.3 Identification of SKOV3-derived EXO Subpopulations

In order to get a more in-depth view of heterogeneity in protein composition, in addition to size (Fig. 4.2) we set out to perform western blots for commonly used EXO marker proteins. However, the high volume of each individual HR-SEC fraction (4.0 mL) in combination with low EV concentration ruled out the possibility of directly determining protein expression in each fraction by western blot. Concentrating each fraction with centrifugal filters or dUC resulted in high EV loss, and most importantly unequal EV loss between fractions, further complicating comparisons of protein presence and expression between HR-SEC fractions.

As an alternative, we decided to resort to the simplified version of western blot, also known as dot or slot blot (167). This allowed for direct application of each individual HR-SEC fraction on a membrane in a single spot. More importantly, it also enabled applying high sample volumes by consecutively loading the same HR-SEC fraction in the same well.

The presence and distribution of a number of commonly used EXO proteins (CD63, CD9, ALIX, SDCBP), and previously identified EXO subpopulation protein (ACTN4) was successfully determined using this approach (Fig. 4.4).

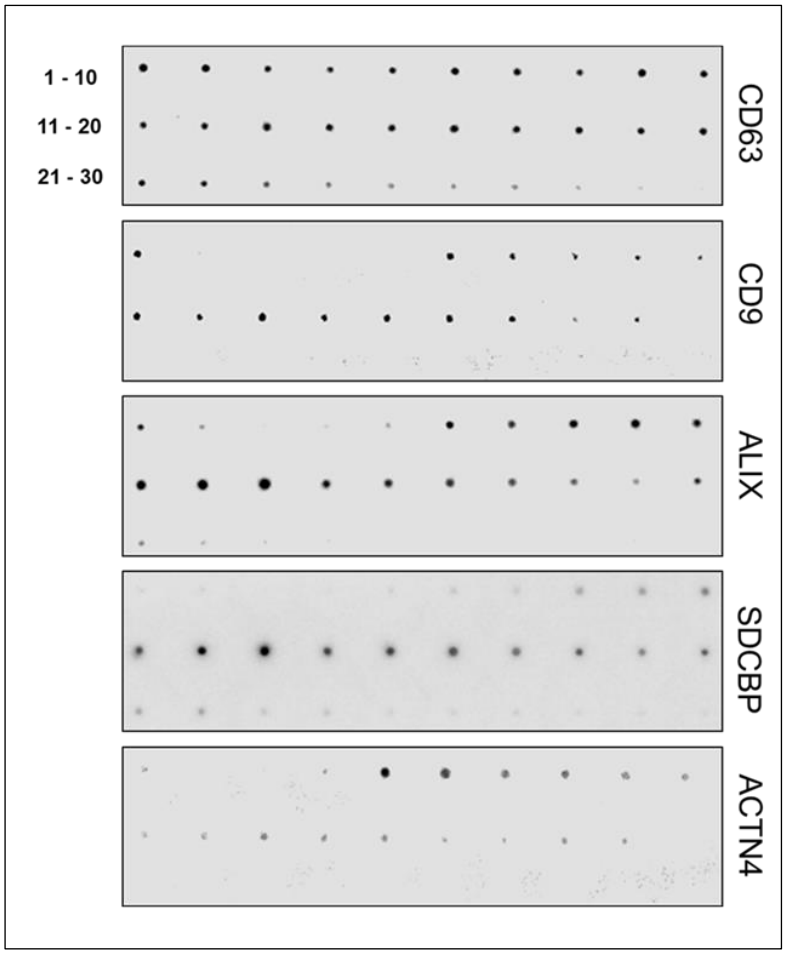


Figure 4.7 Differential expression of a panel of EV proteins in individual HR-SEC fractions. Equal volumes of each individual HR-SEC fraction were blotted onto nitrocellulose membranes to determine the expression of a number of EV marker proteins.

As shown in Fig. 4.4, the distribution of commonly used EXO marker proteins over HR-SEC fractions differed from one another. As expected ACTN4, a marker for larger EXOs, was more abundant in the early HR-SEC fractions containing larger EXOs. CD63 showed a more uniform distribution. In contrast, CD9, ALIX, and SDCBP, were found to be more abundant in HR-SEC fractions containing smaller EXOs.

On the basis of the EXO size distribution (Fig. 4.2), protein distribution (Fig. 4.4), and elution profile (Supplementary Fig. S 4.2), four pools of EXOs were produced for further characterisation: Pool 1 (HR-SEC fractions 1 - 8), Pool 2 (10 - 15), Pool 3 (17 - 20), and Pool 4 (22 - 30). To minimise potential overlap and carry-over one fraction between each pool was discarded.

NTA analysis on the four selected EXO pools revealed clear differences between the size distribution profiles of each pool (Fig. 4.5A). Pool 1 contained the largest EXOs with a broad size distribution, with a mode size and SD of 126.3±49.2 nm. Pool 2 (106.6±33.7 nm) and Pool 3 (88.7±35.6 nm) contained smaller EXOs with a narrower size distribution. In accordance with HR-SEC elution the smallest particles were expected to elute in Pool 4. Unfortunately, accurate size determination of the smallest vesicles present in Pool 4 turned out to be challenging, Pool 4 measured 85.5±39.4 nm. The majority of vesicles were most likely below the detection limit of NTA (approx. 60 nm), and NTA measurements were overshadowed by strong light scattering of larger particles more easily detected and tracked. Measures such as 0.22 µm filtration prior to measurement or alterations of the camera level did not increase the sensitivity.

SKOV3-derived EXOs were also successfully fractionated according to a recently published AF4 protocol (149). As shown in Supplementary Fig. S 4.5, using this approach allowed us to obtain three subpopulations: Exo-L, Exo-S, and exomeres. Determination of the size distribution through NTA confirms presence of particles in all three obtained subpopulations, Exo-L 139.4±69.2 nm, Exo-S 72.3±54.4 nm, and exomeres 72.1±68.3 nm. In line with expectations Exo-L contains the largest EXOs, a difference in size distribution between Exo-S and exomeres could however not be observed with NTA. Comparative studies of

composition (western blotting) and detailed study of size (TEM) of the AF4 subpopulations to HR-SEC subpopulations will be performed in the near future.

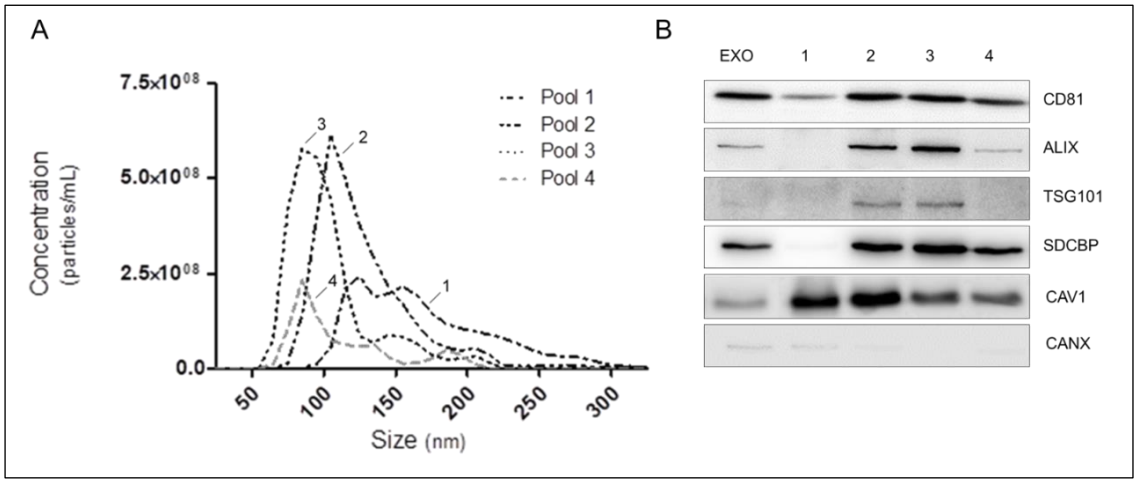


Figure 4.8 SKOV3 HR-SEC pools contain EXOs with distinct size and protein composition. Size distribution determined with NTA (A). Expression of EXO proteins by Western blot on equal amounts (15 µg) of protein. EXO = unfractionated SKOV3 EXOs.

Analysis of protein expression by western blot revealed a differential distribution of a number of EXO marker proteins (Fig. 4.5B). Larger EXOs present in Pool 1 and Pool 2 show a higher relative abundance of CAV1. Pool 1 appears to contain large EXOs which express CAV1, whilst lacking common EXO proteins ALIX, TSG101, and SDBCBP. Abundance of ALIX, TSG101, and SDCBP was the highest in EXOs present in Pool 2 and Pool 3. Pool 4 shows a similar expression pattern as Pool 2 and 3 although expression levels are lower, but interestingly Pool 4 lacks TSG101 and seems to express very little ALIX.

4.2.4 Functional roles of SKOV3-derived EXO subpopulations

Given the fact that the HR-SEC pools differ in size (Fig. 4.5A) and protein composition (Fig. 4.5B) we next set out to explore whether this would result in differences in biological functionality in cancer. Effects of SKOV3 EXOs on proliferative signalling of SKOV3 cells and effects on endothelial migration were evaluated through live-cell time-lapse microscopy (IncuCyte®). Making use of this approach allowed for monitoring of effects over time.

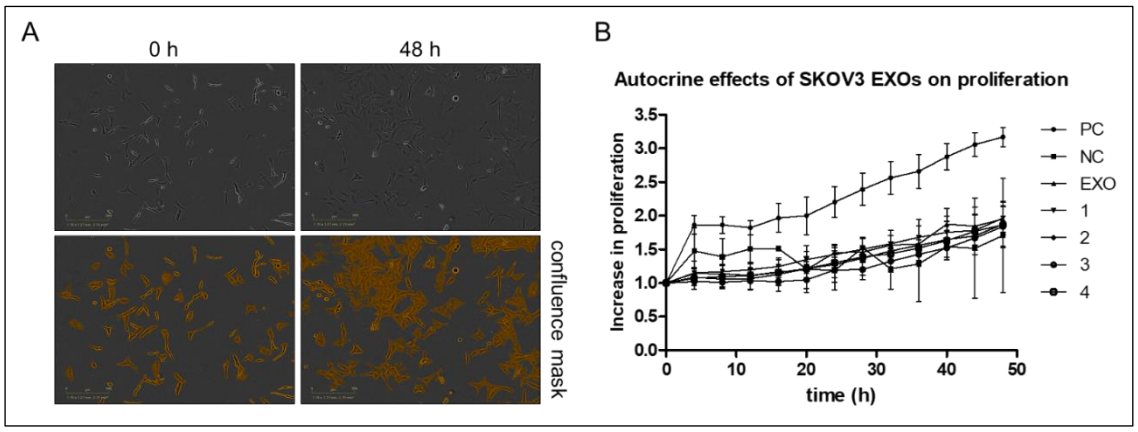


Figure 4.6 SKOV3-derived EXOs do not affect ovarian cancer proliferation. (A) Human ovarian cancer cells SKOV3 were treated with SKOV3-derived EXOs and cell proliferation was followed over 48 h. (B) Proliferation was quantified with built-in IncuCyte® software to determine cell confluence. Values are mean ± SD; n=3. PC, positive control (1% FBS); NC, negative control (PBS); EXO, unfractionated EXOs; 1, Pool 1; 2, Pool 2; 3, Pool 3; 4, Pool 4

Sustained and enhanced proliferative ability is one of the hallmarks of cancer, and is relatively easy to evaluate in an *in vitro* assay. Promotion of cancer cell proliferation after treatment with cancer-derived EVs is commonly reported throughout literature (168–171). In our hands SKOV3-dervided EXOs did however not show any enhancing effects on SKOV3 proliferation (Fig. 4.6).

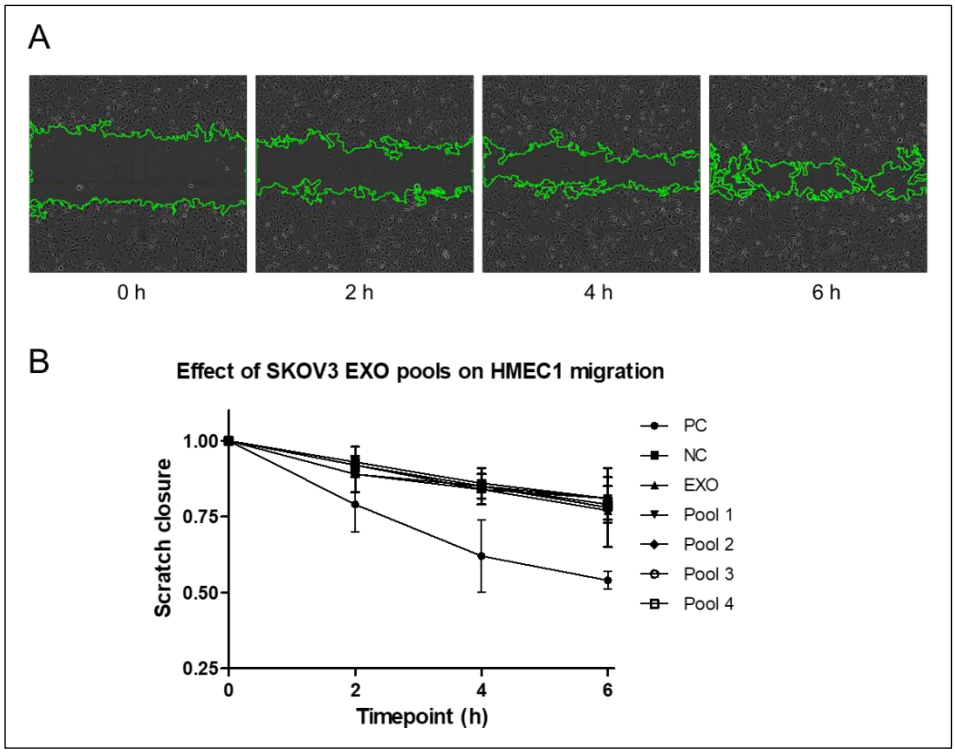


Figure 4.7 SKOV3 EXOs do not affect HMEC1 migration. (A) Scratches were made in confluent monolayers of human microvascular endothelial cells HMEC-1. Cells were subsequently incubated in presence or absence of (1.0 µg/mL) SKOV3 EXOs, migration was followed using time-lapse microscopy (IncuCyte®). (B) Total area of each scratch was quantified through ImageJ. Values are mean ± SD; n=3. PC, positive control (1% FBS); NC, negative control (PBS); EXO, unfractionated EXOs

In addition to proliferation, the effect of SKOV3-derived EXOs on endothelial migration was evaluated. Migration without passing through obstructive barriers (i.e. invasion) was studied by scraping HMEC1 monolayers to generate well-defined scratches (Fig. 4.7A). No effects of SOV3-derived EXOs on migration of endothelial cells could be observed.

4.2.5 The role of SKOV3-derived EXOs in adhesion

Failing to observe any effects of SKOV3-derived EXOs on cell proliferation and migration, we set out to explore alternative functional roles to evaluate. We hypothesised that SKOV-derived EXOs could be important in the preparation of metastatic niche, as reported for other EVs (53). In particular, we became interested in the specific role of ovarian cancer-derived EXO subpopulations in cell adhesion because of the two following reasons. First of all, unfractionated EXOs containing a specific composition of integrins (i.e. proteins that directly mediate cell adhesion) have been shown to play a major role in determining cancer metastasis locations (99,172,173). Secondly, ovarian cancer derived EXOs in particular are reported to control dissemination sites from primary ovarian cancer M-Trap (174).

Metastasis of ovarian cancer cells has unique characteristics, since ovarian cancer has the ability to metastasise at an early stage onto the peritoneal mesothelial surface of the abdominal cavity (175). Detached or exfoliated cancer cells from the primary tumour are able to migrate to the peritoneum through the physiological movement of peritoneal fluid (175–177). This is perfectly in line with Stephen Paget's 'seed and soil' hypothesis, where the seed (i.e. disseminated ovarian cancer cells) travels to the peritoneum where it will encounter its preferred and favoured soil (i.e. mesothelium) (86). Interestingly, the disseminated ovarian cancer cells do not establish just anywhere on the peritoneum, a surface of approximately 1 – 2 m^2. This highlights the possibility that this process is most likely dependent on certain secondary influences or characteristics which create pockets or niches with characteristics favourable to

establishment of the secondary tumour (178). The role of tumour-derived EVs in the formation of the pre metastatic niche (PMT) is well established (66,87).

The precise role of ovarian cancer-derived EXOs in the formation of the PMT and establishment of the secondary tumours in the peritoneum are not clear (179). Commonly observed effects of cancer-derived EVs (i.e. promotion of proliferation and endothelial migration) were not observed for ovarian cancer-derived vesicles in our hands. As discussed, ovarian cancer-derived vesicles could play a role by providing a direct scaffold for binding of the disseminated cancer cell. A characteristic which has been exploited for the development of therapeutic PMT mimics (174,180). One such mimic called M-TRAP (metastatic trap) made up of EXOs purified from ovarian cancer patient ascites embedded onto a 3D-Polystyrene/Polycaprolactone insert. The device was implanted into the peritoneum and preferentially captured intraperitoneally injected SKOV3 cells (174). As a result mice implanted with M-TRAP survived significantly longer than those without implants, with improved survival demonstrated upon removal of the implant carrying the metastatic disease.

4.2.6 SKOV3-derived EXO subpopulations show differential ability to support adhesion

We set-out to study this observed effect in an *in vitro* setting. Firstly we confirmed that EXOs released by SKOV3 support adhesion (of SKOV3 cells) (Fig. 4.8). An equal amount of protein obtained from the non-EV (i.e. PROT) fraction released by SKOV3 cells showed no support of adhesion.

Integrins represent a large family of adhesion molecules that mediate cell-cell and cell-extracellular matrix interaction and adhesion (181). The transmembrane proteins of the tetraspanin superfamily, which are commonly found to be enriched in EVs (e.g. CD9, CD63), have been shown to function as key regulators on cell adhesion molecules (182). More interestingly the 2015 landmark publication by the Lyden lab highlights that integrins present on tumour-derived EXOs determine organotropic metastasis (99).

In order to evaluate whether integrins are involved in the observed effects of SKOV3-derived EXOs we employed a blocking monoclonal antibody (mAb Lia 1/2) specific for integrin beta 1 subunit. Inhibition of adhesion in presence of Lia 1/2 highlighted a central role of integrin beta 1 in the interaction between SKOV3-derived EXOs and SKOV3 cells (Fig. 4.8). Other factors seemed to play a role in adhesion to factors present in the PROT fraction, since inhibition of adhesion by Lia 1/2 was not observed.

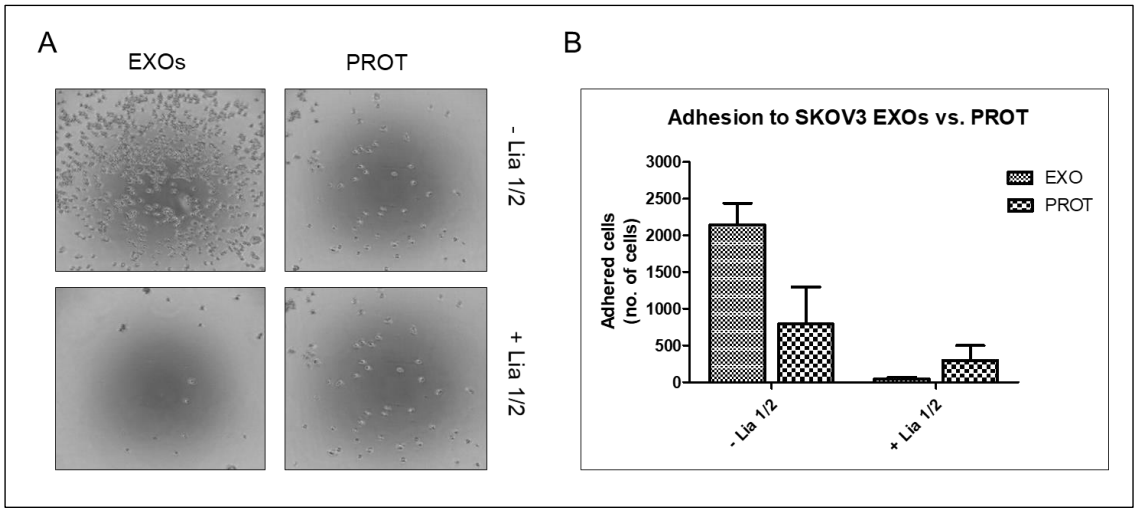


Figure 4.8 SKOV3 –derived EXOs support adhesion of ovarian cancer cells in an Integrin beta 1 dependent process. SKOV3 cells were allowed to adhere to coated EXO (1.0 µg) or PROT (1.0 µg) in absence (top row) or presence (bottom row) of Lia1/2 (1:500). Values are mean ± SD; n=3. EXO = unfractionated exosomes, PROT = protein or non-exosome fraction, Lia1/2 = integrin beta 1 antibody. Images are representative of 5 individual experiments.

Taking into account this interesting observation we set out to explore whether SKOV3 EXO Pools show differential ability to support adhesion. As shown in Fig. 4.9 a clear difference was observed between the EXO Pools. Pool 1 and Pool 2, containing larger EXOs, showed a low level of SKOV3 adhesion. In contrast, small EXOs present in Pool 3 and Pool 4, showed a very high level.

Adhesion by the different EXO Pools was found to be beta 1 dependent (Fig. 4.9 lower panel). These findings provide an indication about the potential unique/different roles of EXO subpopulations in ovarian cancer adhesion.

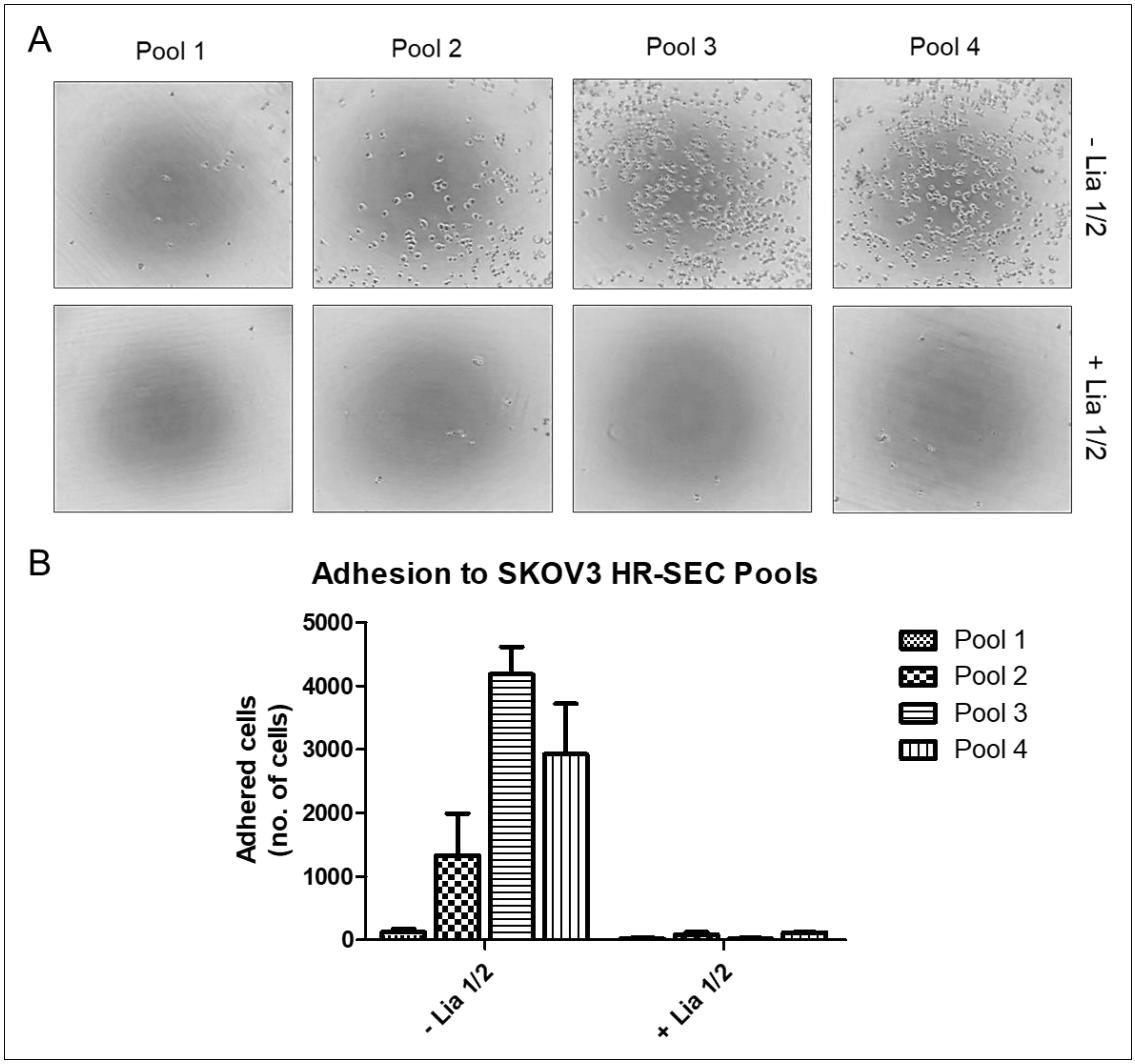


Figure 4.9 Large and small SKOV3-derived EXOs show differential ability in support of ovarian cancer adhesion. SKOV3 cells were allowed to adhere to coated HR-SEC EXO pools (1.0 µg) in absence (top row) or presence (bottom row) of Lia1/2 (1:500). EXO = unfractionated exosomes, PROT = protein or non-exosome fraction, Lia 1/2 = integrin beta 1 antibody. Images are representative of 5 individual experiments.

4.3 Discussion and conclusion

Increasing evidence points to the fact that, in contrast to previous and currently held views, EXOs represent a heterogeneous population of EVs (20,22,24,111,131). Elucidating EV and in particular EXO heterogeneity has become a key subject of research in the EV field. Getting a more in depth and precise understanding of heterogeneity and of distinct populations released by cells will aid progression in many areas of EV-research. Despite significant recent advances EV isolation techniques, separation is still relatively crude, thus not allowing for isolation of 'pure' vesicle populations. Additionally, the study of EVs on a single vesicle level is highly needed yet technologically extremely challenging due to their very small size, complex composition and underdeveloped analysis methods. We here describe our approach which successfully allowed for fractionation of isolated EXOs according to size (Fig. 4.2). Optimisation of a SEC based isolation and subsequent fractionation was achieved through appropriate choice of column dimensions and resin. NTA analysis showed that isolated EXOs ranged in size from 168 nm down to 68 nm, a wide distribution which is normally obscured by bulk analysis of the isolated EXO populations.

Fractionation of dUC isolated B16F10 derived EXOs and subsequent pooling of fractionated EXOs according to size allowed for identification of previously identified EXO subpopulations LD-Exo and HD-Exo, as shown in Fig. 4.3 and described in Chapter 2. Confirming first of all that our HR-SEC method, similar to density gradient approaches, allows for fractionation of EXOs. Secondly it confirms that cells release EXO subpopulations with distinct size and composition.

The higher degree of fractionation achieved with HR-SEC compared to DG centrifugation led us to believe that this approach could allow for more in-depth study of heterogeneity. Study of the distribution of common EXO markers in each individual fraction highlighted heterogeneity in protein composition within isolated EXOs (Fig. 4.4). ACTN4 was found associated with fractions containing larger EXOs, whereas CD63 showed a more uniform distribution. In contrast, CD9, ALIX, and SDCBP, were detected in fractions containing smaller EXOs.

Leading on from these findings, four Pools (i.e. subpopulations) of EXOs were composed for further characterisation. As shown in Fig. 4.5, the largest EXOs were detected in Pool 1 with a mode size and SD of 126.3±49.2 nm, followed by Pool 2 (106.6±33.7 nm) and Pool 3 (88.7±35.6 nm). In contrast to our expectations Pool 4 did according to the NTA measurements not contain the smallest EXOs, 85.5±39.4 nm. This is most likely due to the fact that the majority of EXOs have a size below the detection limit of NTA, size determination using TEM should allow us to accurately study the differences between the four obtained Pools. Recent findings by Zhang et al. using AF4 for fractionation of isolated EXOs, and TEM for determination of size, allowed for identification of two distinct subpopulations of EXOs, Exo-L (large EXO vesicles, 90–120 nm) and Exo-S (small EXO vesicles, 60–80 nm). More importantly a novel population of very small non-membranous nanoparticles was identified (~35 nm), which they term exomeres (116). It is tempting to speculate that Pool 4 might contain a low percentage of EXOs and mainly exomeres, with the latter particles falling below the detection limits of NTA. Similar to Zhang et al. TEM analysis should allow us to confirm whether exomeres are present in Pool 4. More importantly I have

successfully fractionated SKOV3-derived EXOs according to the AF4 protocol published by Zhang et al. Three subpopulations (i.e. Exo-L, Exo-S, and exomeres) were obtained after fractionation (Supplementary Fig. S 4.5). Determination of the size distribution through NTA confirmed presence of particles in all three obtained subpopulations, Exo-L 139.4±69.2 nm, Exo-S 72.3±54.4 nm, and exomeres 72.1±68.3 nm. Exo-L contained the largest EXOs, a difference in size distribution between Exo-S and exomeres was however not observed with NTA. Comparative studies of composition (western blotting) and more accurate studies of size (TEM) of these samples to the four HR-SEC pools will be performed in the near future.

Current study of protein composition of HR-SEC Pools using western blotting shows that larger EXOs present in Pool 1 and Pool 2 have a higher relative abundance of CAV1. Pool 1 appears to contain large EXOs which express CAV1, whilst lacking common EXO proteins ALIX, TSG101, CD81, and SDBCBP. Interestingly large oncosomes (LOs), a population of atypical large tumour-derived EVs, have been found to be enriched in CAV1 whilst expressing low levels of tetraspanins CD9, CD63, and CD81 (25). In contrast to LOs, vesicles present in Pool 1 do not fall within the commonly observed size range of LOs.

Abundance of common EXO marker proteins CD81, ALIX, TSG101, and SDCBP was highest in EXOs present in Pool 2 and Pool 3, indicating that they are to be likely derived through ESCRT-dependent biogenesis pathways. Pool 4 has a low expression of aforementioned EXO markers, and lacks TSG101. Given the fact that equal amount of protein was loaded for each pool, these findings could

indicate that Pool 4 contains a small amount of EXOs. The majority of protein and particles in Pool 4 however is likely to constitute the previously mentioned exomeres, which lack expression of the studied EXO markers. The latter finding is in line with result published on the protein composition of exomeres by Zhang et al. In-depth comparison of the protein content using proteomics could provide a better understanding of the HR-SEC subpopulations, and their comparison to populations described by others (21,116,183).

Based on the observed differences in size and composition we next set out to evaluate functional effects of the obtained subpopulations. Effects of cancer-derived EVs and EXOs on proliferation and endothelial migration are reported throughout EV literature. As such we were expecting to observe effects in both cases. In our hands EXOs did neither promote proliferation nor endothelial migration, and differences between subpopulations were not observed (Fig. 4.6 & 4.7). A number of approaches was taken to optimise the assay, such as serum starvation (data not shown). Although surprising, there are a large number of experimental parameters at play that can influence the outcome of applied functional assays (e.g. differences in growth conditions, cell confluency, and concentration). Difference in cell source and EXO isolation method perhaps provide another likely explanation for this discrepancy. The tendency for underrepresentation of negative or null effects in available scientific EV literature, and scientific literature in general, might be worth taking into consideration as well.

Although further changes in experimental parameters could perhaps lead to observable functional differences in the assays described above, given the origin of the used EXOs. We decided to focus on a functional effect important specifically in the context of ovarian cancer, in particular the potential effect of SKOV3-derived EXOs to support ovarian cancer dissemination and metastasis. As hypothesised by others, ovarian cancer derived EVs could play a role by providing a direct scaffold for binding of the disseminated cancer cell (173,177,179). A potential role which is supported by the fact that ovarian cancer derived EXOs have been successfully used as so called PMT mimics, altering the dissemination pattern of ovarian cancer (174,180).

As shown in Fig. 4.8 and Supplementary Fig. S 4.3 and S 4.4, SKOV3-derived EXOs show a strong support of SKOV3 adhesion. When evaluating EXO subpopulations a clear difference was observed between the EXO Pools (Fig. 4.9). Pool 1 and Pool 2 showed a low level of SKOV3 adhesion whereas Pool 3 and Pool 4 showed a very high level of support. Observed adhesive effects were found to be integrin beta 1 dependent (Fig. 4.9 lower panel). Although more experiments need to be performed in order to understand specific mechanisms of this observation, these findings although basic provide an indication about possible differential roles of EXO subpopulations in ovarian cancer.

Even though our experimental setup proves the direct functional involvement of integrins in this process, it does not distinguish whether the key interaction mediators are integrins present on EXOs or on SKOV3 tumour cells themselves.

Literature suggests an important and strong role of exosomal integrins. The relevance of exosomal integrins has been emphasised since the landmark paper by Hoshino et al. showing that integrin 'fingerprints' present on tumour-derived EXOs dictate organotropic metastasis (99). Earlier work by Clayton et al. shows that B cell-derived EXOs express functional integrins, which may present a novel mode for cells of delivering adhesion signals at distances beyond that of direct cell-cell contact (184).

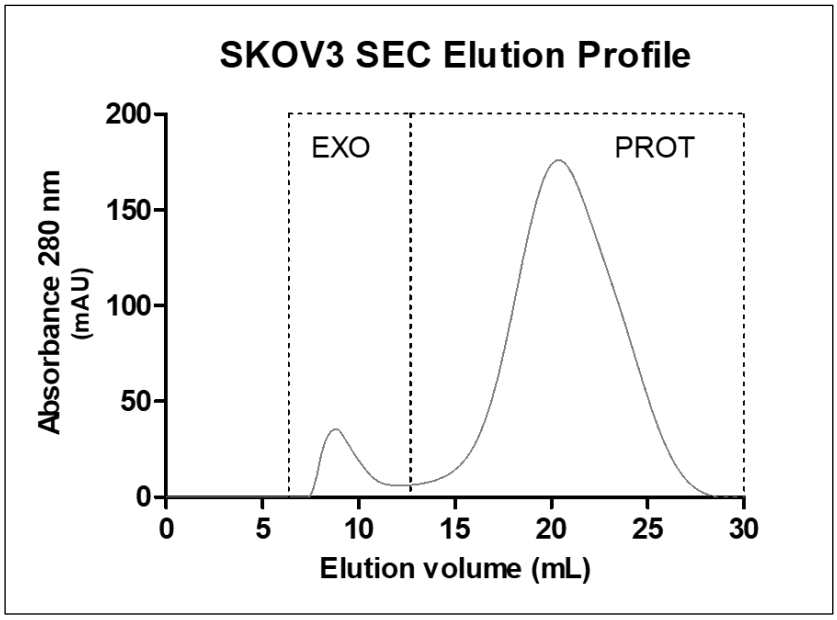
Perhaps the strongest body of evidence supporting our findings is provided by work on the involvement of EVs in the maintenance of anchorage independent growth, adhesion, cellular motility and invasion of breast cancer cells (185,186). Data presented by the authors show rapid adhesion and spreading of breast cancer cells after treatment with EVs. Furthermore an increase in secretion of EVs from rapidly adhering metastatic cancer cells is observed compared to cancer cells that take longer to adhere and spread. The authors suggest that metastatic cells display this EV-mediated increase in adherence capacity to gain a foothold for growth advantage at distant metastatic niches (187,188).

Our findings and aforementioned important findings clearly show that it's worth looking deeper into the role of EXOs in ovarian cancer adhesion and of exosomal integrins present on SKOV3- derived EXO subpopulations, even though other mechanisms may be involved too. More experiments are needed to get a better understanding of the underlying mechanistics.

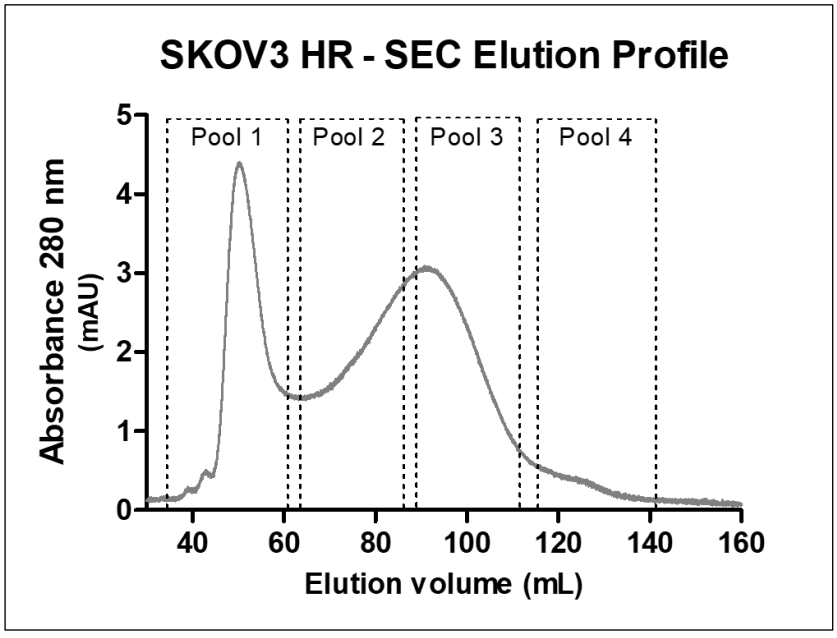
Furthermore it would be worthwhile to explore the distribution and EV-mediated transfer of CD44, which has been shown to promote invasion of ovarian cancer through effects on mesothelial cells (189). An immortalised human mesothelial cell line (HMrSV5) has been acquired, which will allow us to investigate these findings and study if SKOV3-derived subpopulations have unique functional effects. In addition it would be relevant to study whether SKOV3 cells show increased adhesion to HMrSV5 cells treated with SKOV3-derived EXOs, a set-up which resembles the *in vivo* conditions more closely.

Studying functional effects of EVs will always remain a challenge due to the fact that EXOs are composed of multiple molecules (i.e. proteins, lipids, and nucleic acids). The combination (i.e. the package) of all these different components will dictate the functionality, however it is likely that certain cargoes are functionally more important than others. Successful fractionation, approaching single vesicle level, and obtaining a detailed view and understanding of the composition of secreted EV populations and EXO subpopulations will allow for studies on the unique role(s) of each (sub)population. It's however worth taking into consideration that cells are constantly undergoing change. As such the observed effects might be more dependent on the state of the host cell than the actual composition of the EV. Along the same lines, the state of the EV recipient cell might also partially dictate whether EV cargoes can mediate their functional effects or not.

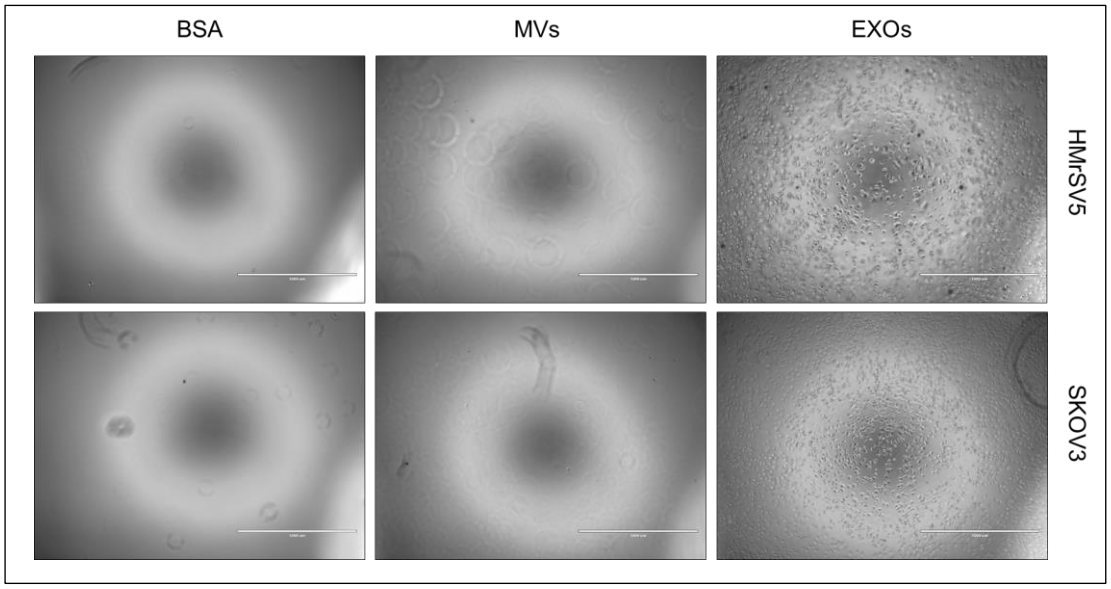
4.4 Supplementary figures



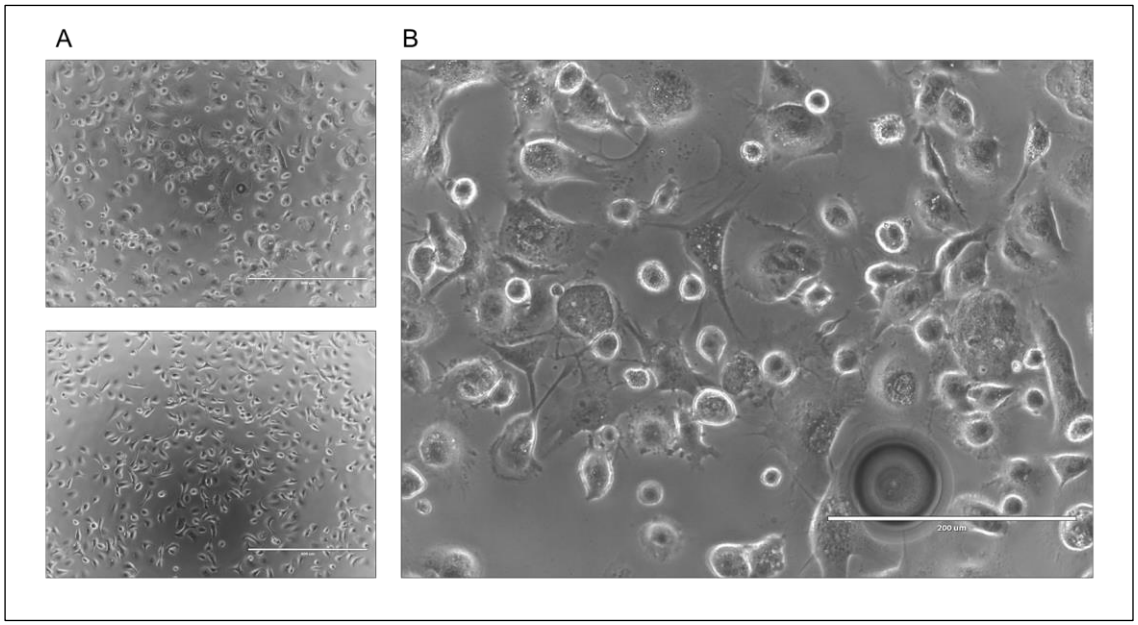
Supplementary Figure S 4.1 Representative SEC elution profile for isolation of SKOV3 EXOs. EXO, exosomes; PROT, protein or non-EV fraction.



Supplementary Figure S 4.2 Representative HR-SEC elution profile for fractionation of SKOV3 – derived EXOs.

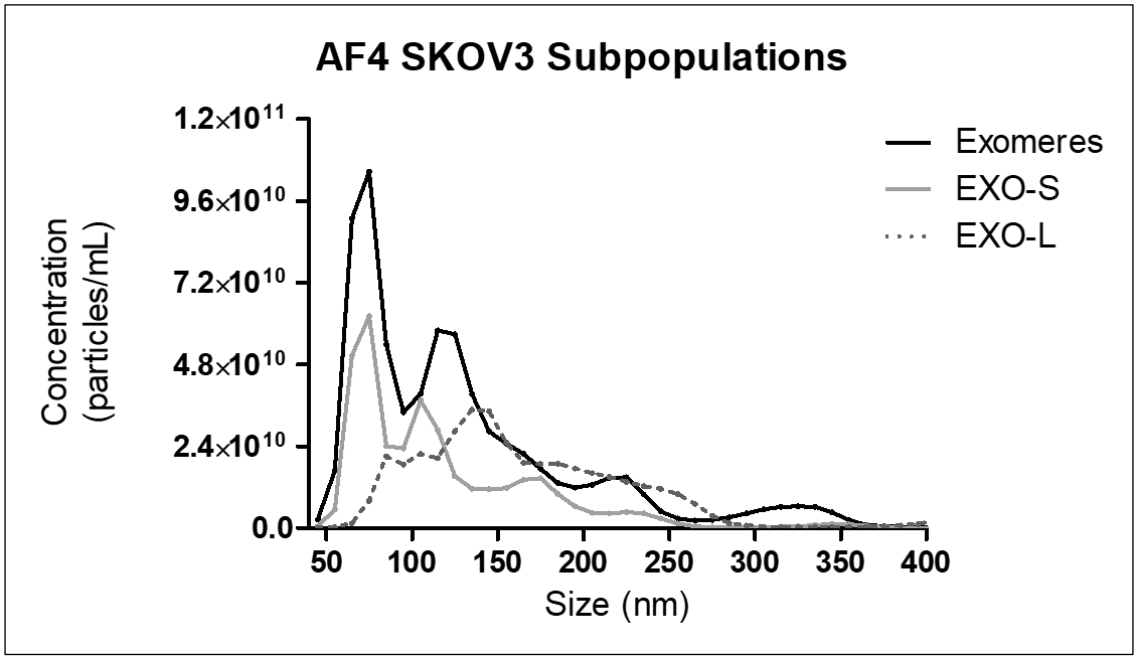


Supplementary Figure S 4.3 SKOV3 – derived EXOs support adhesion of ovarian cancer cells (SKOV3) and mesothelial cells (HMrSV5). SKOV3 cells or HMrSV5 cells were allowed to adhere for 30 mins to coated SKOV3-derived EXOs (1.0 µg), SKOV3-derved MVs (1.0 µg), or BSA (1.0 µg). Images taken on EVOS microscope at 4x magnification.



Supplementary Figure S 4.4 SKOV3 – derived EXOs support adhesion and spreading of ovarian cancer cells (SKOV3) and mesothelial cells (HMrSV5). A) SKOV3 (A, bottom panel) or HMrSV5 mesothelial cells (A, top panel) were

allowed to adhere for 30 mins to coated SKOV3-derived EXOs (1.0 µg) Images taken on EVOS microscope at 4x magnification. B) Image of HMrSV5 mesothelial taken on EVOS microscope at 20x magnification after cells were allowed to adhere to SKOV3-derived EXOs for 30 minutes (1.0 µg).



Supplementary Figure S 4.5 Asymmetrical flow field flow fractionation (AF4) allows for successful fractionation of SKOV3-derived EXOs. SKOV3 EXOs were isolated using SEC and subsequently fractionated according to AF4 protocol published by Zhang et al. (149). Exomeres (black solid) 72.1±68.3 nm; EXO-S (grey solid) 72.3±54.4 nm; EXO-L (dotted) 139.4±69.2 nm

5 Results 3

Development of scFv targeted exosomes

Abstract

Exosomes are a population of extracellular vesicles that mediate cell-to-cell communication mainly through delivery of their content into recipient cells. Exploiting their natural characteristics represents a promising approach for intracellular delivery of therapeutics into diseased or malignant cells. Expression of cell surface antigens CD19 and CD22 is restricted to B cells and as such they represent ideal candidates for B cell targeted nanomedicines, with potential applications in B cell malignancies such as lymphoma and leukemia. Single chain variable fragments targeting CD19 and CD22 were successfully expressed on the exosome surface, through genetic engineering of exosome producing cells. Uptake of CD22-targeted exosomes by CD22-expressing recipient cells was higher and occurred more rapidly compared to uptake of CD19-targeted exosomes. Differences in uptake of exosome subpopulations indicate potential implications of exosome heterogeneity for development of exosome based therapeutics. Whether observed differences in uptake could influence intracellular delivery of biotherapeutics into malignant B cells remains to be addressed.

5.1 Introduction

As outlined in section 1.5 - 1.6 of this DPhil thesis, EVs have emerged as attractive vehicles for delivery of therapeutics. Within the field of nanomedicine and drug delivery, many different types of nanocarriers have been explored and developed (190). However, most of these have major drawbacks, such as immunogenicity, low drug packaging efficiency, rapid clearance, and low *in vivo* stability (190). It is therefore not surprising that interest of the field has shifted towards naturally occurring nano-sized vesicles (EVs), which seem to have favourable characteristics such as low immunogenicity (if derived from appropriate cell types) and ability to overcome natural barriers (132,133).

Increased understanding of the composition, underlying biogenesis, and secretion of EVs have allowed for more precise engineering of EVs secreted by cells. Engineering EVs can allow for successful exploitation of their natural cell-penetrating characteristics for delivery of therapeutics.

5.1.1 Targeting of EVs

Targeting is a strategy commonly employed in nanomedicine to increase the exposure of specific organs, tissues, or cells, to a therapeutic, relative to other organs, tissues, or cells (191). Expression of certain tissue- or cell-type-specific targeting ligands on the surface of EVs can lead to increased accumulation, internalisation into target cells, and retention at the target site, with subsequent enhanced therapeutic effects (192–194).

Multiple methods of EV targeting have been explored (135,192,195–198), most efforts have focused on manipulation of the EV surface through tailoring naturally occurring EV components (i.e. proteins and lipids). For instance, Professor Matthew Wood's lab has made use of the Lamp2b protein, an exosomal membrane protein found abundantly in EXOs. Fusion of the RVG peptide, a central nervous system–specific rabies viral glycoprotein (RVG) peptide, to the extra-exosomal N terminus of Lamp2b, allowed for efficient expression on the EXO surface. Mouse-derived dendritic cells were engineered to overexpress the targeting construct (i.e. endogenous loading), and isolated EXOs displayed targeting to the mouse brain (135).

Recently Gao et al. identified a peptide (CP05) that specifically binds to tetraspanin CD63 (198). The CP05 peptide binds to the second extracellular loop of CD63, which enabled decoration of the EXO surface with different targeting moieties or therapeutics irrespective of EXO source. Anchoring of a muscle-targeting peptide (M12) redirected systemic distribution to specific tissues, including peripheral muscle.

Along similar lines, researchers have developed a method coined 'Exosome Display technology' which makes use of a specific domain of Lactadherin (C1C2) for sorting of proteins to EXOs (195). Fusion of proteins with the C1C2 domain, a domain which belongs to a family of related domains that peripherally associate with the outer exosome membrane by interaction with abundantly expressed phosphatidylserine (PS), enables efficient loading onto the surface of purified vesicles (195). This approach has been successfully applied to express tumour

associated antigens to the surface of EVs and in doing so increase the immunogenicity of the presented antigens (199–201).

5.1.2 Single chain variable fragments for targeting of CD19 and CD22

Recently Longatti et al. combined two aforementioned strategies to generate EXOs targeted towards the surface receptor ERBB2 (Her2) (202). EV-producing cells (HEK293) were genetically engineered to express single chain variable fragment (scFv) domains targeted towards surface receptor ERBB2 (Her2), fused to the C1C2 domain of lactadherin. scFvs are small fusion proteins of the heavy and light chain of an antibody (i.e. the antigen-binding site), as such they represent the smallest antibody derivate that retains the antigen-binding and recognition site (203). By varying the affinity of the expressed scFv and the Her2 receptor expression level on recipient cells, it was determined that both high affinity anti-Her2-scFv (KD ≤ 1 nM) and recipient cells expressing a high level ($\geq 10^6$ copies per cell) of Her2 were optimally required to enable selective uptake. The requirement for the expression of high numbers of receptors may limit the choice of therapeutic targets to those that are highly expressed on target cells, and these may not represent receptors most selectively expressed. As suggested by the authors this finding could also result from the slow internalisation of the Her2 receptor, and targeting of a more rapidly internalising receptor (e.g. CD22) could thus overcome these limitations.

A basis for supporting this hypothesis can be found in the work of Professor Ira Pastan, who has worked on development of recombinant immunotoxins for the treatment of B cell malignancies (e.g. leukemia). B-cell-specific transmembrane

glycoproteins CD19 and CD22 are commonly found on the surface of B cells, and have emerged as targets for treatment of B cell malignancies (204,205).

Immunotoxins (fusion proteins of an antibody and toxin) directed against CD19 have however not shown durable responses in clinical trials (206,207). In contrast, anti-CD22 immunotoxins (composed of the Fv fragment of an anti-CD22 monoclonal antibody fused to a fragment of Pseudomonas exotoxin A) have produced striking results in clinical trials which has resulted in recent approval of Lumoxiti (CD22 immunotoxin; moxetumomab pasudotox) (208–210). Pastan et al. were able to show that this disparity in effect arises due to the rapid internalisation of large amounts of CD22-targeted immunotoxins compared to CD19-targeted immunotoxins (211).

Targeting of B cell surface antigens CD19 and CD22 thus offers a suitable model for studying the dynamics and optimisation of targeting and exosome-based delivery of therapeutics. Furthermore, expression of both antigens is restricted to and upregulated in B cells, which makes off-target effects less likely to occur (204,205).

In line with the approach taken by Longatti et al. (202) scFvs were chosen as B cell surface antigen targeting moieties. Sequences encoding four different scFvs with varying affinities developed by the industrial collaborator Medimmune, two directed against CD19 (6C11 and 3649) and two directed against CD22 (A10 and RFB4), were provided for this work. Due to time constraints only two scFvs were compared, one anti-CD19-scFV (6C11) with an affinity of 30 pM, and anti-CD22-scFV (RFB4) with an affinity 85 nM respectively. Expression on the exosomal

surface was achieved by fusion to the C1C2 domain of lactadherin.

5.1.3 Delivery of biotherapeutics

Most therapeutics are directed exclusively against extracellular molecules or those on the surface of cells which are readily accessible to proteins and molecules. There are however a wealth of molecules present inside of cells which play a role in disease, that currently cannot be targeted in an efficient way due to the inability of therapeutics to enter cells (212).

One of the most intriguing features of EVs is their inherent ability to reach the intracellular environment of recipient cells, and subsequently transmit their content. Early findings report transfer of mRNAs present in EVs derived from embryonic stem cells and cancer cells, which were shown to induce phenotypic changes in recipient haematopoietic progenitor cells and monocytes (13). Since then the ability of EVs to transfer proteins has been observed as well (213,214). Harnessing the content transporting and delivering capacity of EVs represents a promising approach to reach intracellular drug targets. The Wood laboratory was one of the first groups to publish findings on delivery of exogenous siRNA using EXOs (135). As previously described EXOs were derived from mouse dendritic cells which had been engineered to express Lamp2b fused with a brain-specific peptide (rabies virus glycoprotein (RVG)-derived peptide), preferentially directing EXOs to the mouse brain. Targeted EXOs were loaded with beta-secretase 1 (BACE1) siRNA by electroporation. Reducing the expression of BACE1 would prevent build-up of beta-amyloid and may help attenuate disease progression in Alzheimers disease (215).

Strong *in vivo* knockdown of BACE1 mRNA (60%) and protein (62%) in wild-type mice highlights the potential of applying EVs for delivery of therapeutics. Leading on from these findings the interest in EVs as drug delivery tools has grown rapidly, as outlined in detail by Pinheiro et al (216).

5.1.4 Intracellular targets for treatment of B cell malignancies

Two intracellular targets relevant for potential treatment of B cell malignancies are members of the Bcl-2 family of proteins: Bcl-2 (B cell lymphoma 2) and Bcl-xL (B cell lymphoma extra large) (217,218). These proteins govern the process of apoptosis, deregulation of this process allows tumour cells to evade apoptosis, which is one of the hallmarks of cancer (219). Binding of Bcl-2/xL to pro-apoptotic proteins (BAK, BAD, BID and BAX) inhibits the release of cytochrome c release form mitochondria. Cytochrome c release activates apoptotic protease-activating factor 1 (APAF-1), which in turn can trigger the caspase cascade to drive apoptosis. Overexpression of anti-apoptotic Bcl-2 family proteins, which is commonly observed in B cell malignancies, allows malignant B cells to evade apoptosis and plays key role in promoting cell survival. Blocking binding of Bcl-2 and Bcl-xL could thus represent a strong strategy for the induction of apoptosis in B cell malignancies.

Findings below describe the efforts taken to develop EXOs targeted towards B cell surface antigens CD19 and CD22. Loading of targeted EXOs with biotherapeutics was unfortunately not explored due to time limitations. Development of EXO based therapeutics could for a number of reasons outlined in the introduction of this thesis benefit from elucidation of heterogeneity. As such, targeted EXOs were fractionated with both HR-SEC and AF4, uptake of obtained subpopulations was evaluated in an attempt to optimise targeted EXOs.

5.2 Results

5.2.1 Generation of targeted EXOs

In order to generate EXOs which target naturally overexpressed B cell surface antigens CD19 or CD22, transgenes were constructed to encode either anti-CD19 (6C11 and 3649) or anti-CD22 (A10 and RFB4) scFvs, fused to a myc tag and the C1C2 domain of lactadherin (Fig. 5.1 A). Since high expression of the constructs is essential for achieving successful targeting, we generated overexpressing HEK cells via lentiviral transduction. Using this approach four stable cell lines, each expressing a different targeting scFv, were generated. As shown in Fig. 5.1 B, expression of the CD22 targeting construct (RFB4) in HEK293 cells was confirmed through immunoblotting for the expressed myc tag. EXOs were isolated from all four cell lines using SEC.

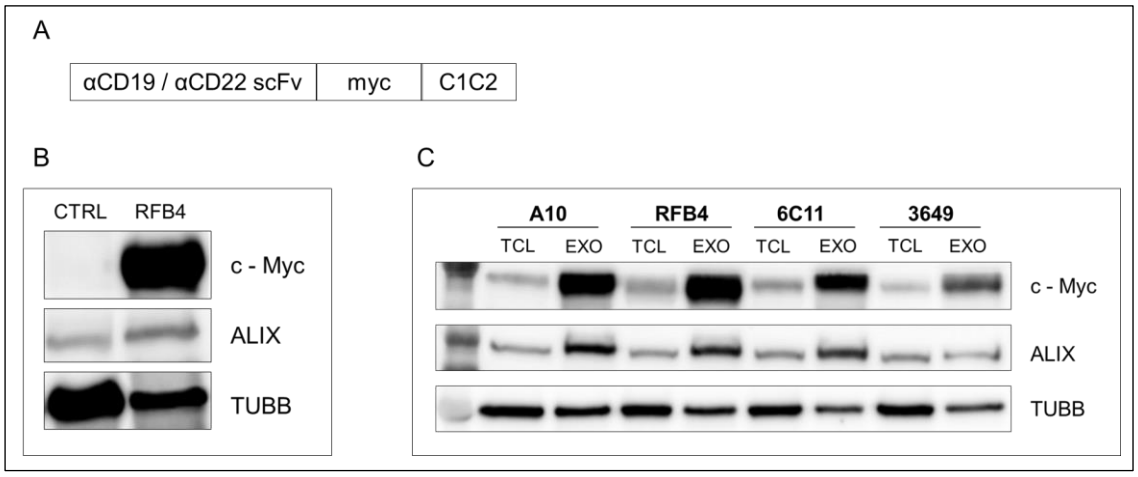


Figure 5.1 Successful generation of CD19 and CD22 targeted EXOs through genetic manipulation of HEK293 cells. A) Schematic illustration of expressed fusion protein design αCD19 / 22, anti-hCD19 or anti-hCD22; myc, myc-tag; C1C2, C1C2-domain of lactadherin. B) Immunoblot analysis of cell lysate from parental HEK293 and HEK293 expressing RFB4-scFv. Equal amounts of protein were loaded. TUBB, beta-tubulin C) Immunoblot analysis of cell lysate and exosomes from HEK293 expressing fusion proteins. Equal amounts of protein were loaded. TCL, total cell lysate; EXO, exosomes; TUBB, beta- tubulin

First of all, immunoblotting to detect the commonly used EXO marker ALIX confirmed successful isolation of EXOs. Secondly, high expression of myc in the isolated EXOs compared to cells confirmed expression and enrichment of the targeting constructs in EXOs (Fig. 5.1 B). Expression of the anti-CD19 scFv 3649 was found to be much lower compared to the other constructs. Subsequent comparison in differences between CD19 and CD22 targeting were made on the basis of anti-CD22 RFB4 and anti-CD19 6C11.

5.2.2 Uptake by target-expressing recipient cells

Next, we set out to determine whether expression of generated targeting constructs on the surface of EXOs would result in differences in uptake efficiency. To obtain EXOS, cell culture supernatant was collected after RFB4 and 6C11 cells had been cultured in serum free conditions (OptiMEM medium) for 48 h. The supernatant was cleared from cellular debris by low speed centrifugation (2,000 x g), and MVs by centrifugation at higher speed (10,000 x g). EXOs were subsequently isolated from the MV depleted supernatant by SEC.

Isolated EXOs were labelled with an Alexa Fluor™ 647 fluorophore through protein crosslinking with primary amines. Making use of this N-hydroxysuccinimide (NHS) ester-mediated derivitisation allows for covalent crosslinking of the label with primary amines, which are present on the outside surfaces of tertiary protein structures. As such they are an easy target for conjugation of the Alexa Fluor™ 647 fluorophore on the EXO surface. Any unbound fluorophore was removed through SEC purification.

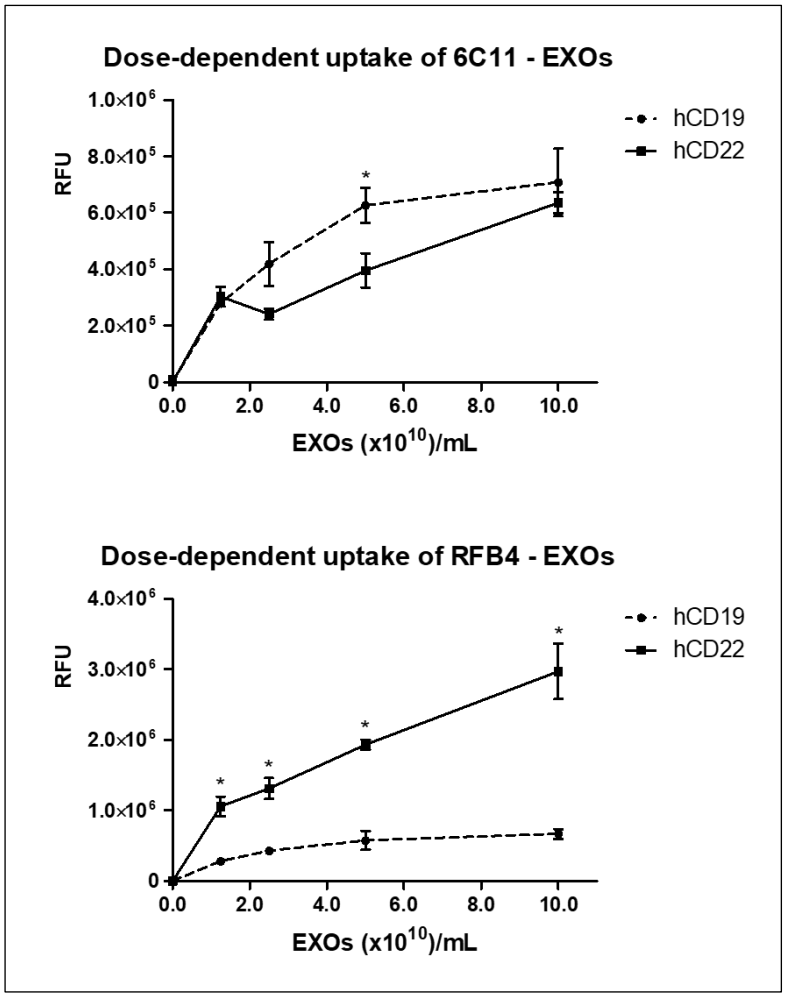


Figure 5.2 Dose - dependent uptake of targeted – EXOs by recipient hCD19 and hCD22 expressing cells. Recipient HEK293 cells expressing hCD19 (dotted line) or hCD22 (solid line) were exposed to increasing amounts of Alexa Fluor™ 647 labelled 6C11 (CD19 targeted) – EXOs (top graph) or RFB4 (CD22 targeted) – EXOs (bottom graph) for four hours. Cells were washed and four images per well were acquired at 20x magnification on an ImageXpress Micro widefield high content microscope (Molecular Devices). Uptake was quantified through Multi-Wavelength Cell Scoring (MetaXpress, Molecular Devices). Values are mean ± SD; n=3. Statistical analysis was performed using the GraphPad Prism 6 software. Uptake at different concentrations was compared using the multiple t-test analysis and corrected for multiple comparisons using the Holm-Sidak correction. * denotes statistically significant difference. Control (0.0 EXOs ($x10^{10}$)/mL), free Alexa Fluor™ 647 NHS Ester; RFU, relative fluorescence units; EXOs, exosomes

Uptake was evaluated by widefield imaging of the recipient cells expressing hCD19 or hCD22 after four hours of incubation, to allow sufficient uptake of EXOs to occur. In all cases dose-dependent uptake of labelled-EXOs was observed (Fig. 5.2). A significant increase in uptake of CD22 targeted RFB4–EXOs by hCD22 expressing cells was observed (Fig. 5.2 lower panel). Uptake of CD19 targeted 6C11-EXOs by hCD19 expressing cells was found to be increased as well, although there was no significant difference in uptake between the hCD19 and hCD22 cells, even after incubation with the highest dose of $10x10^{10}$ EXOs/mL (Fig. 5.2 upper panel).

Subsequently, a time course over four hours was performed by treating the recipient cells with 6C11-EXOs or RFB4-EXOs at the dose of $10x10^{10}$ EXOs/mL. 6C11-EXOs showed a similar uptake profile in both hCD19 and hCD22 expressing cells (Fig. 5.3). A small but significant increase in uptake by hCD22 was observed.

A significant increase in uptake of CD22-targeted RFB4 - EXOs by hCD22 compared to hCD19 expressing cells was already observed after 30 minutes, and continued to increase strongly over the four hour period. Uptake of RFB4-EXOs by hCD19 expressing cells was low compared to uptake by hCD22 expressing cells, and reached a similar level of uptake observed in hCD19 expressing cells after four hours (Fig. 5.3). Aforementioned findings indicate that targeting of hCD22 offers a successful strategy to increase EXO uptake.

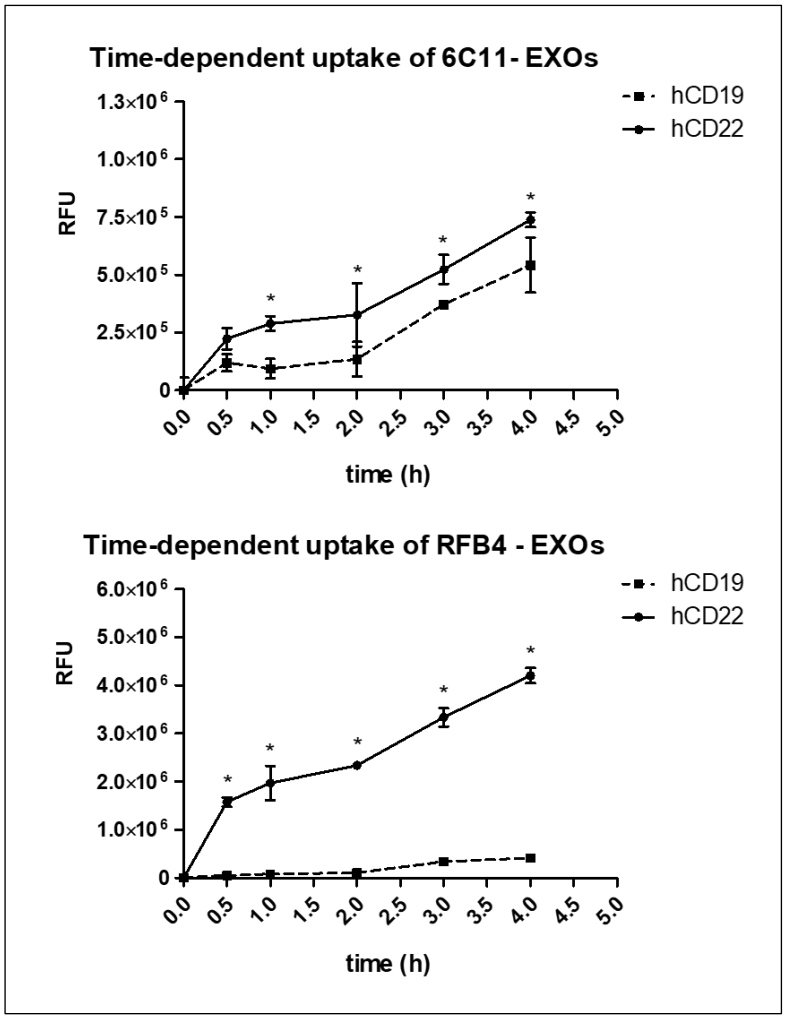


Figure 5.3 Time – dependent uptake of targeted – EXOs by recipient hCD19 and hCD22 expressing cells. Recipient HEK293 cells expressing hCD19 (dotted line) or hCD22 (solid line) were exposed to 10 x 10^{10} EXOs/mL of Alexa Fluor™ 647 labelled 6C11 – EXOs (top graph) or RFB4 – EXOs (bottom graph) for increasing amounts of time. Cells were washed and fixed at indicated time-points. Four images per well were acquired at 20x magnification on an ImageXpress Micro widefield high content microscope (Molecular Devices). Values are mean ± SD; n=3. Uptake was quantified through Multi-Wavelength Cell Scoring (MetaXpress, Molecular Devices). Statistical analysis was performed using the GraphPad Prism 6 software. Uptake at different time points was compared using the multiple t-test analysis and corrected for multiple comparisons using the Holm-Sidak correction. * denotes statistically significant difference. Control, free Alexa Fluor™ 647 NHS Ester; RFU, relative fluorescence units; EXOs, exosomes

5.3 Uptake of EV populations and EXO subpopulations

As outlined in section 1.6 of this DPhil thesis, development of EV-based therapeutics could benefit from understanding which population of EVs is uptake-competent within the highly heterogeneous mix of all secreted vesicles. Indeed, emerging evidence highlights a vast heterogeneity in secreted EVs (24,36,116,183). It is therefore highly likely that cells will release a certain subpopulation of EVs that display characteristics which make them more suitable for targeted delivery of biotherapeutics.

For example, cells may release one subpopulation which displays the following characteristics: high uptake efficiency, low immunogenicity, efficient intracellular delivery capacity, and high stability in circulation, while another subpopulation might interact with cell surface receptors without triggering the uptake event. Aforementioned characteristics make this specific uptake-competent EV subpopulation an excellent candidate for the delivery of biotherapeutics. Specifically engineering an EV producing cell to express the biotherapeutic solely in this subpopulation, or developing a method to allow isolation of only this specific subpopulation would thus be of great importance.

Overexpression of cargo (e.g. biotherapeutics or targeting constructs), such as the approach described in this chapter, will most likely result in the vast majority of secreted EVs expressing the construct especially when cargo is guided to EVs by taking advantage of general EV marker proteins. As such, cargo will end up in most if not all secreted EVs, including the subpopulation displaying characteristics favourable to the therapeutic application as well. Since expression level of cargos in EV producing cells is not unlimited, this strategy might not be

optimal because valuable bioactive cargo is wasted in inherently inactive EVs to a certain extent.

Furthermore, current isolation methods mainly allow for bulk isolation of EV populations. As a result specific benefits of subpopulations or potential subpopulations with negative characteristics (e.g. highly immunogenic and/or rapidly cleared) will be present in the isolated EVs as well.

Therefore, as discussed above, it is important to make sure that the overexpressed cargo proteins would not be expelled to the extracellular environment via EVs as excess molecular garbage – a function of at least some EVs according to a hypothesis of early EV studies (220,221). In order to be able to focus on biologically active EVs, methods must be developed which allow for isolation and characterisation of EV populations in phenotypic assays, and the engineering and purification of only the desired EV subpopulation.

In an attempt to shed light on this hypothesis EXOs from RFB4 and 6C11 were fractionated making use of two independent methods. Firstly the HR-SEC approach described in this DPhil thesis and secondly a recently published AF4 approach (116,149).

5.3.1 HR-SEC Subpopulations

Firstly, classic EV populations MVs and EXOs were isolated from the cell culture supernatant of RFB4 cells. MVs were obtained by centrifugation at 10,000 x g and washed through resuspension in PBS and a second round of centrifugation at 10,000 x g. EXOs were isolated by subjecting the supernatant cleared of MVs (10,000 x g supernatant) to SEC. The isolated populations were labelled with an Alexa Fluor™ 647 fluorophore as described earlier. As shown in Fig. 5.4, NTA measurement confirmed successful isolation of larger heterogeneous MVs (mode size 171.4±60.9 nm), and smaller EXOs (74.9±42.5 nm).

Labelled EXOs were subsequently fractionated according to size using the previously described HR-SEC approach. Four EXO subpopulations (Pool 1 – 4) were obtained through fractionation, NTA measurement confirmed successful fractionation and differences in size of the obtained subpopulations: Pool 1, 156.1±81.6 nm; Pool 2, 114.1±61.9 nm; Pool 3, 90.1 ±58.8 nm; Pool 4, 90.2± 72.7 nm (Fig. 5.4).

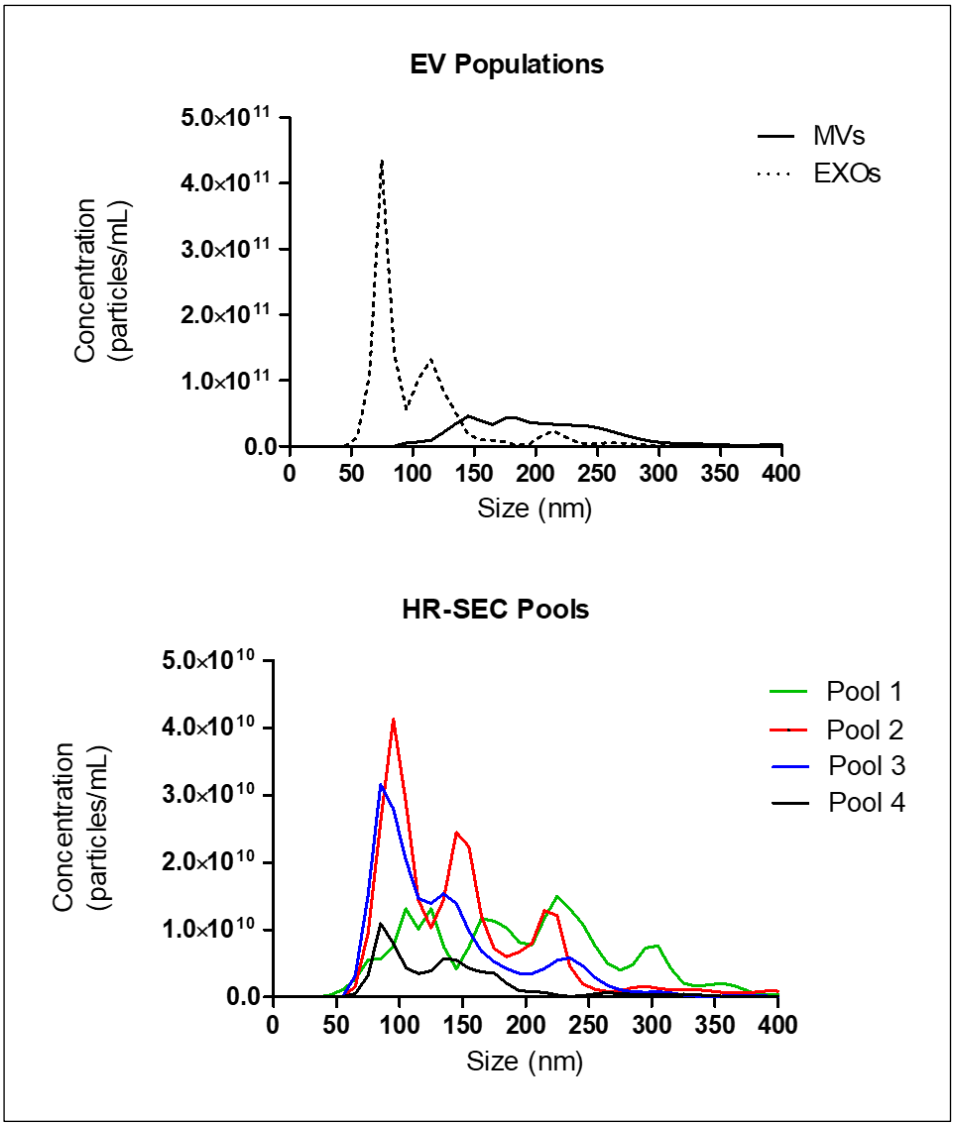


Figure 5.4 EV Populations and HR-SEC EXO subpopulations isolated from RFB4 cells have distinct size distribution profiles. Size distribution of isolated MVs (microvesicles) and EXOs (exosomes) was determined with NTA (top panel). MVs mode size 171.4±60.9 nm; EXOs 74.9±42.5 nm. B) Size distribution of HR-SEC Pools (bottom panel); Pool 1 (green), 156.1± 81.6 nm; Pool 2 (red), 114.1±61.9 nm; Pool 3 (blue), 90.1±58.8 nm; Pool 4 (black), 90.2±72.7 nm.

In order to evaluate potential differences in uptake between the isolated EV populations (MVs and EXOs) and EXO subpopulations (Pool 1-4) HEK293 hCD22 expressing recipient cells were incubated with $2.5x10^{10}$ EVs/mL, for four hours. As shown in Fig. 5.5, no difference in uptake of labelled MVs and EXOs

was observed in HEK293 hCD22 expressing recipient cells. Interestingly, EXO subpopulations showed differential levels of uptake. EXOs present in Pool 2 were found to show a higher level of uptake compared to any of the other EXO subpopulations (i.e. Pool 1, Pool 3, and Pool 4) and EV populations MVs and EXOs. Other EXO subpopulations showed low levels of uptake compared to Pool 2 and EV populations. This finding seems to indicate that EXOs present in Pool 2 might have characteristics which are favourable for uptake and as such engineering of EXOs in Pool 2 could potentially be beneficial.

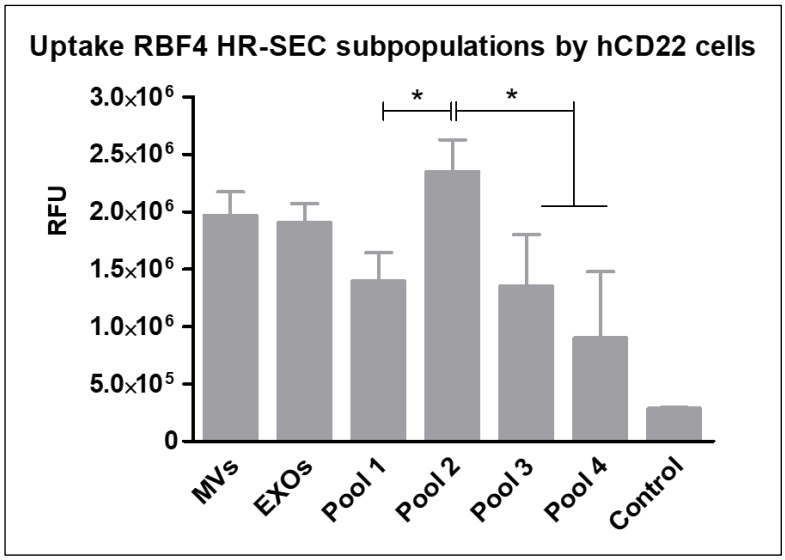


Figure 5.5 Labelled RFB4 - EV Populations and RFB4 - EXO subpopulations show different levels in uptake by hCD22 expressing recipient cells. Recipient cells were exposed to equal amounts of Alexa Fluor™ 647 labelled EVs and Alexa Fluor™ 647 HR-SEC EXO subpopulations ($2.5x10^{10}$ EVs/mL) for four hours, in triplicate. Cells were washed and four images per well were acquired at 20x magnification on an ImageXpress Micro widefield high content microscope (Molecular Devices). Values are mean ± SD; n=3. Uptake was quantified through Multi-Wavelength Cell Scoring (MetaXpress, Molecular Devices). Statistical analysis was performed using the GraphPad Prism 6 software. Uptake of different EV populations was compared using the one-way ANOVA and corrected for multiple comparisons using the Holm-Sidak correction. * denotes statistically significant difference. Control, free Alexa Fluor™ 647 NHS Ester; RFU, relative fluorescence units; MVs, microvesicles; EXOs, exosomes

As shown in Fig. 5.6 and Fig. 5.7, the uptake of all RFB4 - EXO subpopulations could clearly be observed. Closer observation of the cells seem to indicate a potential difference in intracellular localisation of large EXOs (i.e. Pool 1) and small EXOs (Pool 4), which needs further examination.

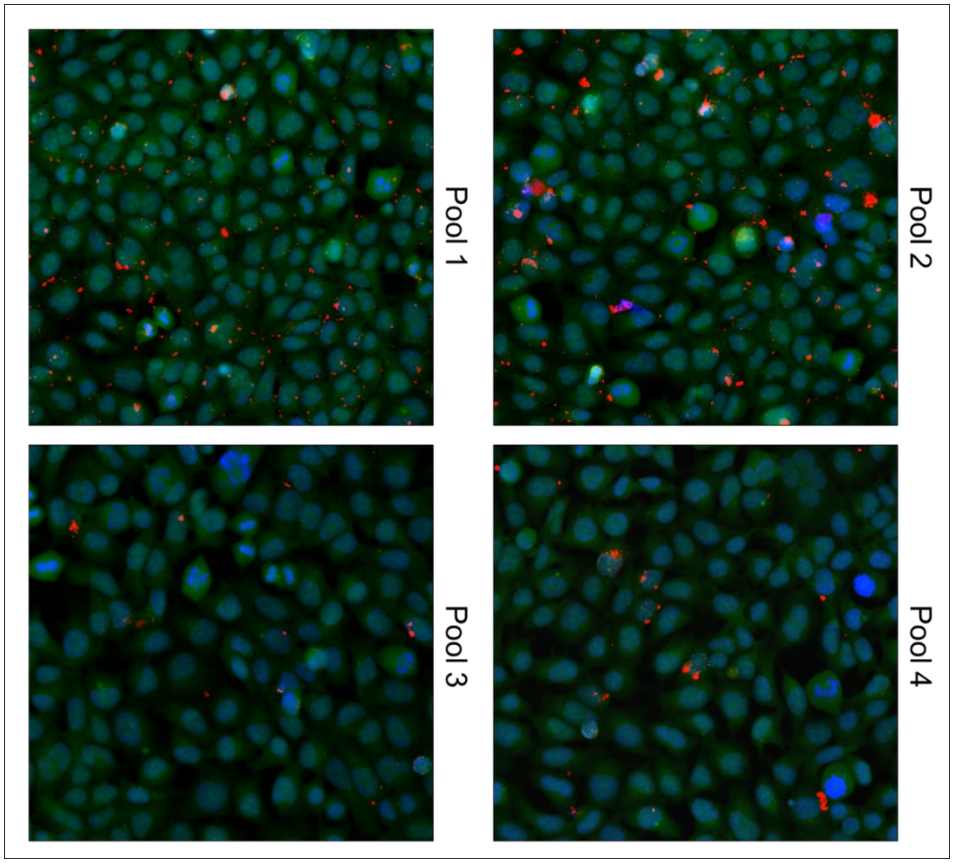


Figure 5.6 HR-SEC EXO Pools show differences in uptake. Alexa Fluor™ 647 labelled EXOs derived from HEK293-αCD22 - RFB4 cells were fractionated through HR-SEC. HEK293-hCD22 expressing cells were incubated with equal amounts of Alexa Fluor™ 647 labelled HR-SEC EXO subpopulations ($2.5x10^{10}$ EVs/mL) for four hours. Images taken on an ImageXpress Micro widefield high content microscope (Molecular Devices). Nuclei in blue, plasma membrane in green, and EXOs in red.

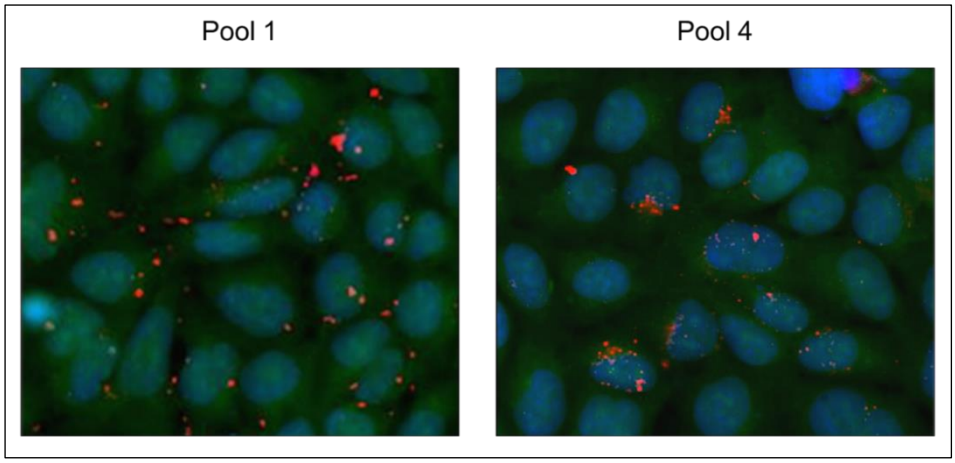


Figure 5.7 Large and small EXOs show a difference in nuclear localisation. Alexa Fluor™ 647 labelled EXOs derived from HEK293-αCD22 - RFB4 cells were fractionated through HR-SEC. HEK293-hCD22 expressing cells were incubated with different pools for 4 hours, in triplicate. Pool 1 (large EXOs), Pool 4 (small EXOs). Nuclei in blue, plasma membrane in green, and EXOs in red.

5.3.2 AF4 Subpopulations

AF4 represents another method which has been used for fractionation of EXOs. We set out to evaluate potential differences in the uptake of 6C11 and RFB4 EXO subpopulations derived using AF4. For this purpose labelled EXOs were fractionated according to the validated protocol into Exo-L, Exo-S, and exomeres (Supplementary Fig. S 5.1). hCD22 expressing recipient cells were subsequently exposed to the different subpopulations for four hours.

As shown in Figure 5.8, a low but significant increase of uptake could only be detected after incubation with the Exo-L subpopulation derived from RFB4 - cells. Interestingly, no uptake could be detected after incubation with any of the other obtained subpopulations.

This finding resembles earlier findings on uptake of HR-SEC subpopulations, larger EXOs present in Pool 2 of HR-SEC EVs were taken up more readily as compared to Pool 3 and 4 which contained smaller vesicles. This could indicate that larger EXOs present in Exo-L display favourable uptake characteristics relevant to development of EV-based therapeutics.

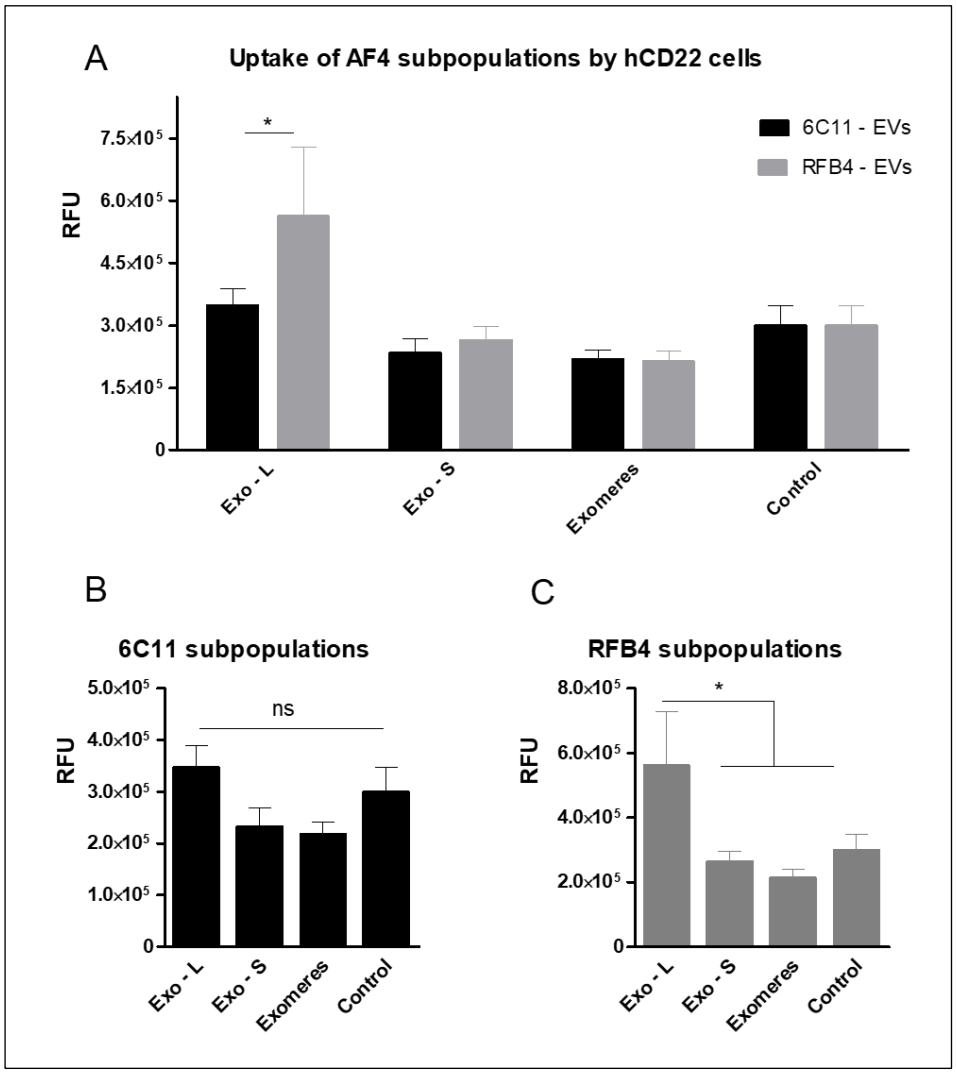


Figure 5.8 Uptake of labelled AF4 - EXO subpopulations by hCD22 expressing recipient cells.

(A) A significant increase in uptake of Exo-L RFB4-EVs compared to Exo-L 6C11-EVs was observed (B) No significant difference in uptake of 6C11-EV populations by hCD22 expressing recipient cells was observed (C) Exo-L RFB4-EVs display a significant increase in uptake by hCD22 expressing recipient cells. Alexa Fluor™ 647 labelled 6C11 - and RFB4 – EVs were fractionated through AF4. Recipient hCD22 expressing cells were incubated for four hours, in triplicate. Cells were washed and four images per well were acquired at 20x magnification on an ImageXpress Micro widefield high content microscope (Molecular Devices). Uptake was quantified through Multi-Wavelength Cell Scoring (MetaXpress, Molecular Devices). Statistical analysis was performed using the GraphPad Prism 6 software. Values are mean ± SD; n=3. Uptake of different subpopulations and sample types were compared using the two-way ANOVA and corrected for multiple comparisons using the Sidak correction. ns, not significant; * denotes statistically significant difference. Control, free Alexa Fluor™ 647 NHS Ester; RFU, relative fluorescence units

5.4 Discussion and conclusions

Findings in this chapter show that targeting of B cell surface antigen CD22 provides an attractive approach for increasing the uptake of EXOs by CD22 expressing cells. HEK293 cells were engineered to express a transgene construct expressing a targeting scFv fused to the C1C2 domain of lactadherin. This approach allowed for efficient expression of both CD22 and CD19 targeting constructs in HEK293-derived EXOs (Fig. 5.1). Although loading of EXOs was found to be efficient, based on the expression of incorporated myc tag, it would be of great interest to determine how many scFv molecules are expressed per isolated EXO. Comparing the level of expressed scFV with levels of the C1C2 binding partner PS, lactadherin, and expressed myc, would provide great insight into the sorting efficiency of engineered cargo into EXOs. scFv expression in other EV populations or EXO subpopulations was not determined, although performed uptake experiments seem to indicate possible differences in expression (Fig. 5.2 and 5.3). The observed differences in uptake could however also be the result of differences in topology of the expressed scFvs between the different EVs, since scFvs have to be expressed on the EV surface in order to interact with CD19 and CD22 on the surface of cells to be taken up.

In our hands HEK293 allowed for successful expression of scFvs in isolated EXOs. HEK293 cells are commonly used as a tool for recombinant expression approaches (222). However, it remains to be determined whether this is the most suitable EV source cell to use for targeting and delivery of cargo into B cells. In addition, concerns around the clinical application of HEK293-derived EVs have been raised. Oncogenic (e.g. epidermal growth factor receptor) and immunogenic proteins and mRNA have been detected in HEK293-derived EVs

(223). Nevertheless, they provide a useful tool for initial study and development of EV based therapeutic approaches.

We next evaluated uptake of scFv-expressing EXOs by recombinant hCD19 and hCD22 receptor expressing HEK293 cells. To this end, 6C11-EXOs (CD19-targeted EXOs) and RFB4-EXOs (CD22-targeted EXOs) were labeled with an Alexa Fluor™ 647 fluorophore. This labelling approach crosslinks the fluorophore with primary amines (224). Detailed studies to determine stability of the labeled EXOs and efficiency of labelling were not performed. However, this covalent crosslinking approach should overcome the drawbacks observed with commonly applied lipid membrane dyes (e.g. cellular dye transfer) (225). However, the crosslinking could change the overall EV charge, subsequently affecting uptake properties.

As shown in Figure 5.2 dose-dependent uptake of EXOs by all recipient cell lines was observed. As hypothesised, RFB4-EXOs were taken up more efficiently and at a very high level by hCD22 expressing cells compared to 6C11-EXOs. However, increased uptake of 6C11-EXO was observed by hCD19 expressing cells. There was no significant difference in uptake by hCD19 cells when cells had been exposed high numbers of EXOs (10×10^{10} EXOs/mL).

Evaluation of uptake over a four hour period revealed interesting differences in uptake dynamics between hCD22 and hCD19 expressing cells (Fig. 5.4). 6C11-EXOs (10×10^{10} EXOs/mL) showed a similar uptake profile in both hCD19 and hCD22 expressing cells. A significant but very small increase in uptake by hCD22 was observed.

In contrast, uptake of RFB4-EXOs by hCD22 expressing cells could already be observed after 30 minutes of exposure and increased rapidly over time. These findings are in line with findings on uptake differences between CD22-targeted immunotoxins (IT) compared to CD19-targeted ITs (211). Internalisation rates of labelled Alexa - 488 ITs by CA46 lymphoma cells was determined by comparing the internalised IT levels with the amount of IT which was bound to the cell surface at a saturated concentration (i.e. 100%) at time point t=0. After 15 minutes 40,000 molecules of CD19-targeted IT (11%) were internalised by CA46 cells and 82,000 molecules (23%) after 4 hours, compared to 216,000 molecules of CD22-targeted IT (230%) after 15 minutes and 229,000 molecules (240%) after 4 hours. The fact that amount of internalised CD22-targeted IT exceeds 100% indicates that, in addition to the initial surface CD22, there might be additional CD22 receptors recruited to the cell surface over time (208,211).

The observed differences in internalisation of CD22-targeted ITs are in line with our observations on uptake of CD22-targeted EXOs compared to CD19-targeted EXOs by recombinant hCD22-overexpressing cells. It remains to be established whether this increase in uptake also occurs in cell lines relevant to B cell malignancies (e.g. CA46 or Ri-1). Rapid internalisation could be a favourable characteristic for *in vivo* application of EVs, ensuring EVs are taken up by target expressing cells before they are cleared out of the systemic circulation (194).

Whether increased EXO uptake can subsequently allow for increased delivery of biotherapeutics remains to be determined. Due to time constraints loading of targeted-EXOs with therapeutics inhibiting anti-apoptotic functions of Bcl-2 and Bcl-xL was not addressed. The described model of targeting B cell surface

antigens CD19 and CD22 with CD19/CD22-scFvs expressing EXOs would be very suitable to explore delivery of EXO loaded biotherapeutics into malignant B cells. Based on the uptake results, higher numbers of CD22-targeted EXOs will most likely reach the intracellular environment of CD22-expressing cells. Whether the internalised EXOs will release their cargo, and whether EXOs are trafficked to reach and release their content in the correct intracellular location remains to be determined. Findings by Longatti et al. indicate that expression of C1C2-scFv constructs can alter intracellular trafficking of EXOs (202).

Uptake of an EXO and its subsequent intracellular fate might also be dependent on individual characteristics such as composition and size. As outlined in this DPhil thesis cells release a heterogeneous population of EVs and distinct EXO subpopulations have been identified (24,116,183). Subpopulations might carry specific surface signatures which dictate their uptake efficiency and intracellular fate. Differences in the specific repertoire of exosomal surface molecules of tumour-derived EXOs has been shown to dictate their homing to their target cell types (99). Harnessing the natural targeting properties of such specific subpopulations could thus be a promising approach.
The relevance of EV heterogeneity for development of EV-based therapeutics has been outlined in section 5.3 of this DPhil thesis.

For example, differences in EV composition might result in differences in scFv expression on the EXO surface and subsequent efficiency of targeting. In an attempt to shed light on heterogeneity of engineered RFB4 and 6C11 EXOs two methods of EXO fractionation were employed (HR-SEC and AF4).

Differences in uptake of four RBF4 EXO subpopulations obtained with HR-SEC were determined. A significant increase in uptake of the RFB4 subpopulation Pool 2 was observed compared to uptake of the three other obtained subpopulations. Uptake of Pool 2 was not significantly increased compared to uptake of the total EXO population. Pool 2 is most likely the major contributor to observed uptake of the EXO population.

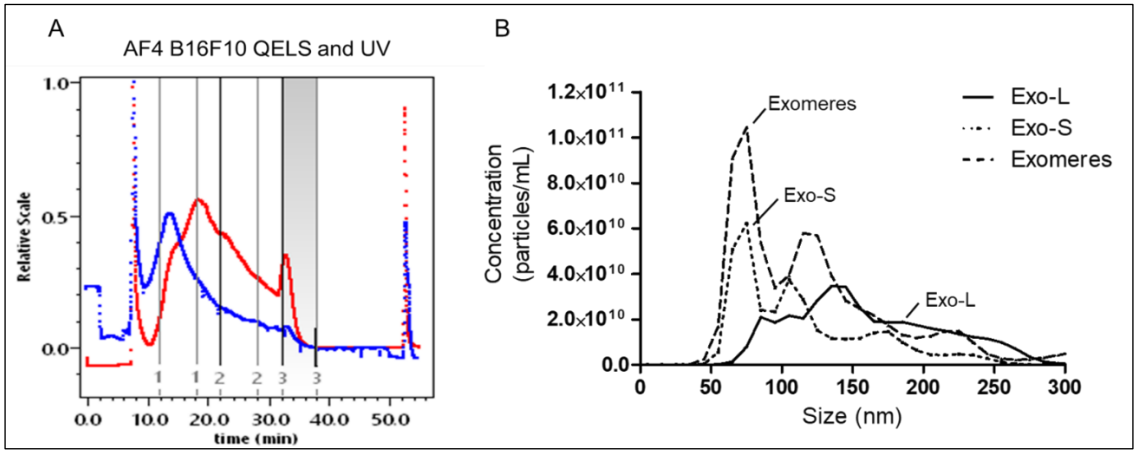
A novel method of EXO fractionation (i.e. AF4) was explored as well in order to address potential differences in uptake of EXO subpopulations. This novel method was used as an orthogonal method to HR-SEC in order to exclude potential method-specific artefacts. AF4 allowed for fractionation of 6C11-EXOs and RFB4-EXOs intro three subpopulations, Exo-L, Exo-S and exomeres, recently defined by Zhang et al. Uptake was only observed when hCD22 expressing cells were exposed to the Exo-L, and uptake of RFB4 Exo-L was significantly higher compared to uptake of 6C11 Exo-L. (Fig. 5.8). Levels of detected uptake and uptake of the other AF4- subpopulations were low, most likely resulting from the fact that EXO yield after AF4 fractionation was low. Interestingly, subpopulations displaying the highest level of uptake (HR-SEC subpopulation Pool 2 and AF4-subpopulation Exo-L) both contain larger EXOs, Pool 2 114.1±61.9 nm and Exo-L 139.4±69.2 nm.

On the basis of the preliminary findings we can't draw any conclusion as to why the larger EXOs display higher uptake. This could be the result of differences in level of scFv expression or differences in topology of the expressed scFv.

The aforementioned findings indicate that development of EXO based nanomedicines could benefit from addressing vesicle heterogeneity and is as such an interesting area to explore. It could for instance allow for identification of subpopulations which display superior uptake or delivery capabilities. Furthermore, the employed fractionation methods could offer an approach to exclude non-engineered EVs not expressing targeting ligands or therapeutic cargo. This might be essential to minimise the risk of potential adverse effects or to increase efficacy of EV-based treatments. Applicability of these techniques for fractionation of engineered EVs on a large scale remains to be evaluated.

In summary, scFvs are successfully expressed on EXOs and used as EXO targeting moieties. Targeting of the rapidly internalising hCD22 with anti-CD22-scFv-containing EXOs allows for rapid and efficient uptake of EXOs. Whether this translates in increased delivery of biotherapeutics, and as such represents a promising EV-based delivery strategy remains to be determined.

5.5 Supplementary figures



Supplementary Figure S 5.1 Fractionation of exosomes and exomeres with AF4. A) Representative fractionation profile of EXOs. Red and blue line illustrate the QELS (DLS) intensity (red line) and UV absorbance (blue line). Fractions were divided into three pools and concentrated with 10 kDa centrifugal units. Pool 1 – Exomeres- (12-18 min); Pool 2 – Exo-S (22-28 min), Pool 3 – Exo-L- (32-38 min). (B) NTA confirms presence of larger EXOs in Exo-L with a mode size of 139.4±69.2 nm and smaller EXOs in Exo-S with a mode size of 72.0±53.1 nm. The < 50 nm size of particles present in Pool 1 (Exomeres) could not be confirmed with NTA analysis, 71.1±67.6 nm respectively.

6 Discussion and conclusion

6.1 Summary of main findings

This DPhil thesis set out to study two important aspects of the EV field: EV heterogeneity and the development of EV - based therapeutics.

The important roles of EVs in intercellular communication were outlined in the introductory chapter. The characteristics of EVs, their biological roles, biogenesis of EVs, and their application as therapeutics are outlined. The role of EVs in cancer has been extensively researched, and as such it provides a strong body of evidence for their biological functions. Increasing evidence highlights the heterogeneous nature of EVs. Heterogeneity and unique functional roles of different EV populations are discussed in the light of cancer. Studies on heterogeneity can benefit from development of innovative EV isolation methods that allow fractionation of populations. I have therefore given an overview of current and emerging methods of EV isolation and the applicability of these methods for studies on heterogeneity (Table 1).

In chapter 3, I set out to study the following hypothesis which proposed that despite the proposed homogenous characteristics of EXOs a wide range of putative functions have so far been reported. On the basis of these diverse reported functions it seemed likely that cells release EXO subpopulations, and that each subpopulation carries out unique functions. The application of density gradient flotation allowed for fractionation of EXOs into two distinct subpopulations. These subpopulations were found to be different in size and composition. Importantly, they are released by a number of different cell lines and

could be retrieved from different EXO sources. Differences observed in the effects of melanoma-derived EXO subpopulations on the gene expression of recipient cells, provided evidence for potential unique functional roles of these two identified subpopulations.

Taken together this chapter showed that two subpopulations of EXOs are present in the total population of EXOs released by cells, and isolated EXOs obtained with commonly used EXO isolation methods. The release and presence of these findings has since then also been reported by others (20,36,226).

In Chapter 4 of this thesis I described a chromatography approach (HR-SEC) that allowed fractionation of isolated EXO. This method provided a tool to study EXO heterogeneity in more detail. Subpopulations with different size and composition were isolated from ovarian-cancer cells. These subpopulations were found to have differential ability to support cellular adhesion. Reported findings, although preliminary, highlight that EXO subpopulations might have unique roles in the processes underlying metastasis of ovarian cancer.

In Chapter 5 I described my approach taken to explore the application of targeted EVs in B cell malignancies. Cells were engineered to release EVs expressing scFvs constructs with high affinity to surface antigens CD19 and CD22. These surface antigens are exclusively expressed by B cells and have therefore been identified and successfully used as targets in the development of treatments for B cell malignancies (227,227–230). Expression of a CD22 targeting scFv on EXOs significantly increased their uptake by CD22 expressing recipient cells.

As outlined in section 1.6 and 5.3, a better understanding of the heterogeneous nature of EXOs and their potential distinct functions, will be crucial for optimising EV-based engineering approaches and development of well-designed EV-based therapeutics. Differences in the uptake efficiency of subpopulations of CD22-targeted EXOs by CD22 expressing recipient cells was observed. This finding illustrated how development of EV-based therapies can benefit from addressing heterogeneity.

6.2 Future prospects for EV heterogeneity research

Addressing the heterogeneous nature of EVs, identifying unique populations, and improving our understanding of respective functions of EV populations released by cells has become of major importance to the EV field (142). Development of new methods for EXO isolation and fractionation will have benefits for all areas of EV research. They can allow us to get a better understanding of the physiological and pathophysiological roles of EVs, as well as improve their clinical application as nanomedicines and biomarkers. Currently there is only a small number of techniques available that can resolve these nano-sized EV populations and even smaller EXO subpopulations (Table 1). Techniques like IM or FC allow for precise studies on the composition of EVs, but are limited by the fact that they first of all currently only allow for study of EV surface proteins. Secondly, study of functionality is not possible because EVs will be bound to the surface of beads utilized for these techniques.

The HR-SEC fractionation approach described in this DPhil thesis therefore represent an attractive approach to study EV heterogeneity. Differences in the

observed functional role of ovarian cancer-derived EXO subpopulations in cellular adhesion indicates the potential of subpopulations serving different roles in ovarian cancer pathology. More detailed studies on their composition are however needed to ascertain a better understanding of their unique components. Obtaining this information can also shed light on potential differences in underlying biogenesis, which have not been explored yet.

The precise role of EVs in ovarian cancer pathology remains to be determined. However, EVs seem to play a role in the spread of ovarian cancer cells from the primary tumour into the peritoneal cavity. This role of EVs has been successfully exploited to develop so called PMT mimics. Disseminated ovarian cancer cells were found to home and adhere to inserts containing ovarian cancer derived EVs (174). Furthermore, as this example illustrates, having an understanding of which specific population is most effective at mediating the functional properties, could directly benefit development of EV-based therapies.

AF4 represent another promising technique that, similar to HR-SEC, allows fractionation of EXOs. A novel particle population termed exomeres has recently been isolated using this technique. Exomeres are even smaller than previously identified EXO subpopulations. Accurate characterisation of EVs remains to be a major challenge. Differences in quantification could bias findings on differences between subpopulations. In order for researchers to make accurate comparisons between subpopulations of different size, the accurate quantification of size and concentration is essential.

Nevertheless, current and emerging evidence on EV populations highlights the importance of addressing EV heterogeneity.

6.3 Future prospects for EV-based therapeutics

EVs have gained great interest because of their potential application as nanomedicine. The natural characteristics of EVs can be harnessed to gain access to the intracellular environment of cells where numerous druggable targets that play a role in disease pathology can be found. However, these targets are challenging to reach due to biological barriers and lack of suitable drug delivery vehicles to overcome those barriers. In an attempt, the field of drug delivery has focused on the development of synthetic lipid drug delivery vesicles such as liposomes.

In contrast to liposomes, the application of EVs for delivery of therapeutics is still in its infancy. Many aspects remain to be addressed to allow successful clinical application of EVs. First of all underlying EV biogenesis and the biological effects of EVs are still not fully understood. Second of all practical issues, such as large-scale production of EVs, large-scale isolation of EVs, and methods of storage might propose difficulties. The EV field can learn from developments made in the liposome field and in return the liposome field can learn from a better understanding of EVs.

6.4 Concluding remarks

The role of EVs in intercellular communication has been well established and developments for their therapeutic application are promising. Findings in this DPhil thesis shed light on one of the major current challenges for the EV field: heterogeneity. Novel isolation and fractionation approaches such as method described this thesis will allow for more in-depth studies on the diverse types of EVs released by cells. A better understanding of the diversity will in turn allow for more precise studies on the underlying biogenesis and unique roles in physiological and pathophysiological processes of EV populations, and provide a strong foundation for the rational development of EV-based therapeutics.

7 References

1. Hargett LA, Bauer NN. On the origin of microparticles: From “platelet dust” to mediators of intercellular communication. Pulm Circ. 2013;3(2):329–40.

2. Wolf P. The nature and significance of platelet products in human plasma. Br J Haematol. 1967 May;13(3):269–88.

3. Anderson HC. Vesicles associated with calcification in the matrix of epiphyseal cartilage. J Cell Biol. 1969 Apr;41(1):59–72.

4. Johnstone RM, Adam M, Hammond JR, Orr L, Turbide C. Vesicle formation during reticulocyte maturation. Association of plasma membrane activities with released vesicles (exosomes). J Biol Chem. 1987 Jul 5;262(19):9412–20.

5. Harding C, Heuser J, Stahl P. Receptor-mediated endocytosis of transferrin and recycling of the transferrin receptor in rat reticulocytes. J Cell Biol. 1983 Aug;97(2):329–39.

6. Johnstone RM, Mathew A, Mason AB, Teng K. Exosome formation during maturation of mammalian and avian reticulocytes: evidence that exosome release is a major route for externalization of obsolete membrane proteins. J Cell Physiol. 1991 Apr;147(1):27–36.

7. Pan BT, Teng K, Wu C, Adam M, Johnstone RM. Electron microscopic evidence for externalization of the transferrin receptor in vesicular form in sheep reticulocytes. J Cell Biol. 1985 Sep;101(3):942–8.

8. Raposo G, Nijman HW, Stoorvogel W, Liejendekker R, Harding CV, Melief CJ, et al. B lymphocytes secrete antigen-presenting vesicles. J Exp Med. 1996 Mar 1;183(3):1161–72.

9. Valadi H, Ekström K, Bossios A, Sjöstrand M, Lee JJ, Lötvall JO. Exosome-mediated transfer of mRNAs and microRNAs is a novel mechanism of genetic exchange between cells. Nat Cell Biol. 2007 Jun;9(6):654–9.

10. Subra C, Grand D, Laulagnier K, Stella A, Lambeau G, Paillasse M, et al. Exosomes account for vesicle-mediated transcellular transport of activatable phospholipases and prostaglandins. J Lipid Res. 2010 Aug;51(8):2105–20.

11. Colombo M, Raposo G, Théry C. Biogenesis, secretion, and intercellular interactions of exosomes and other extracellular vesicles. Annu Rev Cell Dev Biol. 2014;30:255–89.

12. Gatti S, Bruno S, Deregibus MC, Sordi A, Cantaluppi V, Tetta C, et al. Microvesicles derived from human adult mesenchymal stem cells protect

against ischaemia-reperfusion-induced acute and chronic kidney injury. Nephrol Dial Transplant Off Publ Eur Dial Transpl Assoc - Eur Ren Assoc. 2011 May;26(5):1474–83.

13. Ratajczak J, Miekus K, Kucia M, Zhang J, Reca R, Dvorak P, et al. Embryonic stem cell-derived microvesicles reprogram hematopoietic progenitors: evidence for horizontal transfer of mRNA and protein delivery. Leukemia. 2006 May;20(5):847–56.

14. Del Conde I, Shrimpton CN, Thiagarajan P, López JA. Tissue-factor-bearing microvesicles arise from lipid rafts and fuse with activated platelets to initiate coagulation. Blood. 2005 Sep 1;106(5):1604–11.

15. Bellingham SA, Coleman BM, Hill AF. Small RNA deep sequencing reveals a distinct miRNA signature released in exosomes from prion-infected neuronal cells. Nucleic Acids Res. 2012 Nov;40(21):10937–49.

16. Buzas EI, György B, Nagy G, Falus A, Gay S. Emerging role of extracellular vesicles in inflammatory diseases. Nat Rev Rheumatol. 2014 Jun;10(6):356–64.

17. Mack M, Kleinschmidt A, Brühl H, Klier C, Nelson PJ, Cihak J, et al. Transfer of the chemokine receptor CCR5 between cells by membrane-derived microparticles: a mechanism for cellular human immunodeficiency virus 1 infection. Nat Med. 2000 Jul;6(7):769–75.

18. Kalluri R. The biology and function of exosomes in cancer. J Clin Invest. 2016 Apr 1;126(4):1208–15.

19. van Niel G, D'Angelo G, Raposo G. Shedding light on the cell biology of extracellular vesicles. Nat Rev Mol Cell Biol. 2018 Jan 17;

20. Kowal J, Arras G, Colombo M, Jouve M, Morath JP, Primdal-Bengtson B, et al. Proteomic comparison defines novel markers to characterize heterogeneous populations of extracellular vesicle subtypes. Proc Natl Acad Sci. 2016 Feb 8;201521230.

21. Tkach M, Kowal J, Zucchetti AE, Enserink L, Jouve M, Lankar D, et al. Qualitative differences in T-cell activation by dendritic cell-derived extracellular vesicle subtypes. EMBO J. 2017 16;36(20):3012–28.

22. Sork H, Corso G, Krjutskov K, Johansson HJ, Nordin JZ, Wiklander OPB, et al. Heterogeneity and interplay of the extracellular vesicle small RNA transcriptome and proteome. Sci Rep. 2018 Jul 17;8(1):10813.

23. Palma J, Yaddanapudi SC, Pigati L, Havens MA, Jeong S, Weiner GA, et al. MicroRNAs are exported from malignant cells in customized particles. Nucleic Acids Res. 2012 Oct;40(18):9125–38.

24. Willms E, Johansson HJ, Mäger I, Lee Y, Blomberg KEM, Sadik M, et al. Cells release subpopulations of exosomes with distinct molecular and biological properties. Sci Rep. 2016 Mar 2;6.

25. Minciacchi VR, You S, Spinelli C, Morley S, Zandian M, Aspuria P-J, et al. Large oncosomes contain distinct protein cargo and represent a separate functional class of tumor-derived extracellular vesicles. Oncotarget. 2015 Mar 14;6(13):11327–41.

26. Gould SJ, Raposo G. As we wait: coping with an imperfect nomenclature for extracellular vesicles. J Extracell Vesicles. 2013;2.

27. Chevillet JR, Kang Q, Ruf IK, Briggs HA, Vojtech LN, Hughes SM, et al. Quantitative and stoichiometric analysis of the microRNA content of exosomes. Proc Natl Acad Sci U S A. 2014 Oct 14;111(41):14888–93.

28. Squadrito ML, Baer C, Burdet F, Maderna C, Gilfillan GD, Lyle R, et al. Endogenous RNAs modulate microRNA sorting to exosomes and transfer to acceptor cells. Cell Rep. 2014 Sep 11;8(5):1432–46.

29. Pegtel DM, Cosmopoulos K, Thorley-Lawson DA, van Eijndhoven MAJ, Hopmans ES, Lindenberg JL, et al. Functional delivery of viral miRNAs via exosomes. Proc Natl Acad Sci U S A. 2010 Apr 6;107(14):6328–33.

30. Alexander M, Hu R, Runtsch MC, Kagele DA, Mosbruger TL, Tolmachova T, et al. Exosome-delivered microRNAs modulate the inflammatory response to endotoxin. Nat Commun. 2015;6:7321.

31. Bronisz A, Wang Y, Nowicki MO, Peruzzi P, Ansari K, Ogawa D, et al. Extracellular vesicles modulate the glioblastoma microenvironment via a tumor suppression signaling network directed by miR-1. Cancer Res. 2014 Feb 1;74(3):738–50.

32. Kahlert C, Kalluri R. Exosomes in tumor microenvironment influence cancer progression and metastasis. J Mol Med Berl Ger. 2013 Apr;91(4):431–7.

33. Becker A, Thakur BK, Weiss JM, Kim HS, Peinado H, Lyden D. Extracellular Vesicles in Cancer: Cell-to-Cell Mediators of Metastasis. Cancer Cell. 2016 Dec 12;30(6):836–48.

34. Kosaka N, Yoshioka Y, Fujita Y, Ochiya T. Versatile roles of extracellular vesicles in cancer. J Clin Invest. 2016 Apr 1;126(4):1163–72.

35. Rak J. Microparticles in cancer. Semin Thromb Hemost. 2010 Nov;36(8):888–906.

36. Collino F, Pomatto M, Bruno S, Lindoso RS, Tapparo M, Sicheng W, et al. Exosome and Microvesicle-Enriched Fractions Isolated from Mesenchymal Stem Cells by Gradient Separation Showed Different Molecular Signatures and Functions on Renal Tubular Epithelial Cells. Stem Cell Rev. 2017;13(2):226–43.

37. Henne WM, Buchkovich NJ, Emr SD. The ESCRT pathway. Dev Cell. 2011 Jul 19;21(1):77–91.

38. Raiborg C, Stenmark H. The ESCRT machinery in endosomal sorting of ubiquitylated membrane proteins. Nature. 2009 Mar 26;458(7237):445–52.

39. Hurley JH. ESCRTs are everywhere. EMBO J. 2015 Oct 1;34(19):2398–407.

40. Colombo M, Moita C, van Niel G, Kowal J, Vigneron J, Benaroch P, et al. Analysis of ESCRT functions in exosome biogenesis, composition and secretion highlights the heterogeneity of extracellular vesicles. J Cell Sci. 2013 Dec 15;126(Pt 24):5553–65.

41. Stuffers S, Sem Wegner C, Stenmark H, Brech A. Multivesicular endosome biogenesis in the absence of ESCRTs. Traffic Cph Den. 2009 Jul;10(7):925–37.

42. van Niel G, Charrin S, Simoes S, Romao M, Rochin L, Saftig P, et al. The tetraspanin CD63 regulates ESCRT-independent and -dependent endosomal sorting during melanogenesis. Dev Cell. 2011 Oct 18;21(4):708–21.

43. Andreu Z, Yáñez-Mó M. Tetraspanins in extracellular vesicle formation and function. Front Immunol. 2014;5:442.

44. Chairoungdua A, Smith DL, Pochard P, Hull M, Caplan MJ. Exosome release of β-catenin: a novel mechanism that antagonizes Wnt signaling. J Cell Biol. 2010 Sep 20;190(6):1079–91.

45. Trajkovic K, Hsu C, Chiantia S, Rajendran L, Wenzel D, Wieland F, et al. Ceramide triggers budding of exosome vesicles into multivesicular endosomes. Science. 2008 Feb 29;319(5867):1244–7.

46. Balusu S, Van Wonterghem E, De Rycke R, Raemdonck K, Stremersch S, Gevaert K, et al. Identification of a novel mechanism of blood-brain communication during peripheral inflammation via choroid plexus-derived extracellular vesicles. EMBO Mol Med. 2016;8(10):1162–83.

47. Edgar JR, Eden ER, Futter CE. Hrs- and CD63-dependent competing mechanisms make different sized endosomal intraluminal vesicles. Traffic Cph Den. 2014 Feb;15(2):197–211.

48. Stenmark H. Rab GTPases as coordinators of vesicle traffic. Nat Rev Mol Cell Biol. 2009 Aug;10(8):513–25.

49. Li W, Hu Y, Jiang T, Han Y, Han G, Chen J, et al. Rab27A regulates exosome secretion from lung adenocarcinoma cells A549: involvement of EPI64. APMIS Acta Pathol Microbiol Immunol Scand. 2014 Nov;122(11):1080–7.

50. Savina A, Vidal M, Colombo MI. The exosome pathway in K562 cells is regulated by Rab11. J Cell Sci. 2002 Jun 15;115(Pt 12):2505–15.

51. Frühbeis C, Fröhlich D, Kuo WP, Amphornrat J, Thilemann S, Saab AS, et al. Neurotransmitter-Triggered Transfer of Exosomes Mediates Oligodendrocyte–Neuron Communication. PLoS Biol. 2013 Jul 9;11(7).

52. Ostrowski M, Carmo NB, Krumeich S, Fanget I, Raposo G, Savina A, et al. Rab27a and Rab27b control different steps of the exosome secretion pathway. Nat Cell Biol. 2010 Jan;12(1):19–30; sup pp 1-13.

53. Peinado H, Alečković M, Lavotshkin S, Matei I, Costa-Silva B, Moreno-Bueno G, et al. Melanoma exosomes educate bone marrow progenitor cells toward a pro-metastatic phenotype through MET. Nat Med. 2012 Jun;18(6):883–91.

54. Bobrie A, Krumeich S, Reyal F, Recchi C, Moita LF, Seabra MC, et al. Rab27a supports exosome-dependent and -independent mechanisms that modify the tumor microenvironment and can promote tumor progression. Cancer Res. 2012 Oct 1;72(19):4920–30.

55. Hugel B, Martínez MC, Kunzelmann C, Freyssinet J-M. Membrane microparticles: two sides of the coin. Physiol Bethesda Md. 2005 Feb;20:22–7.

56. Bevers EM, Comfurius P, Dekkers DW, Zwaal RF. Lipid translocation across the plasma membrane of mammalian cells. Biochim Biophys Acta. 1999 Aug 18;1439(3):317–30.

57. D'Souza-Schorey C, Chavrier P. ARF proteins: roles in membrane traffic and beyond. Nat Rev Mol Cell Biol. 2006 May;7(5):347.

58. Muralidharan-Chari V, Clancy J, Plou C, Romao M, Chavrier P, Raposo G, et al. ARF6-regulated shedding of tumor cell-derived plasma membrane microvesicles. Curr Biol CB. 2009 Dec 1;19(22):1875–85.

59. Thomas LM, Salter RD. Activation of macrophages by P2X7-induced microvesicles from myeloid cells is mediated by phospholipids and is partially dependent on TLR4. J Immunol Baltim Md 1950. 2010 Sep 15;185(6):3740–9.

60. Li B, Antonyak MA, Zhang J, Cerione RA. RhoA triggers a specific signaling pathway that generates transforming microvesicles in cancer cells. Oncogene. 2012 Nov 8;31(45):4740–9.

61. Caruso S, Poon IKH. Apoptotic Cell-Derived Extracellular Vesicles: More Than Just Debris. Front Immunol. 2018;9:1486.

62. Hristov M, Erl W, Linder S, Weber PC. Apoptotic bodies from endothelial cells enhance the number and initiate the differentiation of human endothelial progenitor cells in vitro. Blood. 2004 Nov 1;104(9):2761–6.

63. Halicka HD, Bedner E, Darzynkiewicz Z. Segregation of RNA and separate packaging of DNA and RNA in apoptotic bodies during apoptosis. Exp Cell Res. 2000 Nov 1;260(2):248–56.

64. Morello M, Minciacchi VR, de Candia P, Yang J, Posadas E, Kim H, et al. Large oncosomes mediate intercellular transfer of functional microRNA. Cell Cycle. 2013 Nov 15;12(22):3526–36.

65. Di Vizio D, Kim J, Hager MH, Morello M, Yang W, Lafargue CJ, et al. Oncosome formation in prostate cancer: association with a region of frequent chromosomal deletion in metastatic disease. Cancer Res. 2009 Jul 1;69(13):5601–9.

66. Lobb RJ, Lima LG, Möller A. Exosomes: Key mediators of metastasis and pre-metastatic niche formation. Semin Cell Dev Biol. 2017 Jul;67:3–10.

67. Yuan Y, Jiang Y-C, Sun C-K, Chen Q-M. Role of the tumor microenvironment in tumor progression and the clinical applications (Review). Oncol Rep. 2016 May;35(5):2499–515.

68. Antonyak MA, Li B, Boroughs LK, Johnson JL, Druso JE, Bryant KL, et al. Cancer cell-derived microvesicles induce transformation by transferring tissue transglutaminase and fibronectin to recipient cells. Proc Natl Acad Sci U S A. 2011 Mar 22;108(12):4852–7.

69. Xiao D, Barry S, Kmetz D, Egger M, Pan J, Rai SN, et al. Melanoma cell-derived exosomes promote epithelial-mesenchymal transition in primary melanocytes through paracrine/autocrine signaling in the tumor microenvironment. Cancer Lett. 2016 01;376(2):318–27.

70. Kucharzewska P, Christianson HC, Welch JE, Svensson KJ, Fredlund E, Ringnér M, et al. Exosomes reflect the hypoxic status of glioma cells and mediate hypoxia-dependent activation of vascular cells during tumor development. Proc Natl Acad Sci U S A. 2013 Apr 30;110(18):7312–7.

71. Geddings JE, Hisada Y, Boulaftali Y, Getz TM, Whelihan M, Fuentes R, et al. Tissue factor-positive tumor microvesicles activate platelets and enhance thrombosis in mice. J Thromb Haemost JTH. 2016 Jan;14(1):153–66.

72. Chalmin F, Ladoire S, Mignot G, Vincent J, Bruchard M, Remy-Martin J-P, et al. Membrane-associated Hsp72 from tumor-derived exosomes mediates STAT3-dependent immunosuppressive function of mouse and human myeloid-derived suppressor cells. J Clin Invest. 2010 Feb;120(2):457–71.

73. Costa-Silva B, Aiello NM, Ocean AJ, Singh S, Zhang H, Thakur BK, et al. Pancreatic cancer exosomes initiate pre-metastatic niche formation in the liver. Nat Cell Biol. 2015 Jun;17(6):816–26.

74. Demory Beckler M, Higginbotham JN, Franklin JL, Ham A-J, Halvey PJ, Imasuen IE, et al. Proteomic analysis of exosomes from mutant KRAS colon cancer cells identifies intercellular transfer of mutant KRAS. Mol Cell Proteomics MCP. 2013 Feb;12(2):343–55.

75. Luhtala N, Hunter T. Failure to detect functional transfer of active K-Ras protein from extracellular vesicles into recipient cells in culture. PLOS ONE. 2018 Sep 7;13(9):e0203290.

76. Todorova D, Simoncini S, Lacroix R, Sabatier F, Dignat-George F. Extracellular Vesicles in Angiogenesis. Circ Res. 2017 May

77. Al-Nedawi K, Meehan B, Micallef J, Lhotak V, May L, Guha A, et al. Intercellular transfer of the oncogenic receptor EGFRvIII by microvesicles derived from tumour cells. Nat Cell Biol. 2008 May;10(5):619–24.

78. Thomas GM, Brill A, Mezouar S, Crescence L, Gallant M, Dubois C, et al. Tissue factor expressed by circulating cancer cell-derived microparticles drastically increases the incidence of deep vein thrombosis in mice. J Thromb Haemost JTH. 2015 Jul;13(7):1310–9.

79. Whiteside TL. Exosomes and tumor-mediated immune suppression. J Clin Invest. 2016 Apr 1;126(4):1216–23.

80. Bobrie A, Théry C. Exosomes and communication between tumours and the immune system: are all exosomes equal? Biochem Soc Trans. 2013 Feb 1;41(1):263–7.

81. Greening DW, Gopal SK, Xu R, Simpson RJ, Chen W. Exosomes and their roles in immune regulation and cancer. Semin Cell Dev Biol. 2015 Apr 1;40:72–81.

82. Wieckowski EU, Visus C, Szajnik M, Szczepanski MJ, Storkus WJ, Whiteside TL. Tumor-derived microvesicles promote regulatory T cell expansion and induce apoptosis in tumor-reactive activated CD8+ T lymphocytes. J Immunol Baltim Md 1950. 2009 Sep 15;183(6):3720–30.

83. Taylor DD, Gerçel-Taylor C, Lyons KS, Stanson J, Whiteside TL. T-cell apoptosis and suppression of T-cell receptor/CD3-zeta by Fas ligand-containing membrane vesicles shed from ovarian tumors. Clin Cancer Res Off J Am Assoc Cancer Res. 2003 Nov 1;9(14):5113–9.

84. Umansky V, Blattner C, Gebhardt C, Utikal J. The Role of Myeloid-Derived Suppressor Cells (MDSC) in Cancer Progression. Vaccines. 2016 Nov 3;4(4).

85. Ricklefs FL, Alayo Q, Krenzlin H, Mahmoud AB, Speranza MC, Nakashima H, et al. Immune evasion mediated by PD-L1 on glioblastoma-derived extracellular vesicles. Sci Adv. 2018 Mar;4(3):eaar2766.

86. Paget S. The distribution of secondary growths in cancer of the breast. 1889. Cancer Metastasis Rev. 1989 Aug;8(2):98–101.

87. Hood JL, San RS, Wickline SA. Exosomes released by melanoma cells prepare sentinel lymph nodes for tumor metastasis. Cancer Res. 2011 Jun 1;71(11):3792–801.

88. Gardiner C, Di Vizio D, Sahoo S, Théry C, Witwer KW, Wauben M, et al. Techniques used for the isolation and characterization of extracellular vesicles: results of a worldwide survey. J Extracell Vesicles. 2016;5:32945.

89. Keerthikumar S, Gangoda L, Liem M, Fonseka P, Atukorala I, Ozcitti C, et al. Proteogenomic analysis reveals exosomes are more oncogenic than ectosomes. Oncotarget. 2015 Jun 20;6(17):15375–96.

90. Tauro BJ, Greening DW, Mathias RA, Mathivanan S, Ji H, Simpson RJ. Two distinct populations of exosomes are released from LIM1863 colon carcinoma cell-derived organoids. Mol Cell Proteomics MCP. 2013 Mar;12(3):587–98.

91. Muhsin-Sharafaldine M-R, Saunderson SC, Dunn AC, Faed JM, Kleffmann T, McLellan AD. Procoagulant and immunogenic properties of melanoma exosomes, microvesicles and apoptotic vesicles. Oncotarget. 2016 Aug 30;7(35):56279–94.

92. Falanga A, Schieppati F, Russo D. Cancer Tissue Procoagulant Mechanisms and the Hypercoagulable State of Patients with Cancer. Semin Thromb Hemost. 2015 Oct;41(7):756–64.

93. Minciacchi VR, Spinelli C, Reis-Sobreiro M, Cavallini L, You S, Zandian M, et al. MYC Mediates Large Oncosome-Induced Fibroblast Reprogramming in Prostate Cancer. Cancer Res. 2017 01;77(9):2306–17.

94. Yáñez-Mó M, Gutiérrez-López MD, Cabañas C. Functional interplay between tetraspanins and proteases. Cell Mol Life Sci CMLS. 2011 Oct;68(20):3323–35.

95. Bassani S, Cingolani LA. Tetraspanins: Interactions and interplay with integrins. Int J Biochem Cell Biol. 2012 May;44(5):703–8.

96. Berditchevski F. Complexes of tetraspanins with integrins: more than meets the eye. J Cell Sci. 2001 Dec;114(Pt 23):4143–51.

97. Rana S, Yue S, Stadel D, Zöller M. Toward tailored exosomes: the exosomal tetraspanin web contributes to target cell selection. Int J Biochem Cell Biol. 2012 Sep;44(9):1574–84.

98. Yue S, Mu W, Erb U, Zöller M. The tetraspanins CD151 and Tspan8 are essential exosome components for the crosstalk between cancer initiating cells and their surrounding. Oncotarget. 2014 Dec 10;6(4):2366–84.

99. Hoshino A, Costa-Silva B, Shen T-L, Rodrigues G, Hashimoto A, Tesic Mark M, et al. Tumour exosome integrins determine organotropic metastasis. Nature. 2015 Nov 19;527(7578):329–35.

100. Théry C, Amigorena S, Raposo G, Clayton A. Isolation and characterization of exosomes from cell culture supernatants and biological fluids. Curr Protoc Cell Biol. 2006 Apr;Chapter 3:Unit 3.22.

101. Menck K, Klemm F, Gross JC, Pukrop T, Wenzel D, Binder C. Induction and transport of Wnt 5a during macrophage-induced malignant invasion is mediated by two types of extracellular vesicles. Oncotarget. 2013 Nov;4(11):2057–66.

102. Crescitelli R, Lässer C, Szabó TG, Kittel A, Eldh M, Dianzani I, et al. Distinct RNA profiles in subpopulations of extracellular vesicles: apoptotic bodies, microvesicles and exosomes. J Extracell Vesicles. 2013 Sep 12;2.

103. Jeppesen DK, Hvam ML, Primdahl-Bengtson B, Boysen AT, Whitehead B, Dyrskjøt L, et al. Comparative analysis of discrete exosome fractions obtained by differential centrifugation. J Extracell Vesicles. 2014;3:25011.

104. Cvjetkovic A, Lötvall J, Lässer C. The influence of rotor type and centrifugation time on the yield and purity of extracellular vesicles. J Extracell Vesicles. 2014;3.

105. Aalberts M, van Dissel-Emiliani FMF, van Adrichem NPH, van Wijnen M, Wauben MHM, Stout TAE, et al. Identification of distinct populations of prostasomes that differentially express prostate stem cell antigen, annexin A1, and GLIPR2 in humans. Biol Reprod. 2012 Mar;86(3):82.

106. Sahlén GE, Egevad L, Ahlander A, Norlén BJ, Ronquist G, Nilsson BO. Ultrastructure of the secretion of prostasomes from benign and malignant epithelial cells in the prostate. The Prostate. 2002 Nov 1;53(3):192–9.

107. Bobrie A, Colombo M, Krumeich S, Raposo G, Théry C. Diverse subpopulations of vesicles secreted by different intracellular mechanisms are present in exosome preparations obtained by differential ultracentrifugation. J Extracell Vesicles. 2012;1.

108. Mol EA, Goumans M-J, Doevendans PA, Sluijter JPG, Vader P. Higher functionality of extracellular vesicles isolated using size-exclusion chromatography compared to ultracentrifugation. Nanomedicine Nanotechnol Biol Med. 2017 Aug;13(6):2061–5.

109. Nordin JZ, Lee Y, Vader P, Mäger I, Johansson HJ, Heusermann W, et al. Ultrafiltration with size-exclusion liquid chromatography for high yield isolation of extracellular vesicles preserving intact biophysical and

functional properties. Nanomedicine Nanotechnol Biol Med. 2015 May;11(4):879–83.

110. Benedikter BJ, Bouwman FG, Vajen T, Heinzmann ACA, Grauls G, Mariman EC, et al. Ultrafiltration combined with size exclusion chromatography efficiently isolates extracellular vesicles from cell culture media for compositional and functional studies. Sci Rep. 2017 Nov 10;7(1):15297.

111. Willis GR, Kourembanas S, Mitsialis SA. Toward Exosome-Based Therapeutics: Isolation, Heterogeneity, and Fit-for-Purpose Potency. Front Cardiovasc Med. 2017;4.

112. Xu R, Simpson RJ, Greening DW. A Protocol for Isolation and Proteomic Characterization of Distinct Extracellular Vesicle Subtypes by Sequential Centrifugal Ultrafiltration. Methods Mol Biol Clifton NJ. 2017;1545:91–116.

113. Xu R, Greening DW, Rai A, Ji H, Simpson RJ. Highly-purified exosomes and shed microvesicles isolated from the human colon cancer cell line LIM1863 by sequential centrifugal ultrafiltration are biochemically and functionally distinct. Methods San Diego Calif. 2015 Oct 1;87:11–25.

114. Introduction to Tangential Flow Filtration for Laboratory and Process Development Applications.

115. Andriolo G, Provasi E, Lo Cicero V, Brambilla A, Soncin S, Torre T, et al. Exosomes From Human Cardiac Progenitor Cells for Therapeutic Applications: Development of a GMP-Grade Manufacturing Method. Front Physiol. 2018;9:1169.

116. Zhang H, Freitas D, Kim HS, Fabijanic K, Li Z, Chen H, et al. Identification of distinct nanoparticles and subsets of extracellular vesicles by asymmetric flow field-flow fractionation. Nat Cell Biol. 2018 Mar;20(3):332–43.

117. Giddings JC. A New Separation Concept Based on a Coupling of Concentration and Flow Nonuniformities. Sep Sci. 1966 Jan 1;1(1):123–5.

118. Citkowicz A, Petry H, Harkins RN, Ast O, Cashion L, Goldmann C, et al. Characterization of virus-like particle assembly for DNA delivery using asymmetrical flow field-flow fractionation and light scattering. Anal Biochem. 2008 May 15;376(2):163–72.

119. Sitar S, Kejžar A, Pahovnik D, Kogej K, Tušek-Žnidarič M, Lenassi M, et al. Size characterization and quantification of exosomes by asymmetrical-flow field-flow fractionation. Anal Chem. 2015 Sep 15;87(18):9225–33.

120. Kang D, Oh S, Ahn S-M, Lee B-H, Moon MH. Proteomic analysis of exosomes from human neural stem cells by flow field-flow fractionation

and nanoflow liquid chromatography-tandem mass spectrometry. J Proteome Res. 2008 Aug;7(8):3475–80.

121. Flack K, Jimenez LA, Zhong W. Analysis of the Distribution Profiles of Circulating MicroRNAs by Asymmetrical Flow Field Flow Fractionation. Methods Mol Biol Clifton NJ. 2017;1509:161–8.

122. Bousse T, Shore DA, Goldsmith CS, Hossain MJ, Jang Y, Davis CT, et al. Quantitation of influenza virus using field flow fractionation and multi-angle light scattering for quantifying influenza A particles. J Virol Methods. 2013 Nov;193(2):589–96.

123. Petersen KE, Manangon E, Hood JL, Wickline SA, Fernandez DP, Johnson WP, et al. A review of exosome separation techniques and characterization of B16-F10 mouse melanoma exosomes with AF4-UV-MALS-DLS-TEM. Anal Bioanal Chem. 2014 Dec;406(30):7855–66.

124. Yang JS, Lee JC, Byeon SK, Rha KH, Moon MH. Size Dependent Lipidomic Analysis of Urinary Exosomes from Patients with Prostate Cancer by Flow Field-Flow Fractionation and Nanoflow Liquid Chromatography-Tandem Mass Spectrometry. Anal Chem. 2017 Feb 21;89(4):2488–96.

125. Gholizadeh S, Shehata Draz M, Zarghooni M, Sanati-Nezhad A, Ghavami S, Shafiee H, et al. Microfluidic approaches for isolation, detection, and characterization of extracellular vesicles: Current status and future directions. Biosens Bioelectron. 2017 May 15;91(Supplement C):588–605.

126. Shin S, Han D, Park MC, Mun JY, Choi J, Chun H, et al. Separation of extracellular nanovesicles and apoptotic bodies from cancer cell culture broth using tunable microfluidic systems. Sci Rep. 2017 Aug 30;7(1):9907.

127. Welsh JA, Holloway JA, Wilkinson JS, Englyst NA. Extracellular Vesicle Flow Cytometry Analysis and Standardization. Front Cell Dev Biol. 2017 Aug 30;5.

128. Nolte-’t Hoen ENM, van der Vlist EJ, Aalberts M, Mertens HCH, Bosch BJ, Bartelink W, et al. Quantitative and qualitative flow cytometric analysis of nanosized cell-derived membrane vesicles. Nanomedicine Nanotechnol Biol Med. 2012 Jul;8(5):712–20.

129. Groot Kormelink T, Arkesteijn GJA, Nauwelaers FA, van den Engh G, Nolte-’t Hoen ENM, Wauben MHM. Prerequisites for the analysis and sorting of extracellular vesicle subpopulations by high-resolution flow cytometry. Cytom Part J Int Soc Anal Cytol. 2016 Feb;89(2):135–47.

130. Higginbotham JN, Zhang Q, Jeppesen DK, Scott AM, Manning HC, Ochieng J, et al. Identification and characterization of EGF receptor in

individual exosomes by fluorescence-activated vesicle sorting. J Extracell Vesicles. 2016;5:29254.

131. Koliha N, Wiencek Y, Heider U, Jüngst C, Kladt N, Krauthäuser S, et al. A novel multiplex bead-based platform highlights the diversity of extracellular vesicles. J Extracell Vesicles. 2016;5:29975.

132. Vader P, Mol EA, Pasterkamp G, Schiffelers RM. Extracellular vesicles for drug delivery. Adv Drug Deliv Rev. 2016 Nov 15;106(Pt A):148–56.

133. EL Andaloussi S, Mäger I, Breakefield XO, Wood MJA. Extracellular vesicles: biology and emerging therapeutic opportunities. Nat Rev Drug Discov. 2013 May;12(5):347–57.

134. O'Loughlin AJ, Mäger I, Jong OG de, Varela MA, Schiffelers RM, Andaloussi SE, et al. Functional Delivery of Lipid-Conjugated siRNA by Extracellular Vesicles. Mol Ther. 2017 Jul 5;25(7):1580–7.

135. Alvarez-Erviti L, Seow Y, Yin H, Betts C, Lakhal S, Wood MJ. Delivery of siRNA to the mouse brain by systemic injection of targeted exosomes. Nature Biotechnol. 2011.

136. Zhang Y, Liu D, Chen X, Li J, Li L, Bian Z, et al. Secreted monocytic miR-150 enhances targeted endothelial cell migration. Mol Cell. 2010 Jul 9;39(1):133–44.

137. Pascucci L, Coccè V, Bonomi A, Ami D, Ceccarelli P, Ciusani E, et al. Paclitaxel is incorporated by mesenchymal stromal cells and released in exosomes that inhibit in vitro tumor growth: a new approach for drug delivery. J Control Release Off J Control Release Soc. 2014 Oct 28;192:262–70.

138. Kanuma T, Yamamoto T, Kobiyama K, Moriishi E, Masuta Y, Kusakabe T, et al. CD63-Mediated Antigen Delivery into Extracellular Vesicles via DNA Vaccination Results in Robust CD8+ T Cell Responses. J Immunol Baltim Md 1950. 2017 15;198(12):4707–15.

139. Zhou H, Yuen PST, Pisitkun T, Gonzales PA, Yasuda H, Dear JW, et al. Collection, storage, preservation, and normalization of human urinary exosomes for biomarker discovery. Kidney Int. 2006 Apr;69(8):1471–6.

140. Skog J, Wurdinger T, van Rijn S, Meijer D, Gainche L, Sena-Esteves M, et al. Glioblastoma microvesicles transport RNA and protein that promote tumor growth and provide diagnostic biomarkers. Nat Cell Biol. 2008 Dec;10(12):1470–6.

141. Thompson AG, Gray E, Heman-Ackah SM, Mäger I, Talbot K, Andaloussi SE, et al. Extracellular vesicles in neurodegenerative disease - pathogenesis to biomarkers. Nat Rev Neurol. 2016 Jun;12(6):346–57.

142. Tkach M, Kowal J, Théry C. Why the need and how to approach the functional diversity of extracellular vesicles. Philos Trans R Soc Lond B Biol Sci. 2018 Jan 5;373(1737).

143. Kanada M, Bachmann MH, Hardy JW, Frimannson DO, Bronsart L, Wang A, et al. Differential fates of biomolecules delivered to target cells via extracellular vesicles. Proc Natl Acad Sci U S A. 2015 Mar 24;112(12):E1433–42.

144. Caponnetto F, Manini I, Skrap M, Palmai-Pallag T, Di Loreto C, Beltrami AP, et al. Size-dependent cellular uptake of exosomes. Nanomedicine Nanotechnol Biol Med. 2017;13(3):1011–20.

145. Soares Martins T, Catita J, Martins Rosa I, A. B. da Cruz e Silva O, Henriques AG. Exosome isolation from distinct biofluids using precipitation and column-based approaches. PLoS ONE. 2018 Jun 11;13(6).

146. Jeyaram A, Jay SM. Preservation and Storage Stability of Extracellular Vesicles for Therapeutic Applications. AAPS J. 2017 Nov 27;20(1):1.

147. Lőrincz ÁM, Timár CI, Marosvári KA, Veres DS, Otrokocsi L, Kittel Á, et al. Effect of storage on physical and functional properties of extracellular vesicles derived from neutrophilic granulocytes. J Extracell Vesicles. 2014;3:25465.

148. Yuana Y, Böing AN, Grootemaat AE, van der Pol E, Hau CM, Cizmar P, et al. Handling and storage of human body fluids for analysis of extracellular vesicles. J Extracell Vesicles. 2015;4:29260.

149. Zhang H, Lyden D. A protocol for Asymmetric-Flow Field-Flow Fractionation (AF4) of small extracellular vesicles. 2018 Feb 19.

150. Pfaffl MW. A new mathematical model for relative quantification in real-time RT-PCR. Nucleic Acids Res. 2001 May 1;29(9):e45.

151. Raposo G, Stoorvogel W. Extracellular vesicles: exosomes, microvesicles, and friends. J Cell Biol. 2013 Feb 18;200(4):373–83.

152. Trajkovic K, Hsu C, Chiantia S, Rajendran L, Wenzel D, Wieland F, et al. Ceramide triggers budding of exosome vesicles into multivesicular endosomes. Science. 2008 Feb 29;319(5867):1244–7.

153. van Niel G, Charrin S, Simoes S, Romao M, Rochin L, Saftig P, et al. The tetraspanin CD63 regulates ESCRT-independent and -dependent endosomal sorting during melanogenesis. Dev Cell. 2011 Oct 18;21(4):708–21.

154. Santana SM, Antonyak MA, Cerione RA, Kirby BJ. Cancerous Epithelial Cell Lines Shed Extracellular Vesicles With a Bimodal Size Distribution that is Sensitive to Glutamine Inhibition. Phys Biol. 2014 Nov 26;11(6):065001.

155. van der Vlist EJ, Arkesteijn GJA, van de Lest CHA, Stoorvogel W, Nolte-'t Hoen ENM, Wauben MHM. CD4(+) T cell activation promotes the differential release of distinct populations of nanosized vesicles. J Extracell Vesicles. 2012;1.

156. Lunavat TR, Cheng L, Kim D-K, Bhadury J, Jang SC, Lässer C, et al. Small RNA deep sequencing discriminates subsets of extracellular vesicles released by melanoma cells--Evidence of unique microRNA cargos. RNA Biol. 2015;12(8):810–23.

157. Keerthikumar S, Gangoda L, Liem M, Fonseka P, Atukorala I, Ozcitti C, et al. Proteogenomic analysis reveals exosomes are more oncogenic than ectosomes. Oncotarget. 2015 Apr 12;6(17):15375–96.

158. Honda K, Yamada T, Hayashida Y, Idogawa M, Sato S, Hasegawa F, et al. Actinin-4 increases cell motility and promotes lymph node metastasis of colorectal cancer. Gastroenterology. 2005 Jan;128(1):51–62.

159. Van Raemdonck GAA, Tjalma WAA, Coen EP, Depuydt CE, Van Ostade XWM. Identification of protein biomarkers for cervical cancer using human cervicovaginal fluid. PloS One. 2014;9(9):e106488.

160. Liu D, Guest S, Finley RL. Why cyclin Y? A highly conserved cyclin with essential functions. Fly (Austin). 2010 Dec;4(4):278–82.

161. Kuijper S, Turner CJ, Adams RH. Regulation of angiogenesis by Eph-ephrin interactions. Trends Cardiovasc Med. 2007 Jul;17(5):145–51.

162. Gong J, Körner R, Gaitanos L, Klein R. Exosomes mediate cell contact-independent ephrin-Eph signaling during axon guidance. J Cell Biol. 2016 Jul 4;214(1):35–44.

163. Pasquale EB. Eph receptors and ephrins in cancer: bidirectional signalling and beyond. Nat Rev Cancer. 2010 Mar;10(3):165–80.

164. Zhao Y, Yin L, Zhang H, Lan T, Li S, Ma P. Eph/ephrin Family Anchored on Exosome Facilitate Communications between Cells. Cell Biol Int. 2018 Apr 6.

165. Jenjaroenpun P, Kremenska Y, Nair VM, Kremenskoy M, Joseph B, Kurochkin IV. Characterization of RNA in exosomes secreted by human breast cancer cell lines using next-generation sequencing. PeerJ. 2013;1:e201.

166. Corso G, Mäger I, Lee Y, Görgens A, Bultema J, Giebel B, et al. Reproducible and scalable purification of extracellular vesicles using combined bind-elute and size exclusion chromatography. Sci Rep. 2017 Sep 14;7.

167. Towbin H, Gordon J. Immunoblotting and dot immunobinding--current status and outlook. J Immunol Methods. 1984 Sep 4;72(2):313–40.

168. Ozawa PMM, Alkhilaiwi F, Cavalli IJ, Malheiros D, de Souza Fonseca Ribeiro EM, Cavalli LR. Extracellular vesicles from triple-negative breast cancer cells promote proliferation and drug resistance in non-tumorigenic breast cells. Breast Cancer Res Treat. 2018 Sep.

169. Wei M, Yang T, Chen X, Wu Y, Deng X, He W, et al. Malignant ascites-derived exosomes promote proliferation and induce carcinoma-associated fibroblasts transition in peritoneal mesothelial cells. Oncotarget. 2017 Feb 2;8(26):42262–71.

170. Qu J-L, Qu X-J, Zhao M-F, Teng Y-E, Zhang Y, Hou K-Z, et al. Gastric cancer exosomes promote tumour cell proliferation through PI3K/Akt and MAPK/ERK activation. Dig Liver Dis. 2009 Dec 1;41(12):875–80.

171. Li C, Liu D-R, Li G-G, Wang H-H, Li X-W, Zhang W, et al. CD97 promotes gastric cancer cell proliferation and invasion through exosome-mediated MAPK signaling pathway. World J Gastroenterol. 2015 May 28;21(20):6215–28.

172. Paolillo M, Schinelli S. Integrins and Exosomes, a Dangerous Liaison in Cancer Progression. Cancers. 2017 Jul 26;9(8).

173. Strobel T, Cannistra SA. Beta1-integrins partly mediate binding of ovarian cancer cells to peritoneal mesothelium in vitro. Gynecol Oncol. 1999 Jun;73(3):362–7.

174. de la Fuente A, Alonso-Alconada L, Costa C, Cueva J, Garcia-Caballero T, Lopez-Lopez R, et al. M-Trap: Exosome-Based Capture of Tumor Cells as a New Technology in Peritoneal Metastasis. JNCI J Natl Cancer Inst. 2015 Jul 6;107(9).

175. Lengyel E. Ovarian Cancer Development and Metastasis. Am J Pathol. 2010 Sep 1;177(3):1053–64.

176. Halkia E, Spiliotis J, Sugarbaker P. Diagnosis and Management of Peritoneal Metastases from Ovarian Cancer. Gastroenterology Research and Practice. 2012.

177. Burleson KM, Casey RC, Skubitz KM, Pambuccian SE, Oegema TR, Skubitz APN. Ovarian carcinoma ascites spheroids adhere to extracellular matrix components and mesothelial cell monolayers. Gynecol Oncol. 2004 Apr 1;93(1):170–81.

178. Sandoval P, Jiménez-Heffernan JA, Rynne-Vidal Á, Pérez-Lozano ML, Gilsanz Á, Ruiz-Carpio V, et al. Carcinoma-associated fibroblasts derive from mesothelial cells via mesothelial-to-mesenchymal transition in peritoneal metastasis. J Pathol. 2013 Dec;231(4):517–31.

179. Worzfeld T, Pogge von Strandmann E, Huber M, Adhikary T, Wagner U, Reinartz S, et al. The Unique Molecular and Cellular Microenvironment of Ovarian Cancer. Front Oncol. 2017;7:24.

180. De Vlieghere E, Gremonprez F, Verset L, Mariën L, Jones CJ, De Craene B, et al. Tumor-environment biomimetics delay peritoneal metastasis formation by deceiving and redirecting disseminated cancer cells. Biomaterials. 2015 Jun;54:148–57.

181. Huang R, Rofstad EK. Integrins as therapeutic targets in the organ-specific metastasis of human malignant melanoma. J Exp Clin Cancer Res CR. 2018 Apr 27;37(1):92.

182. Reyes R, Monjas A, Yánez-Mó M, Cardeñes B, Morlino G, Gilsanz A, et al. Different states of integrin LFA-1 aggregation are controlled through its association with tetraspanin CD9. Biochim Biophys Acta. 2015 Oct;1853(10 Pt A):2464–80.

183. Kowal J, Arras G, Colombo M, Jouve M, Morath JP, Primdal-Bengtson B, et al. Proteomic comparison defines novel markers to characterize heterogeneous populations of extracellular vesicle subtypes. Proc Natl Acad Sci U S A. 2016 Feb 23;113(8):E968-977.

184. Clayton A, Turkes A, Dewitt S, Steadman R, Mason MD, Hallett MB. Adhesion and signaling by B cell-derived exosomes: the role of integrins. FASEB J Off Publ Fed Am Soc Exp Biol. 2004 Jun;18(9):977–9.

185. Zigler M, Dobroff AS, Bar-Eli M. Cell adhesion: implication in tumor progression. Minerva Med. 2010 Jun;101(3):149–62.

186. Koumangoye RB, Sakwe AM, Goodwin JS, Patel T, Ochieng J. Detachment of breast tumor cells induces rapid secretion of exosomes which subsequently mediate cellular adhesion and spreading. PloS One. 2011;6(9):e24234.

187. Watson K, Koumangoye R, Thompson P, Sakwe AM, Patel T, Pratap S, et al. Fetuin-A triggers the secretion of a novel set of exosomes in detached tumor cells that mediate their adhesion and spreading. FEBS Lett. 2012 Sep 21;586(19):3458–63.

188. Nangami G, Koumangoye R, Shawn Goodwin J, Sakwe AM, Marshall D, Higginbotham J, et al. Fetuin-A associates with histones intracellularly and shuttles them to exosomes to promote focal adhesion assembly resulting in rapid adhesion and spreading in breast carcinoma cells. Exp Cell Res. 2014 Nov 1;328(2):388–400.

189. Nakamura K, Sawada K, Kinose Y, Yoshimura A, Toda A, Nakatsuka E, et al. Exosomes Promote Ovarian Cancer Cell Invasion through Transfer of CD44 to Peritoneal Mesothelial Cells. Mol Cancer Res. 2017 Jan 1;15(1):78–92.

190. Tran S, DeGiovanni P-J, Piel B, Rai P. Cancer nanomedicine: a review of recent success in drug delivery. Clin Transl Med. 2017 Dec 11;6.

191. Torchilin VP. Drug targeting. Eur J Pharm Sci Off J Eur Fed Pharm Sci. 2000 Oct;11 Suppl 2:S81-91.

192. Kooijmans SAA, Gitz-Francois JJJM, Schiffelers RM, Vader P. Recombinant phosphatidylserine-binding nanobodies for targeting of extracellular vesicles to tumor cells: a plug-and-play approach. Nanoscale. 2018 Feb 1;10(5):2413–26.

193. Shen B, Wu N, Yang J-M, Gould SJ. Protein targeting to exosomes/microvesicles by plasma membrane anchors. J Biol Chem. 2011 Apr 22;286(16):14383–95.

194. Wiklander OPB, Nordin JZ, O'Loughlin A, Gustafsson Y, Corso G, Mäger I, et al. Extracellular vesicle in vivo biodistribution is determined by cell source, route of administration and targeting. J Extracell Vesicles. 2015;4:26316.

195. Delcayre A, Estelles A, Sperinde J, Roulon T, Paz P, Aguilar B, et al. Exosome Display technology: applications to the development of new diagnostics and therapeutics. Blood Cells Mol Dis. 2005 Oct;35(2):158–68.

196. Stickney Z, Losacco J, McDevitt S, Zhang Z, Lu B. Development of exosome surface display technology in living human cells. Biochem Biophys Res Commun. 2016 Mar 25;472(1):53–9.

197. Antes TJ, Middleton RC, Luther KM, Ijichi T, Peck KA, Liu WJ, et al. Targeting extracellular vesicles to injured tissue using membrane cloaking and surface display. J Nanobiotechnology. 2018 Aug 30;16(1):61.

198. Gao X, Ran N, Dong X, Zuo B, Yang R, Zhou Q, et al. Anchor peptide captures, targets, and loads exosomes of diverse origins for diagnostics and therapy. Sci Transl Med. 2018 06;10(444).

199. Rountree RB, Mandl SJ, Nachtwey JM, Dalpozzo K, Do L, Lombardo JR, et al. Exosome targeting of tumor antigens expressed by cancer vaccines can improve antigen immunogenicity and therapeutic efficacy. Cancer Res. 2011 Aug 1;71(15):5235–44.

200. Hartman ZC, Wei J, Glass OK, Guo H, Lei G, Yang X-Y, et al. Increasing vaccine potency through exosome antigen targeting. Vaccine. 2011 Nov 21;29(50):9361–7.

201. Zeelenberg IS, Ostrowski M, Krumeich S, Bobrie A, Jancic C, Boissonnas A, et al. Targeting tumor antigens to secreted membrane vesicles in vivo induces efficient antitumor immune responses. Cancer Res. 2008 Feb 15;68(4):1228–35.

202. Longatti A, Schindler C, Collinson A, Jenkinson L, Matthews C, Fitzpatrick L, et al. High affinity single-chain variable fragments are specific and versatile targeting motifs for extracellular vesicles. Nanoscale. 2018 Aug 7;10(29):14230–44.

203. Ahmad ZA, Yeap SK, Ali AM, Ho WY, Alitheen NBM, Hamid M. scFv antibody: principles and clinical application. Clin Dev Immunol. 2012;2012:980250.

204. Tedder TF, Tuscano J, Sato S, Kehrl JH. CD22, a B lymphocyte-specific adhesion molecule that regulates antigen receptor signaling. Annu Rev Immunol. 1997;15:481–504.

205. Wang K, Wei G, Liu D. CD19: a biomarker for B cell development, lymphoma diagnosis and therapy. Exp Hematol Oncol. 2012 Nov 29;1:36.

206. Multani PS, O'Day S, Nadler LM, Grossbard ML. Phase II clinical trial of bolus infusion anti-B4 blocked ricin immunoconjugate in patients with relapsed B-cell non-Hodgkin's lymphoma. Clin Cancer Res Off J Am Assoc Cancer Res. 1998 Nov;4(11):2599–604.

207. Szatrowski TP, Dodge RK, Reynolds C, Westbrook CA, Frankel SR, Sklar J, et al. Lineage specific treatment of adult patients with acute lymphoblastic leukemia in first remission with anti-B4-blocked ricin or high-dose cytarabine: Cancer and Leukemia Group B Study 9311. Cancer. 2003 Mar 15;97(6):1471–80.

208. Mansfield E, Amlot P, Pastan I, FitzGerald DJ. Recombinant RFB4 immunotoxins exhibit potent cytotoxic activity for CD22-bearing cells and tumors. Blood. 1997 Sep 1;90(5):2020–6.

209. US FDA approves Lumoxiti (moxetumomab pasudotox-tdfk) for certain patients with relapsed or refractory hairy cell leukaemia. [2018 Sep 28].

210. Ghetie MA, Richardson J, Tucker T, Jones D, Uhr JW, Vitetta ES. Antitumor activity of Fab' and IgG-anti-CD22 immunotoxins in disseminated human B lymphoma grown in mice with severe combined immunodeficiency disease: effect on tumor cells in extranodal sites. Cancer Res. 1991 Nov 1;51(21):5876–80.

211. Du X, Beers R, FitzGerald DJ, Pastan I. Differential Cellular Internalization of Anti-CD19 and CD22 Immunotoxins Results in Different Cytotoxic Activity. Cancer Res. 2008 Aug 1;68(15):6300–5.

212. Panyam J, Labhasetwar V. Targeting intracellular targets. Curr Drug Deliv. 2004 Jul;1(3):235–47.

213. Zhang H, Liu J, Qu D, Wang L, Wong CM, Lau C-W, et al. Serum exosomes mediate delivery of arginase 1 as a novel mechanism for endothelial dysfunction in diabetes. Proc Natl Acad Sci U S A. 2018 17;115(29):E6927–36.

214. Guo BB, Bellingham SA, Hill AF. Stimulating the Release of Exosomes Increases the Intercellular Transfer of Prions. J Biol Chem. 2016 Mar 4;291(10):5128–37.

215. Barage SH, Sonawane KD. Amyloid cascade hypothesis: Pathogenesis and therapeutic strategies in Alzheimer's disease. Neuropeptides. 2015 Aug;52:1–18.

216. Pinheiro A, Silva AM, Teixeira JH, Gonçalves RM, Almeida MI, Barbosa MA, et al. Extracellular vesicles: intelligent delivery strategies for therapeutic applications. J Control Release Off J Control Release Soc. 2018 Sep 24;

217. Janumyan YM, Sansam CG, Chattopadhyay A, Cheng N, Soucie EL, Penn LZ, et al. Bcl-xL/Bcl-2 coordinately regulates apoptosis, cell cycle arrest and cell cycle entry. EMBO J. 2003 Oct 15;22(20):5459–70.

218. Kim R. Unknotting the roles of Bcl-2 and Bcl-xL in cell death. Biochem Biophys Res Commun. 2005 Jul 29;333(2):336–43.

219. Hanahan D, Weinberg RA. The hallmarks of cancer. Cell. 2000 Jan 7;100(1):57–70.

220. Nagarajah S. Exosome Secretion — More Than Simple Waste Disposal? Implications for Physiology, Diagnostics and Therapeutics. J Circ Biomark. 2016 Apr 1;5.

221. H. Rashed M, Bayraktar E, K. Helal G, Abd-Ellah MF, Amero P, Chavez-Reyes A, et al. Exosomes: From Garbage Bins to Promising Therapeutic Targets. Int J Mol Sci. 2017 Mar 2;18(3).

222. Thomas P, Smart TG. HEK293 cell line: a vehicle for the expression of recombinant proteins. J Pharmacol Toxicol Methods. 2005 Jun;51(3):187–200.

223. Li J, Chen X, Yi J, Liu Y, Li D, Wang J, et al. Identification and Characterization of 293T Cell-Derived Exosomes by Profiling the Protein, mRNA and MicroRNA Components. PLOS ONE. 2016 Sep 20;11(9):e0163043.

224. Nanda JS, Lorsch JR. Labeling a protein with fluorophores using NHS ester derivitization. Methods Enzymol. 2014;536:87–94.

225. Takov K, Yellon DM, Davidson SM. Confounding factors in vesicle uptake studies using fluorescent lipophilic membrane dyes. J Extracell Vesicles. 2017 Oct 12;6(1).

226. Chen Q, Takada R, Noda C, Kobayashi S, Takada S. Different populations of Wnt-containing vesicles are individually released from polarized epithelial cells. Sci Rep. 2016 Oct 21;6:35562.

227. Sullivan-Chang L, O'Donnell RT, Tuscano JM. Targeting CD22 in B-cell malignancies: current status and clinical outlook. BioDrugs Clin Immunother Biopharm Gene Ther. 2013 Aug;27(4):293–304.

228. Wayne AS, Kreitman RJ, Findley HW, Lew G, Delbrook C, Steinberg SM, et al. Anti-CD22 immunotoxin RFB4(dsFv)-PE38 (BL22) for CD22-positive hematologic malignancies of childhood: preclinical studies and phase I clinical trial. Clin Cancer Res Off J Am Assoc Cancer Res. 2010 Mar 15;16(6):1894–903.

229. Kato J, O'Donnell RT, Abuhay M, Tuscano JM. Efficacy and toxicity of a CD22-targeted antibody-saporin conjugate in a xenograft model of non-Hodgkin's lymphoma. Oncoimmunology. 2012 Dec 1;1(9):1469–75.

230. Chen WC, Sigal DS, Saven A, Paulson JC. Targeting B lymphoma with nanoparticles bearing glycan ligands of CD22. Leuk Lymphoma. 2012 Feb;53(2):208–10.

8 Appendices

8.1 Manuscripts accepted for publication

Willms E, Johansson HJ, Mäger I, Lee Y, Blomberg KEM, Sadik M, et al. Cells release subpopulations of exosomes with distinct molecular and biological properties.
Scientific Reports 2016

Willms E, Cabañas C, Mäger I, Wood MJA, Vader P. Extracellular Vesicle Heterogeneity: Subpopulations, Isolation Techniques, and Diverse Functions in Cancer Progression.
Frontiers in Immunology 2018

8.2 Attended conferences

December 2014

The First UK Extracellular Vesicle Forum (UKEV), London, United Kingdom

April 2015

ISEV Annual Meeting (International Society for Extracellular Vesicles), Washington DC, United States

December 2015

UKEV (UK Extracellular Vesicle Forum), Cardiff, United Kingdom, Poster Presentation

May 2016

ISEV Annual Meeting (International Society for Extracellular Vesicles, Rotterdam, The Netherlands. Oral presentation Characterisation and functional evaluation of distinct exosome subpopulations

September 2016

Oxosome meeting (The Oxford Extracellular Vesicle Group), Oxford, United Kingdom, Oral Presentation Characterisation of distinct exosome subpopulations

January 2017

Extracellular vesicles and the tumour microenvironment, The Royal Society, London, United Kingdom

May 2017

ISEV Annual Meeting (International Society for Extracellular Vesicles), Toronto, Canada. Oral Presentation High resolution size exclusion chromatography allows detailed study of exosome heterogeneity

October 2017

Oxosome Meeting (The Oxford Extracellular Vesicle Group), Oxford, United Kingdom. Part of organising committee

May 2018

The Oxford Interdisciplinary Bioscience Networking Event 2018, Oxford, United Kingdom. Oral Presentation: Exosomes: smuggling drugs into cells